

CHARLES UNIVERSITY IN PRAGUE

Faculty of Science

Department of Physical and Macromolecular Chemistry



STRUCTURAL STUDY OF THE ASK1:THIOREDOXIN
COMPLEX

Diploma thesis
of study program Biophysical Chemistry

Prague 2015

Bc. Katarína Pšenáková

Prohlášení

Prohlašuji, že jsem tuto diplomovou práci vypracovala samostatně pod vedením mého školitele prof. RNDr. Tomáše Obšila, Ph.D. a všechny použité informační zdroje a literaturu jsem řádně citovala. Tato práce ani její podstatná část nebyla předložena k získání jiného nebo stejného akademického titulu.

V Praze dne 07.05.2015

Podpis

Acknowledgments

I would like to thank both of my supervisors, prof. Tomáš Obšil and dr. Veronika Obšilová, for their patient guidance of my work, for their time devoted to me, for the encouragement they have always provided and for the support and advice they have always given me. I have been extremely lucky to have two supervisors who cared so much about my work and it was a real privilege to work under their supervision.

I would like to thank doc. Miroslav Štěpánek for his kind help and assistance with DLS measurements and Ing. Pavlína Novotná for her help with CD measurements.

I thank to all my colleagues in laboratories for their constant help and friendly, optimistic and joyful work environment. Especially to Salome Kylarová, Jakub Ptáček, Dalibor Košek, Miroslava Kopecká, Olívia Petrválská, Miroslava Kacířová, Kateřina Jarosilová and Simona Krausová. I am truly indebted to them for their support.

Special thanks belongs to my family for their unconditional love and for believing in me so much.

ABSTRAKT

Mitogénmi aktivované proteínové kinázy (MAPK) sú najdôležitejšou súčasťou bunkového obranného systému proti stresu. Schopnosť a účinnosť bunkových reakcií na rôzne stresové signály závisí na signálnych dráhach, kde signály z MAPK kinázy kinázy (MAP3K) sú prenášané pomocou fosforylácie na nižší stupeň kaskády tvorený MAPK kinázami (MAP2K) a následne rovnakým spôsobom na MAPK, ktoré tvoria najnižší stupeň signalizačnej kaskády. ASK1 kináza (z angl. Apoptosis signal-regulating kinase 1) je členom MAP3K rodiny a jej aktivácia a inhibícia má významnú rolu v regulácii bunkovej odpovedi na stresové podnety. Regulácia ľudskej formy ASK1 kinázy má silný vplyv na patogenézu mnohých ochorení, jej nadmerná aktivácia, alebo porucha kontroly jej funkcie je spojená s radou kardiovaskulárnych chorôb, neurodegeneratívnych porúch, zápalových ochorení, infekčných ochorení, bunkovým starnutím a s vznikom nádorov, astmy a cukrovky. Aktivita ASK1 je regulovaná interakciami s rôznymi proteínmi, pozornosť je ale sústredená najmä na dva fyziologické inhibítory, cicavčí tioredoxín (TRX) a proteín 14-3-3. Explicitný mechanizmus inhibície ASK1 vytváraním väzieb s TRX a 14-3-3 je však nejasný, vzhľadom na neexistujúce štruktúrne dáta týchto interakcií.

Táto diplomová práca je súčasťou rozsiahleho výskumu ľudskej ASK1 a zameriava sa na biofyzikálnu charakteristiku interakcie medzi ASK1 a TRX. Veríme, že pochopenie štruktúry ASK1 kinázy je rozhodujúce pre akýkoľvek zásah do jej regulácie a že kontrolovaná inhibícia molekuly ASK1 môže byť významná pre liečebný plán rôznych chorôb. Cieľom tejto práce je štruktúrna charakterizácia TRX väzbovej domény N-terminálnej časti ľudskej ASK1 kinázy (ASK1-TBD) a ASK1-TBD:TRX komplexu, a to využitím niekoľkých biofyzikálnych prístupov: natívna elektroforéza testujúca interakcie medzi ASK1 a TRX, dynamický rozptyl svetla pre štúdium polydisperzity a agregácie proteínov, cirkulárny dichroizmus pre štúdium sekundárnej štruktúry proteínov a malo-uhlový rozptyl svetla pre získanie štruktúry ASK1 kinázy s nízkym rozlíšením.

Výsledky ukázali, že ASK1-TBD je rigidná a monoména doména a vytvára stabilný komplex s TRX s veľkým väzbovým rozhraním. Katalytický motív TRX je nevyhnutný pre naviazanie na ASK1 a interakcia nie je spojená s tvorbou medzimolekulárnych disulfidových mostíkov. ASK1-TBD má kompaktný a mierne asymetrický tvar a interaguje s TRX bez vyvolania dramatickej konformačnej zmeny.

ABSTRACT

The mitogen-activated protein kinase (MAPK) cascade is an essential member of the cell defense system against stressors. The capability and efficiency of the cell reactions to different stress signals depend on signal transduction pathway, where signals from MAPK kinase kinase (MAP3K) are transferred through phosphorylation to downstream MAPK kinase (MAP2K) and finally to MAPK. Apoptosis signal-regulating kinase 1 (ASK1) is a member of a MAP3K family and its activation and inhibition has a significant participation in a regulation of cell response to stress stimuli. The regulation of ASK1 has a strong influence in pathogenesis of several diseases, the excessive activation of human ASK1 or failure in the control of its function are associated with cardiovascular diseases, neurodegenerative disorders, inflammatory diseases, infectious diseases, tumorigenesis, asthma, diabetes and ageing. The activity of ASK1 is regulated by its interaction with several proteins, the attention is focused on two physiological inhibitors, mammalian thioredoxin (TRX) and the 14-3-3 protein. ASK1 in its inactive form is inhibited by bonds formation with TRX and 14-3-3, however the explicit mechanism of this interaction is unclear due to the absence of structural data.

This work is a part of an extensive research about human ASK1, focusing on the structural characterization of the interaction between ASK1 and TRX. We believe that the understanding of ASK1 structure is critical for any intervention into its regulation and that the controlled inhibition of ASK1 molecule might be important for a treatment of many different diseases. The aim of this work is the structural characterization of the TRX binding domain of N-terminal human ASK1 (ASK1-TBD) and the ASK1:TRX complex using various biophysical approaches: native gel electrophoresis for the test of the interaction between ASK1 and TRX; dynamic light scattering measurements for a study of polydispersity and aggregation behavior of protein samples; circular dichroism measurements for a study of the protein secondary structure and small angle X-ray scattering measurements for the low resolution structure determination.

Results showed that ASK1-TBD is a rigid and monomeric domain and it forms with TRX a stable complex through a large binding interface. The catalytic motif of TRX is necessary for the ASK1-binding and the interaction is not accompanied by the formation of intermolecular disulfide bridges. ASK1-TBD has a compact and slightly asymmetric shape and it interacts with TRX without inducing any dramatic conformational change.

CONTENT

ABSTRAKT	4
ABSTRACT	5
CONTENT	6
LIST OF ABBREVIATIONS	10
1 INTRODUCTION	13
2 LITERATURE REVIEW.....	14
2.1 Protein kinase ASK1	14
2.1.1 Protein kinases	14
2.1.2 Signal pathways: MAPK pathway.....	16
2.1.3 ASK1.....	18
2.1.4 ASK1 and its regulation: 14-3-3.....	22
2.1.5 ASK1 and its regulation: Thioredoxin	22
2.2 Thioredoxin	24
3 AIMS OF DIPLOMA THESIS	27
4 MATERIAL AND METHODS.....	28
4.1 Used material.....	28
4.1.1 Chemicals	28
4.1.2 Instruments	29
4.1.3 Other material.....	29
4.2 Expression of ASK1-TBD	31
4.2.1 Expression of ASK1 ₈₈₋₃₀₂ C-His	31

4.2.2	Expression of His-GB1-ASK1 fusion constructs	32
4.2.3	Cell harvesting and sonication.....	33
4.3	Purification of ASK1-TBD	35
4.3.1	Nickel chelating chromatography of ASK1 ₈₈₋₃₀₂ C-His.....	35
4.3.2	Nickel chelating chromatography of His-GB1-ASK1 fusion constructs..	37
4.3.2.1	TEV protease cleavage of His-GB1-ASK1 fusion constructs.....	37
4.3.2.2	Removal of a cleaved GB1 protein.....	38
4.3.3	Size exclusion chromatography.....	38
4.4	Expression and purification of TRX.....	39
4.5	Protein concentration	40
4.6	Dialysis.....	41
4.7	SDS electrophoresis	41
4.8	Native gel electrophoresis	45
4.9	Circular dichroism	46
4.10	Dynamic light scattering	50
4.11	Small angle X-ray scattering	53
5	RESULTS.....	55
5.1	Expression and purification of ASK1 ₈₈₋₃₀₂ C-His.....	55
5.1.1	Nickel chelating chromatography.....	55
5.1.2	Size exclusion chromatography.....	56
5.2	Expression and purification of TRX.....	58
5.2.1	Nickel chelating chromatography.....	58
5.2.2	TEV protease cleavage.....	59

5.2.3	Size exclusion chromatography.....	60
5.3	Circular dichroism	61
5.4	Small angle X-ray scattering	64
5.5	Preparation of ASK1-TBD constructs for protein X-ray crystallography	67
5.5.1	Nickel chelating chromatography.....	67
5.5.2	TEV-protease cleavage	72
5.5.3	Removal of a cleaved GB1 protein.....	75
5.5.4	Size exclusion chromatography.....	77
5.6	Native gel electrophoresis	82
5.7	Dynamic light scattering	83
6	DISCUSSION.....	87
7	CONCLUSION	91
8	REFERENCES	92
	SUPPLEMENTS	97

This work was accomplished at the Department of Physical and Macromolecular Chemistry, Faculty of Science at the Charles University in Prague and at the Department of Protein Structures, Institute of Physiology at the Czech Academy of Sciences.

Part of the results presented in this diploma thesis was published in the following article:

1. Kosek D, Kylarova S, **Psenakova K**, Rezabkova L, Herman P, Vecer J, Obsilova V, Obsil T: “Biophysical and Structural Characterization of the Thioredoxin-binding Domain of Protein Kinase ASK1 and Its Interaction with Reduced Thioredoxin”; *The Journal of Biological Chemistry*, vol. 289 p. 24463-24474 (2014)

LIST OF ABBREVIATIONS

A.....	Adenine
ADP.....	Adenosine diphosphate
APS.....	Ammonium persulfate
AS CR.....	Academy of Sciences of the Czech Republic
ASK1.....	Apoptosis signal-regulating kinase 1
ASK1 ₈₈₋₃₀₂ C-His.....	Human N-terminal ASK1-TBD containing amino acid residues 88-302 with a C-terminal His-tag
Asn.....	Asparagine
ATP.....	Adenosine triphosphate
C.....	Cytosine
CaMKII.....	Ca ²⁺ /calmodulin-dependent protein kinase
CD.....	Circular dichroism
CCC.....	C-terminal coiled-coil domain
Cys.....	Cysteine
Da.....	Daltons
DLS.....	Dynamic light scattering
DNA.....	Deoxyribonucleic acid
dNDP.....	Deoxyribonucleotide diphosphate
<i>E. coli</i>	<i>Escherichia coli</i>
EDTA.....	ethylenediaminetetraacetic acid
EM.....	Electron microscopy
ER.....	Endoplasmic reticulum
ERK.....	Extracellular signal-regulated kinase
Eq.....	Equation
FAD.....	Flavin adenine dinucleotide
Fig.....	Figure
G.....	Guanine
g.....	Gravitational force

GB1.....	B1 domain of a streptococcal G protein
Gln.....	Glutamine
Glu.....	Glutamic acid
Gly.....	Glycine
His.....	Histidine
HPLC.....	High performance liquid chromatography
IPTG.....	Isopropyl β -D-1-thiogalactopyranoside
JNK.....	c-Jun N-terminal kinase
LB-medium.....	Luria-Bertani medium
Leu.....	Leucine
LPS.....	Lipopolysaccharide molecules
MAPK.....	Mitogen-activated protein kinase
MKK.....	Mitogen-activated kinase kinase
MRE.....	Mean residue ellipticity
NADPH.....	Nicotinamide adenine dinucleotide phosphate
NCAC.....	Nickel chelating chromatography
NCC.....	N-terminal coiled-coil domain
NMR.....	Nuclear magnetic resonance
OD.....	Optical density
O/N.....	Overnight
P.....	Phosphorylated
PBS.....	Phosphate-buffered saline
Phe.....	Phenylalanine
P _i	Inorganic phosphate
PMSF.....	phenylmethylsulfonyl fluoride
Pro.....	Proline
pSer.....	Phosphoserine
pThr.....	Phosphothreonine
rNDP.....	Ribonucleotide diphosphate
ROS.....	Reactive oxygen species
SAXS.....	Small angle X-ray scattering measurements

SEC.....	Size exclusion chromatography
Ser.....	Serine
SDS-PAGE	Sodium dodecyl sulfate polyacrylamide gel electrophoresis
Tab.....	Table
TBD	Thioredoxin-1 binding domain
TBE.....	Tris-Borate-EDTA buffer
TEMED.....	tetramethylethylenediamine
TEV	Tobacco Etch Virus
Thr	Threonine
TLR.....	Toll-like receptors
TNF α	Tumor necrosis factor α
TRAF.....	TNF receptor-associated factors
Tris.....	tris(hydroxymethyl)aminomethane
Trp	Tryptophan
TRX	Thioredoxin-1
TRXR.....	Thioredoxin reductase
Tyr	Tyrosine
UV	Ultraviolet
6 \times His-tag	six histidine residues
β ME	2-thioethanol

1 INTRODUCTION

Proteins are outstandingly versatile, functionally sophisticated and structurally complicated macromolecules. They contribute not only as a building block for cells, but they also execute almost entire cell function system [1].

It is the essential biological property of a protein to bind to other molecules, based on a specific physical interaction with selected ligands. Protein-protein interactions are mostly based on the formation of a set of noncovalent bonds through various types of interfaces, often affecting the three-dimensional shape of proteins and protein complexes [1]. These interactions create large networks of regulatory responses, forming various cascades and signaling pathways.

Adaptation of the organisms to changes in the external environment is a key feature for their survival. The capability and efficiency of cell reactions to different stress signals depend on interactions between intracellular signaling pathways. The defense system against environmental, extracellular and intracellular stressors is governed by the mitogen-activated protein kinase (MAPK) pathways. They belong to a family of signal transduction pathways, evolutionarily well conserved in eukaryotic organisms, where signals from MAPK kinase kinase (MAP3K) are transferred through phosphorylation to downstream MAPK kinase (MAP2K) and finally to MAPK, leading to adequate cellular response. Apoptosis signal-regulating kinase 1 (ASK1) is a member of a large MAP3K family and its activation plays a key role in regulation of a cell response to stress stimuli [2]. The activity of ASK1 is regulated by its interaction with several proteins, mammalian thioredoxin (TRX) and the 14-3-3 protein are participating in a direct inhibition of ASK1 [3][4].

The explicit mechanism of regulating ASK1 is unclear due to the absence of structural data. This work is concentrating on the structural characterization of the interaction between ASK1 and TRX. The entire sequence of ASK1 molecule contains 1374 amino acids, however the TRX binding domain (TBD) has been previously established within the N-terminal part, between residues 46 and 277 [3][5]. For better understanding of the inhibition mechanism, I performed several biophysical studies on various constructs of the isolated ASK1-TBD and their complexes with TRX (ASK1-TBD:TRX). The aim of this work was the structural characterization of ASK1-TBD and ASK1-TBD:TRX.

2 LITERATURE REVIEW

2.1 Protein kinase ASK1

2.1.1 Protein kinases

Protein kinases belong to a large family of class of enzymes known as transferases. They regulate cellular functions and mediate responses of eukaryotic cells to external stimuli by catalyzing the phosphorylation of proteins. Protein kinases transfer a phosphate group from macroergic nucleoside triphosphate to a substrate (*Fig. 2.1*) [6]. The reverse reaction for the phosphorylation is the hydrolysis dephosphorylation reaction catalyzed by a family of enzymes called protein phosphatases.

The phosphorylation process is carried out by covalently attaching PO_4^{3-} to amino acid with a free hydroxyl group, what involves side chains of serine, threonine and tyrosine. Depending on the type of a phosphorylated amino acid in a protein sequence, protein kinases are divided into serine/threonine kinases and tyrosine kinases

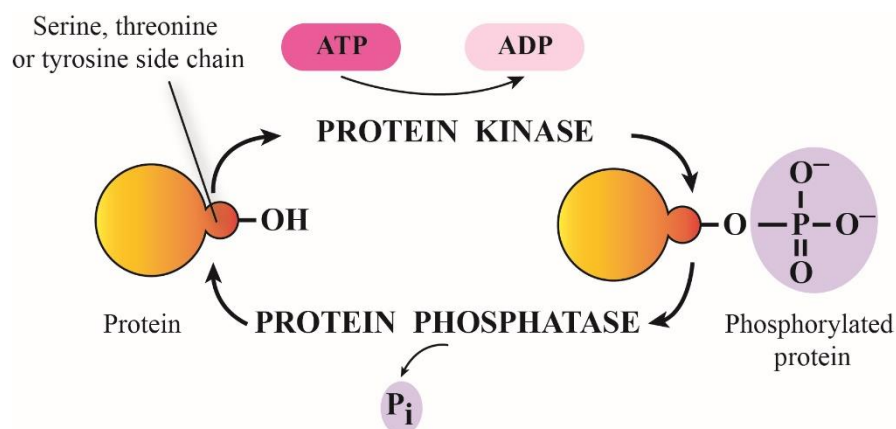


Figure 2.1. Phosphorylation and dephosphorylation of a protein substrate.

Protein kinases catalyze the phosphorylation by transferring a phosphate group from adenosine triphosphate (ATP) to a target protein. During phosphorylation is generated adenosine diphosphate (ATP), dephosphorylation releases inorganic phosphate (P_i). Adapted from [7].

The phosphate group PO_4^{3-} inside a cell is in a deprotonated state. Attachment of this large negatively charged unit alters the protein charge and generally leads to conformational changes (*Fig. 2.2*), thus the phosphorylation state of proteins usually decide about their activity (inactivity). It often occurs in other protein kinase than is the one catalyzing the reaction, what leads to the creation of a kinase cascade that amplifies a cellular signal and improves the ability of its control [1].

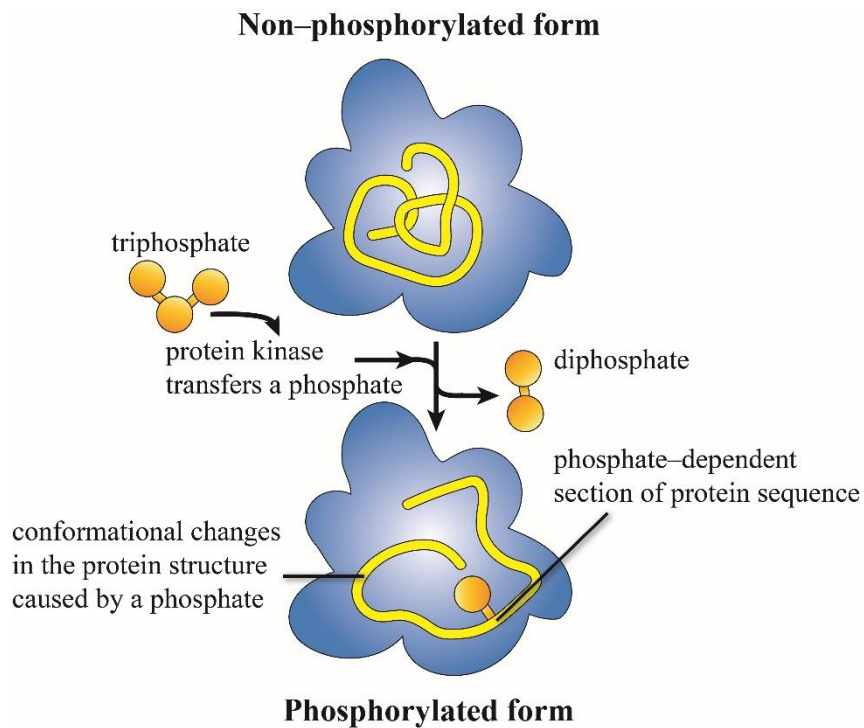


Figure 2.2. Conformational changes in protein during phosphorylation. Protein kinase transfers a phosphate to the phosphate-dependent section of protein sequence. An attachment of this unit leads to conformational changes. Adapted from [7].

2.1.2 Signal pathways: MAPK pathway

The cell signaling is an essential element of a complex system, on which depends the ability of cells to control basic cellular activities and to coordinate most cell actions. All organisms are in constant physical dispute against various stresses and there are a lot of signaling pathways that govern the respond to stresses in cellular microenvironment. The MAPK pathway is one of the stress-activated intracellular signaling pathways in eukaryotes [8].

Multiple, evolutionarily well conserved MAPK pathways occur among all eukaryotic cells regulating cell growth, differentiation and apoptosis. They are activated or inactivated by various extracellular (environmental) stressors, such as UV or γ -ray irradiation, heat shock, bacterial or viral infection; and intracellular stressors, such as endoplasmic reticulum stress, calcium ion influx, osmotic pressure and oxidative stress [8].

Cells and tissues exposed to stress conditions frequently utilize from various organelles the reactive oxygen species (ROS), that may induce oxidative stress, damage cells and subsequently increase the risk of diseases and dysfunction of biochemical systems [9][10]. ROS (hydrogen peroxide, superoxide, hydroxyl radical, singlet oxygen) are generated by aerobic metabolism, specifically by electron transport in the mitochondrial respiratory chain [9]. Minor increase of ROS in an organism is compensated by endogenous antioxidants and reductants, major increase results in a change of redox state in the cell and leads to its death. ROS can therefore function as a messenger in signal transduction, as the generation of ROS causes a fluctuation of the intracellular redox condition, stimulating and modifying other signaling molecules and thus participating in the signaling cascades [9].

Each MAPK cascade consists of three classes of protein kinases: the mitogen-activated protein kinase kinase kinase (MAP3K), the MAPK kinase (MAP2K) and the MAPK. Initially, the MAP3K is triggered by a stimulus. Activated MAP3K phosphorylates and activates MAP2K, which successively phosphorylates and activates MAPK [2][11]. Activated MAPK further phosphorylates other protein kinases and various transcription factors, regulating fundamental cellular responses and functions.

Three crucial MAPK subgroups have been characterized in mammals: extracellular signal-regulated kinase (ERK), c-Jun N-terminal kinase (JNK) and p38 MAPK (Fig. 2.3). ERK pathways are triggered by the growth factors and closely linked to the regulation of a cell proliferation; the JNK and p38 pathways are preferentially activated by the environmental stresses and closely linked to the stress responses [9][10].

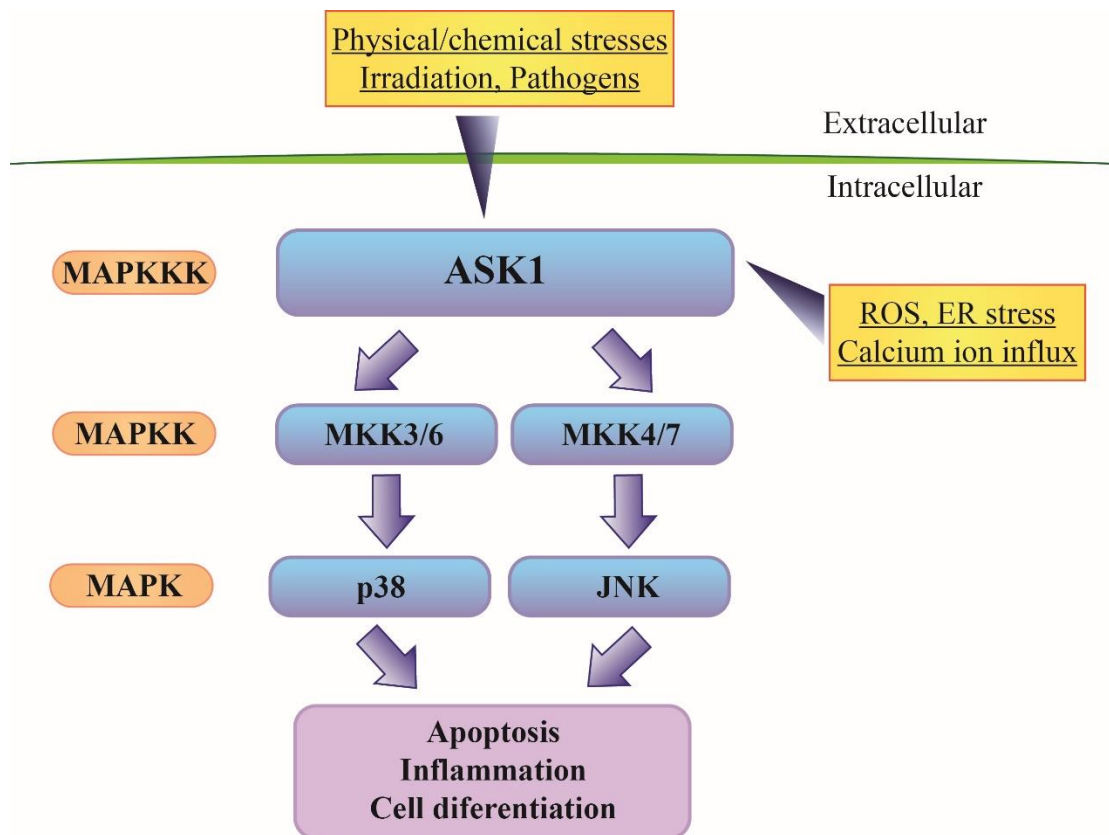


Figure 2.3. Scheme of MAP kinase signaling pathway. Various extracellular and intracellular stressors activate MAP3K, which consequently phosphorylate and activate MAP2K, phosphorylating and activating MAPK. The activation of p38 and JNK pathways lead to cellular responses, such as apoptosis, morphogenesis, proliferative inflammation. Adapted from [12].

2.1.3 ASK1

Apoptosis signal-regulating kinase 1 is a MAP kinase kinase kinase (MAP3K5) and it activates members of a MAPKK family: mitogen-activated kinase kinase MKK3 or MKK6 and MKK4 or MKK7, activating p38 subgroups of MAPKs and stress-activated protein kinase JNK, respectively [2].

The activity of ASK1 depends on various stimuli, including oxidative stress (presence of ROS), endoplasmic reticulum (ER) stress, presence of lipopolysaccharide molecules (LPS) and cytokines (tumor necrosis factors TNF α) or influx of calcium ions (*Fig. 2.4*) [2].

ASK1 functions as a detector for ROS and plays a key role in a signaling for maintaining the redox balance. Overexpression of ASK1 may induce apoptosis, but in the cell's framework it may also promote differentiation or survival [13]. The excessive activation of human ASK1 or failure in the control of its function is associated with many different diseases. ASK1 has been implicated in: (a) cardiovascular diseases; (b) neurodegenerative disorders; (c) inflammatory diseases; (d) infectious diseases; (e) tumorigenesis; (f) asthma, diabetes and ageing [14]. ROS activated kinase pathways are linked to a myocardial ischemia and reperfusion injuries, diabetes mellitus, or chronic hepatitis [15]. ASK1 regulation participates in a trinucleotide repeat expansion (PolyQ) disorders, such as Huntington's disease, Machado-Joseph disease and spinobulbar muscular atrophy. PolyQ diseases are inherited neurodegenerative disorders caused by expanded cytosine, adenine and guanine (CAG) repeats, encoding a long polyglutamine section in the protein sequence and inducing cellular stress [16][17]. ASK1 is also reported to affect the paraquat (parkinsonism toxin) induced neuronal death [18] and the hyperphosphorylation of tau, essential element of neurofibrillary tangles in Alzheimer's disease [19]. List of diseases related to ASK1 is shown in *Table 2.1*.

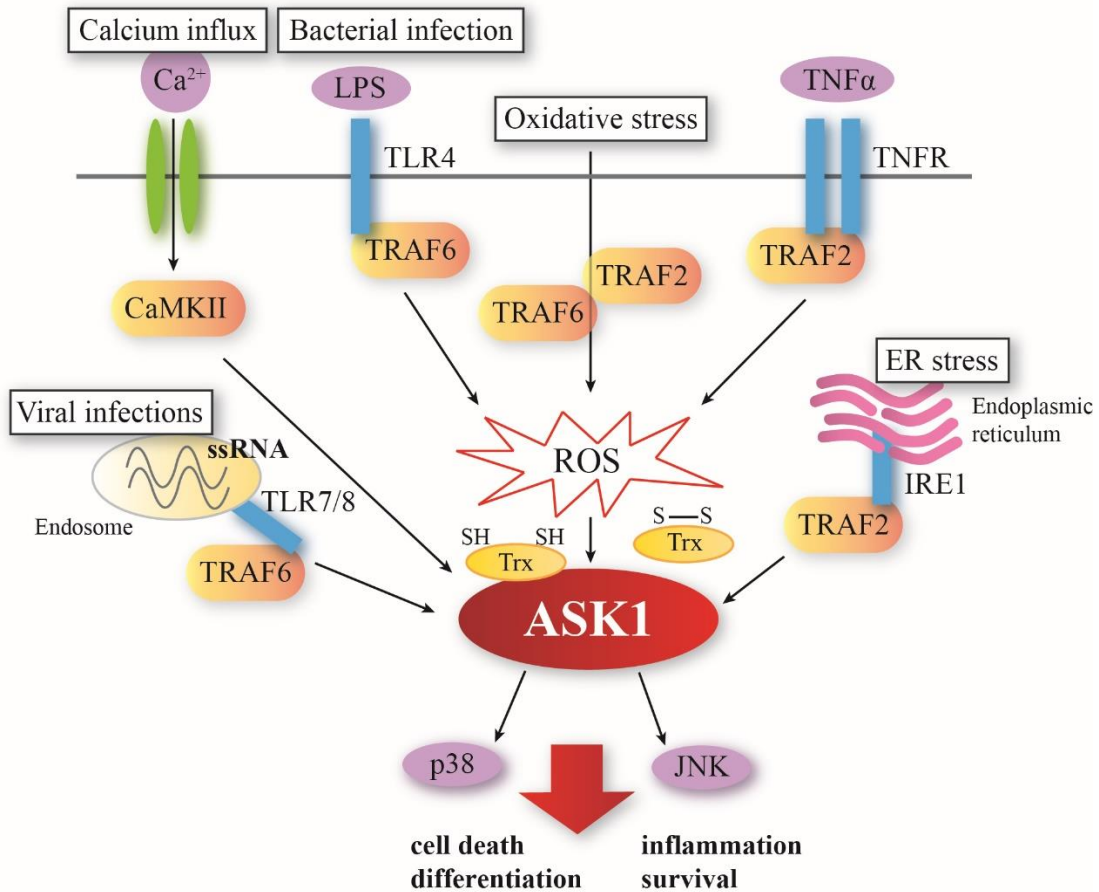


Figure 2.4. Overview of the activation and function of ASK1. ASK1 is activated by the viral infections, calcium influx, bacterial infections, oxidative stress, ER stress, receptor-mediated signaling through Toll-like receptors TLR4/7/8 and tumor necrosis factor TNF receptor. ROS may act as a signaling intermediate for intracellular signaling proteins, such as TNF receptor-associated factors TRAF2/6, Ca²⁺/calmodulin-dependent protein kinase CaMKII. Reduced form of TRX inhibits ASK1 by binding to its N-terminus. Currently accepted hypothesis is that the change in cellular redox state leads to the oxidation of TRX and a dissociation from ASK1, causing its activation. ASK1 activates the MAP kinase signaling pathway p38 and JNK inducing several cellular processes. Adapted from [14].

Table 2.1. Diseases related to ASK1. Adapted from [14].

Disease	Stress	Cell/Pathology
Vascular diseases		
Ischemia/reperfusion injury (cardiac muscle)	ROS, Ca ²⁺	myocardial cell death
Cardiac remodeling	ROS, mechanical stress, inflammatory cytokines	cardiomyocyte death, hyperplasia and fibrosis
Atherosclerosis	disturbed blood flow, TNF α , oxidized low-density lipoprotein	inflammation
Brain ischemia	oxidative stress	apoptosis
Neurodegenerative disorders		
PolyQ disease	ER stress	neuronal cell death
Amyotrophic lateral sclerosis	ER stress	motor neuron death
Alzheimer's disease	oxidative stress	neuronal cell death
Parkinson's disease	oxidative stress, ER stress	dopaminergic neuron death
Mesial temporal lobe epilepsy	ER stress	neuronal cell death
Inflammatory diseases		
Multiple sclerosis	Toll-like receptors	chemokine production
Rheumatoid arthritis	TNF α , lipopolysaccharide	cytokine production
Tumor		
Skin cancer	DNA damage, ROS	inflammation, apoptosis
Colon cancer	Toll-like receptors	inflammation, innate immunity
Breast cancer	DNA damage	cell migration
Liver cancer	DNA damage	apoptosis
Infection		
Influenza virus	TNF α , interleukin 1	apoptosis
HIV-1	Fas ligand (from TNF family)	macrophage apoptosis
Japanese encephalitis virus	ROS	apoptosis
Sepsis	Toll-like receptors, ROS	inflammatory cytokine production, tissue factor expression
Mycobacterium tuberculosis-infected macrophages	Toll-like receptors, ROS	macrophage cytokine production
Other diseases		
Fanconi anemia	TNF α , ROS	hematopoietic cell apoptosis
Diabetes	TNF α , ROS	pancreatic β cell apoptosis, inflammation, insulin resistance
Liver injury induced by drug	ROS	hepatocyte apoptosis
Aging	ROS	

Human ASK1 kinase consists of 1374 amino acids with 11 kinase subdomains and calculated relative molecular mass of 155 kDa [2]. ASK1 consists of serine/threonine catalytic domain located in the middle part of the molecule between two coiled-coil domains which are situated on both the N-terminus (N-terminal coiled-coil domain NCC) and at the C-terminus (C-terminal coiled-coil domain CCC) (Fig. 2.5) [16][11].

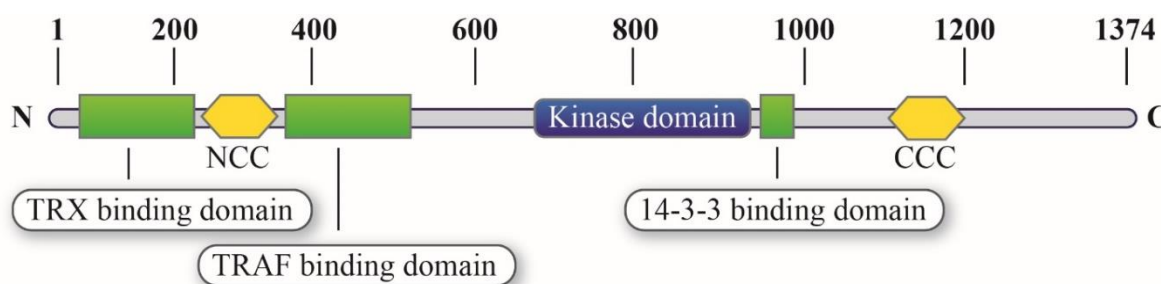


Figure 2.5. Domain configuration of human ASK1. Numbers correspond to amino acids in a protein sequence. NCC and CCC refer to N- or C-terminal coiled coil domain, N and C refer to N- or C-terminus. Adapted from [16].

The structure of the entire molecule has not been solved yet, the crystal structure of human ASK1 catalytic domain in a complex with staurosporine was elucidated by X-ray crystallography analysis in 2007 [16]. The catalytic domain of ASK1 contains three autophosphorylation sites, that are spontaneously phosphorylated in the presence of ATP and magnesium Mg^{2+} cations. First autophosphorylation site is Thr⁸¹³, indirectly influencing catalysis. Second is Thr⁸³⁸ located in the activation loop, playing an essential role in the activation of ASK1 induced by an oxidative stress [20]. This flexible activation motif is conserved among species and its phosphorylation regulates not only ASK1, but also other protein kinases. The third autophosphorylation site is Thr⁸⁴² [16].

Endogenous ASK1 in its inactive state forms the ASK1 signalosome - a complex with high molecular weight (1500-2000 kDa) containing regulatory proteins. Configuration and activity of this unit is based on the homo-oligomerization of ASK1 through CCC domain [21].

2.1.4 ASK1 and its regulation: 14-3-3

Other physiological inhibitors of ASK1 are the 14-3-3 proteins. The 14-3-3 proteins are highly conserved acidic regulatory molecules expressed in all eukaryotic cells. They are important regulators of many cellular processes with an ability to bind and interact with phosphatases, kinases, transmembrane receptors and other functionally differing signaling proteins [22]. The 14-3-3 proteins have specific binding motif that can recognize particular amino acid sequence containing phosphoserine or phosphothreonine (pSer or pThr), thereby significantly affecting the regulation of cellular signal transduction, cell cycle, metabolism, and apoptosis [22].

ASK1 specifically interacts with the 14-3-3 protein through the recognition motif located at the C-terminus of the ASK1 kinase domain. The interaction between ASK1 and 14-3-3 requires the phosphorylation of Ser⁹⁶⁷, crucial for a regulation and inhibition of the catalytic activity of ASK1 under non-stressed conditions [4]. If the ASK1 is exposed to elevated concentrations of ROS, the specific phosphatase is activated, dephosphorylating Ser⁹⁶⁷ results to 14-3-3 dissociation, influencing catalytic activity of ASK1 [23].

2.1.5 ASK1 and its regulation: Thioredoxin

Protein thioredoxin is one of the negative regulators of ASK1, responding to the change of environmental redox potential. TRX has an active site with two cysteine residues that are in their reduced form associated with a regulatory domain of ASK1. TRX inhibits the activity of ASK1 by a specific interaction with the NCC domain of ASK1, preventing a homophilic interaction of two ASK1 molecules through NCC domains [5]. TRX-binding domain in ASK1 sequence is located between amino acid residues 88-277 [5], amino acid sequence of the N-terminal ASK1₁₋₃₂₀ is shown in *Supplement 1*. The explicit mechanism of the interaction between TRX and ASK1 is unknown considering the absence of structural data, the most probable mechanism for the activation of ASK1 signalosome is shown in *Fig. 2.6*.

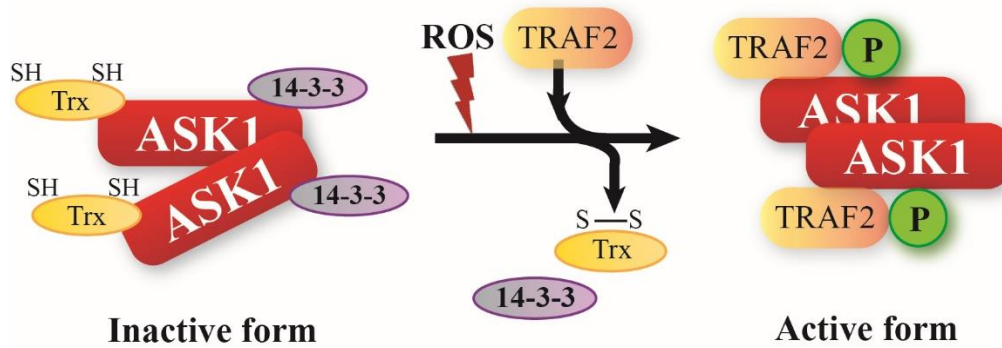


Figure 2.6. Currently accepted model of ASK1 signalosome activation. In the inactive state, the ASK1 is homo-oligomerized through the CCC domain, 14-3-3 binds to the C-terminal, TRX binds to the N-terminal part of ASK1. Oxidative stress (ROS) leads to a 14-3-3 and TRX dissociation from ASK1, the binding site is latched by TRAF2, and the phosphorylated (P) catalytic domain activates ASK1 signalosome. Adapted from [11].

Currently accepted model suggests that an oxidative stress induces formation of a disulfide bridge between Cys³² and Cys³⁵ in the active site of TRX, causing the dissociation of a TRX molecule from the ASK1 dimer (ASK1 dimerization is mediated by CCC regions, *Figs. 2.5, 2.6*). It has been suggested that the release of TRX is followed by a conformational change in ASK1 dimer, resulting in the oligomerization of the N-terminal parts through NCC regions. These structural changes result in the dissociation of a 14-3-3 protein and autophosphorylation of Thr⁸³⁸ in the activation loop of a catalytic domain [20]. The complex between ASK1 and TRX stimulated by ROS is complemented by two tumor necrosis factor receptor-associated factors TRAF2 and TRAF6, establishing an active ASK1 signalosome with higher molecular weight than the inactive system [24].

2.2 Thioredoxin

Thioredoxin-1 (TRX) is a 12kDa oxidoreductase enzyme conserved from archaea to mammal. In oxidative conditions, cysteine dithiol-disulfide exchange in the active site of TRX maintains the intracellular redox state. The oxidized form of TRX is reduced by FAD-containing enzyme thioredoxin reductase (TRXR), allowing to transfer electrons from nicotinamide adenine dinucleotide phosphate (NADPH) to enzymes for cell proliferation and survival. TRX was originally considered as a hydrogen donor for ribonucleotide reductase [25], however TRX has specific protein substrates with particular functional characters for counteracting oxidative stress, therefore playing a pivotal role as a comprehensive disulfide reductase for many crucial enzymes in cells [26].

Thioredoxin system is a cyclic electron transport process transferring electrons via an oxidation-reduction active disulfide, making the capacity of the reducing agent (NADPH) accessible for reductions (*Fig. 2.7*) [27]. The cytoplasmic thioredoxin system involves redox active protein thioredoxin-1 [28], the mitochondrial system involves thioredoxin-2 [29]. Thioredoxin-2 has been far less studied, thioredoxin-1 (TRX) is an essential redox regulator arbitrating the activation of various transcription factors involved in apoptosis, inflammation and cell growth. The role of TRX in embryogenesis - early differentiation and morphogenesis, depends on a defense against oxidative stress and a transcription regulation. Transcription factors with cysteine residues in the DNA binding site are regulated by the change in their redox status, therefore TRX is significant governor of the DNA binding. Other proteins dependent on the TRX system are located (a) outside the cell involved in cell growth simulation and chemotaxis, (b) in the cytoplasm in antioxidant defense system (TRX functioning as a reductant cofactor), (c) in the nucleus involved in DNA synthesis and repair, cell proliferation and gene transcription and (d) in the mitochondria [30].

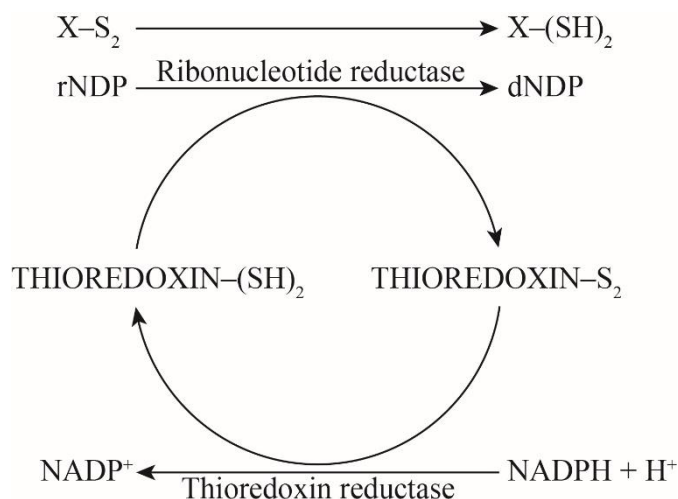


Figure 2.7. Electron transport system. Thioredoxin forms a cyclic electron transport process transferring electrons between disulfide group S_2 and dithiol group $(SH)_2$ in the presence of reductases, allowing to transport electrons from nicotinamide adenine dinucleotide phosphate (NADPH) to enzymes for a cell proliferation and survival. Ribonucleotide reductions provide the formation of deoxyribonucleotide diphosphate dNDP from a ribonucleotide diphosphate rNDP, important in the synthesis of DNA. Adapted from [27].

TRX is an acidic protein with an isoelectric point at 4.8, consisting of 105 amino acid residues. The oxidation-reduction disulfide bridge is established between Cys³² and Cys³⁵ separated by Gly³³ and Pro³⁴ forming a disulfide ring with 14 amino acid residues [31]. The reduction of a disulfide group to a dithiol unit accompanies localized conformational change [32] excessively changing the Trp²⁸ fluorescence emission [33].

The first crystal structure of reduced TRX was solved by a Swedish biochemist Arne Holmgren in 1975. The molecule of reduced TRX consists of a central core with three parallel and two antiparallel β -sheet surrounded by four α -helices [27]. The TRX structure with a full description is shown in *Fig. 2.8*.

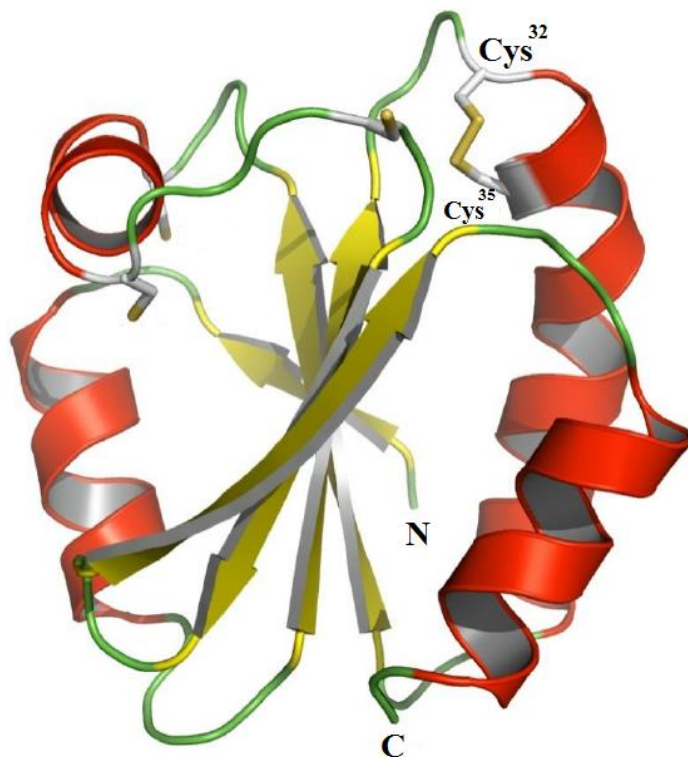


Figure 2.8. Crystal structure of Thioredoxin-S₂. The molecule of a reduced TRX consists of a central core with three parallel and two antiparallel β -sheets surrounded by four α -helices. Amino acid residues 1-72 form one region of molecule: β 1 (the top strand) is formed by residues 2 to 8, α 1 is folded by residues 11 to 18 looping back the chain from residues 22 to 29 to establish middle strand β 2. The disulfide ring with 14 amino acid residues forms a protrusion outside the C-end of β 2, a disulfide bridge is shown between cysteines 32 and 35. The axis of a long α 2 helix (composed from the amino acids 34-49) is parallel to β 2, between β 1 and β 2 is located β 3 (residues 53-58) and α 3 helical turn is included in a loop formed by the residues 59 to 72. A second region is formed by two antiparallel β -sheets 4 and 5 and a carboxy-terminal α 4 helix. Several hydrogen bonds are established between β 2 and β 4, connecting the two regions [27].

Created with The PyMOL Molecular Graphics System, Version 1.7.4 Schrödinger, LLC.

3 AIMS OF DIPLOMA THESIS

- Expression and purification of a human ASK1-TBD containing amino acid residues 88-302 with the C-terminal His-tag (ASK1₈₈₋₃₀₂C-His)
- Expression and purification of a human TRX
- Study of the secondary structure of ASK1₈₈₋₃₀₂C-His and the ASK1₈₈₋₃₀₂C-His:TRX complex using circular dichroism (CD) measurements
- Preparation of ASK1₈₈₋₃₀₂C-His and the ASK1₈₈₋₃₀₂C-His:TRX complex for small angle X-ray scattering (SAXS) measurements

- Optimization of an ASK1-TBD construct for protein X-ray crystallography
 - Expression and purification of seven different constructs of ASK1-TBD
 - Test of the interaction between the selected ASK1-TBD construct and TRX using native gel electrophoresis
 - Study of a polydispersity and aggregation behavior (stability) of selected ASK1-TBD construct using dynamic light scattering (DLS) measurements

4 MATERIAL AND METHODS

4.1 Used material

4.1.1 Chemicals

1,4-dithiotreitol	Carl Roth (Germany)
acetic acid	Lachema a.s. (Czech republic)
ampicillin.....	Sigma (USA)
β-mercaptoethanol	Sigma (USA)
bromophenol blue	Aldrich (Germany)
citric acid	Lachema a.s. (Czech republic)
Coomassie Brilliant Blue R 250	Lachema a.s. (Czech republic)
DNA oligonucleotides.....	Lachema a.s. (Czech republic)
EDTA	Carl Roth (Germany)
ethanol.....	Penta (Czech republic)
glycerol.....	Lachema a.s. (Czech republic)
glycine	Carl Roth (Germany)
hydrochloric acid	Lachema a.s. (Czech republic)
imidazole	Carl Roth (Germany)
IPTG.....	Sigma (USA)
isopropyl alcohol	Lachema a.s. (Czech republic)
LB-medium	Carl Roth (Germany)
lysozyme	Carl Roth (Germany)
methanol.....	Lachema a.s. (Czech republic)
monopotassium phosphate	Lachema a.s. (Czech republic)
PMSF	Sigma (USA)
potassium chloride	Lachema a.s. (Czech republic)
SDS	Sigma (USA)
sodium azide	Sigma (USA)
sodium hydrogenphosphate dihydrate	Lachema a.s. (Czech republic)

sodium hydroxide	Lach-Ner, s.r.o. (Czech republic)
sodium chloride	Carl Roth (Germany)
TEMED	Carl Roth (Germany)
Tris	Carl Roth (Germany)

4.1.2 Instruments

ALV	Langen (Germany)
Centrifuge SIGMA 8K (rotor 12510-H).....	Sigma (Germany)
Centrifuge HERMLE Z323K.....	Hermle (Germany)
Centrifuge 5804 R (rotor A-4-44)	Eppendorf (Germany)
HPLC Watrex	Watrex (Czech republic)
Implen NanoPhotometer P300.....	Implen (Germany)
incubator HT Multitron	Infors (Switzerland)
incubator Shaking Incubator NB-205	N-Biotek (Korea)
laboratory scales HF-200g.....	And (USA)
magnetic stirrer Variomag Maxi, Komet	Thermo Scientific (USA)
peristaltic pump.....	IDEX (Switzerland)
pH meter JenWay 3505	Felsted (United Kingdom)
sonicator 3000 Misonix	Cole-Parmer (USA)
spectrophotometer Agilent 8453.....	Agilent (USA)
thermoblock	Grant (United Kingdom)
vertical polyacrylamide electrophoresis.....	BioRad (USA)
Vortex Zx3.....	Velp Scientifica (Italy)

4.1.3 Other material

automatic pipettes	Eppendorf (Germany)
benzamidin-sepharosa	Amersham Biosciences (Sweden)

centrifuge tubes.....Carl Roth (Germany)
 column HiLoad Superdex 75 (26/60 GL)GE Healthcare (United Kingdom)
 concentrators Amicon UltraMillipore (USA)
 Chelating Sepharose Fast FlowGE Healthcare (United Kingdom)
 dialysis membrane (type 27/32).....Carl Roth (Germany)
E. coli strain BL21(DE3).....Stratagene (USA)
 filters SPARTAN 13/0,45 RCWhatman (Germany)
 filters SPARTAN 13/0,2 RCWhatman (Germany)
 quartz cuvettesAgilent (USA)
 laboratory glassSimax (Czech republic)
 Eppendorf microtubesP-Lab, a.s. (Czech republic)
 nylon filters (0,45 µm)Whatman (Germany)
 Precision Plus Protein Dual Color StandardBioRad (USA)
 SP sepharoseAmersham Biosciences (Sweden)
 syringes.....B. Braun (Germany)
 tips for automatic pipettesAxygen (USA)

4.2 Expression of ASK1-TBD

Eight different constructs of a human ASK1-TBD were used in this diploma thesis. The construct containing ASK1-TBD (amino acid residues 88-302) with the C-terminal His-tag (denoted as ASK1₈₈₋₃₀₂C-His) was a result of a previous work in our laboratory. Seven other constructs with cleavable His-tag and GB1 protein at the N-terminus of ASK1-TBD were designed for structural studies (*Tab. 4.1*).

Table 4.1. List of used ASK1 constructs.

Construct	Plasmid	Construct length (number of amino acids)	Molecular weight (kDa)	Ext. coefficient (M ⁻¹ ·cm ⁻¹)
ASK1₈₈₋₃₀₂C-His *	pST39	215	25.6	13 410
ASK1₈₈₋₃₀₂	pRSFDuet-1	215	24.3	13 410
ASK1₄₆₋₂₅₁	pRSFDuet-1	206	22.8	15 930
ASK1₄₆₋₂₆₇	pRSFDuet-1	222	24.5	15 930
ASK1₄₆₋₂₈₇	pRSFDuet-1	242	27.0	18 910
ASK1₈₈₋₂₅₁	pRSFDuet-1	164	18.9	10 430
ASK1₈₈₋₂₆₇	pRSFDuet-1	180	20.7	10 430
ASK1₈₈₋₂₈₇	pRSFDuet-1	200	23.1	13 410

* ASK1₈₈₋₃₀₂C-His responds to the construct of a human N-terminal ASK1-TBD with the amino acid residues 88-302 and a C-terminal His-tag

4.2.1 Expression of ASK1₈₈₋₃₀₂C-His

ASK1₈₈₋₃₀₂C-His expression construct was prepared by my colleague RNDr. Lenka Řežábková, PhD. For the expression was used pST39 plasmid, with a leakage expression without the necessity of an induction and a resistance to the antibiotic ampicilin. Plasmids are circular double-stranded DNA capable of self-replication, used as the genetically engineered vectors for introducing expression constructs into the host cells (e.g. bacteria).

The sequence encoding human N-terminal ASK1 with amino acid residues 88-302 was inserted between the restriction sites *Xba*I and *Bam*HI in the pST39 vector and to the C-terminus was added a polyhistidine-tag, a motif containing six histidine residues (6×His-tag), simplifying the production of a protein by enabling an affinity chromatography as the first purification step. Also, the C-terminal His-tag in this construct acted as an overall stabilizing element, so ASK1₈₈₋₃₀₂C-His was evaluated as a suitable construct for biophysical studies of ASK1-TBD and its complex with TRX.

The leakage expression of ASK1₈₈₋₃₀₂C-His using pST39 plasmid started with transformation into competent *E. coli* B121 (DE3) bacterial cells. 1 µL of ASK1₈₈₋₃₀₂C-His DNA in pST39 plasmid was added into 45 µL of *E. coli* cell B121 (DE3) suspension and the mixture was incubated on ice for 20 minutes. Heat-shock followed, the mixture was heated to 42 °C for 45 seconds and then cooled again on ice for 2 minutes. 450 µL of the LB-medium (Tab. 4.2) was added in sterile conditions to the mixture and the microtube was incubated at 0.8 g and 37 °C for one hour. Solution of bacteria with the inserted gene of the ASK1₈₈₋₃₀₂C-His was pipetted into a test-tube with 5 mL of a sterile LB-medium containing the ampicilin at the final concentration of 100 µg·mL⁻¹, and these test-tubes were incubated at 0.8 g and 37 °C overnight.

Next, each test-tube was transferred to 1 L of a sterile LB-medium containing ampicilin at the final concentration of 100 µg·mL⁻¹. During a leakage expression these flasks were incubated at 0.8 g and 37 °C for 3 hours for the initiation of proteosynthesis and then the bacterial culture was incubated overnight at 30 °C.

4.2.2 Expression of His-GB1-ASK1 fusion constructs

For crystallographic studies seven different constructs of ASK1-TBD with a cleavable His-tag were prepared using plasmid pRSFDuet-1 with a resistance to the antibiotic kanamycin. Constructs ASK1₈₈₋₃₀₂, ASK1₄₆₋₂₅₁, ASK1₄₆₋₂₆₇, ASK1₄₆₋₂₈₇, ASK1₈₈₋₂₅₁, ASK1₈₈₋₂₆₇ and ASK1₈₈₋₂₈₇ were created by inserting seven different sequences of a human N-terminal ASK1 into the pRSFDuet-1 vector using restriction sites *Pst*I and *Bam*HI. All these constructs contained a cleavage site for a TEV protease followed by 6×His-tag with attached GB1 protein, B1 domain of a streptococcal guanine nucleotide-binding G protein.

Attached GB1 protein significantly improves the stability and solubility of the fusion protein in solution, increasing the ability of concentration and the resulting yield during expression and purification. A cleavage site for TEV protease allows to simply remove 6×His-tag with GB1 by adding TEV protease to the fusion protein solution.

Construct ASK1₈₈₋₃₀₂ was prepared by my colleague Mgr. Kateřina Koláčková, constructs ASK1₄₆₋₂₅₁, ASK1₄₆₋₂₆₇, ASK1₄₆₋₂₈₇, ASK1₈₈₋₂₅₁, ASK1₈₈₋₂₆₇ and ASK1₈₈₋₂₈₇ were prepared by my colleague Kateřina Jarosilová.

The expression of ASK1₄₆₋₂₅₁, ASK1₄₆₋₂₆₇, ASK1₄₆₋₂₈₇, ASK1₈₈₋₂₅₁, ASK1₈₈₋₂₆₇, ASK1₈₈₋₂₈₇ and ASK1₈₈₋₃₀₂ started with the addition of 10 µL of a glycerol stock into the test-tube with 5 mL of sterile LB-medium containing the kanamycin with its final concentration of 30 µg·mL⁻¹, and these test-tubes were incubated at 0.8 g and 37 °C overnight.

Next, each test-tube was transferred to 1 L of a sterile LB-medium containing kanamycin at the final concentration of 30 µg·mL⁻¹. These flasks were than incubated at 0.8 g and 37 °C until the optical density (OD) reached the value of 0.8 at a wavelength of 600 nm. Subsequently, the temperature was reduced to 25 °C and the isopropyl β-D-1-thiogalactopyranoside (IPTG) inductor was introduced to the solution to its final concentration of 1 mmol·dm⁻³. The bacterial culture with initiated proteosynthesis was incubated overnight at 0.8 g and 20 °C.

4.2.3 Cell harvesting and sonication

Bacteria were harvested from the media using the 20 minutes at 2660 g and 4 °C centrifugation. Bacterial pellet was resuspended at 4 °C by vortexing with 50 mL of a lysis buffer (Tab. 4.3). 0.5 mL of a 100 mM stock solution of phenylmethylsulfonyl fluoride (PMSF) in ethanol at the final concentration of 1 mmol·dm⁻³ was added to the homogenized solution of a bacterial culture for the inhibition of serine proteases. The solution was then incubated with 5 mg of a lysozyme at a final concentration of 100 µg·mL⁻¹ with a constant stirring at 4 °C for 20 minutes.

After that, a sonication was performed at 4 °C, with a program: 3 sec. ON/17 sec. OFF, cumulative ON time: 15 minutes, power: 55 W. The solution was then centrifuged for 45 minutes at 19 400 g and 4 °C in order to separate a sonicate from the cells.

The protein was then present in the cytosolic fraction (intracellular fluid), and the protein modified this way was prepared for a purification.

Table 4.2. Luria-Bertani (LB) media

substance	amount
tryptone	10 g
yeast extract	5 g
NaCl	10 g
agar	15 g

Distilled water added to the volume of 1 liter.

Table 4.3. Lysis buffer

substance	amount	final concentration
PBS	10 mL 10× PBS (<i>Tab. 4.4</i>)	1×
NaCl	5.84 g	1 mol·dm ⁻³
β -Mercaptoethanol	27.8 μ L	4 mmol·dm ⁻³
imidazole	0.014 g	2 mmol·dm ⁻³

Distilled water added to the volume of 100 mL.

Table 4.4. 10× Phosphate-buffered saline (PBS) buffer

substance	amount
NaCl	80 g
KCl	2 g
KH ₂ PO ₄	2.4 g
Na ₂ HPO ₄ · 2H ₂ O	14.4 g
NaN ₃	0.4 g

Distilled water added to the volume of 1 liter.

pH adjusted to 7.4 with 10 M NaOH.

4.3 Purification of ASK1-TBD

The purification of proteins is a first step in understanding their function. Protein purification process consists of several steps designed to isolate a protein from a complex mixture of cells, at first separating the protein from the non-protein parts and then isolating the desired protein from all other proteins.

The purification process of ASK1₈₈₋₃₀₂C-His consisted of the nickel chelating chromatography (NCAC) and the size exclusion chromatography (SEC). The purification process of His-GB1-ASK1 fusion constructs consisted of the NCAC, TEV protease cleavage, 2nd NCAC for a removal of cleaved GB1 and a SEC performed the next day.

4.3.1 Nickel chelating chromatography of ASK1₈₈₋₃₀₂C-His

NCAC is a separation method belonging to the group of metal affinity chromatographies. It is based on the ability of formation of a stable reversible complex between the nickel (II) cations and a histidine. ASK1 contains histidine residues at one of its ends attached to the protein sequence as a polyhistidine-tag (6×His-tag). The column in this chromatography is filled with a slurry Chelating Sepharose Fast Flow with bound Ni²⁺ ions. This slurry selectively binds protein molecules containing His-tag, while other molecules and proteins without His-tag pass through the column without capturing. The ASK1 is then eluted with the imidazole, a molecule with an aromatic heterocycle presented in histidine, which binds to Ni²⁺ ions instead of histidine and therefore releasing the protein.

ASK1₈₈₋₃₀₂C-His expressed with a non-cleavable His-tag was purified using the batch form of NCAC. 1 mL of Chelating Sepharose Fast Flow (slurry) was incubated with 50 mL of a 0.1 M solution of Nickel (II) sulfate NiSO₄ for about 10 minutes and washed with 50 mL of distilled water.

Sonicated cells were poured to the Pyrex beaker and incubated with prepared slurry for 30 minutes at 4 °C under the constant stirring. The solution of cells with slurry was equally divided to the 50 mL Falcon conical centrifuge tubes and centrifuged at 430 g for 1 minute.

A supernatant was carefully discarded, a pellet was resuspended with 40 mL of a washing solution with a low concentration of imidazole (elution buffer diluted 1:9 in binding buffer, *Tab. 4.5*), to wash the proteins bound to slurry non-specifically or weakly and again centrifuged at 430 g for 1 minute. This process was repeated 10-12 times, total amount of a washing solution was 500 mL. Slurry with a protein solution was put back to the chromatography column and a protein was eluted at 4 °C with 5 mL of an elution buffer (*Tab. 4.5*) and collected into the tube containing 10 mL of a SEC buffer (*Tab. 4.6*).

To check the result of the expression and purification of ASK1₈₈₋₃₀₂C-His, collected fractions from the elution of protein were analyzed on sodium dodecyl sulfate polyacrylamide gel electrophoresis (SDS-PAGE) (*Chapter 4.7*). Prepared protein was then ready for a concentration and SEC (*Chapter 4.3.3*).

Table 4.5. Buffers for NCAC

Binding buffer

substance	amount	final concentration
PBS	50 mL 10× PBS (<i>Tab. 4.4</i>)	1×
NaCl	14.6 g	0.5 mol·dm ⁻³
β-Mercaptoethanol	70 μL	2 mmol·dm ⁻³
imidazole	0.035 g	1 mmol·dm ⁻³

Distilled water added to the volume of 500 mL.

Elution buffer

substance	amount	final concentration
PBS	50 mL 10× PBS (<i>Tab. 4.4</i>)	1×
NaCl	14.6 g	0.5 mol·dm ⁻³
β-Mercaptoethanol	70 μL	2 mmol·dm ⁻³
imidazole	20.4 g	0.6 mol·dm ⁻³

Distilled water added to the volume of 500 mL.

pH adjusted to 8.0 with concentrated HCl.

4.3.2 Nickel chelating chromatography of His-GB1-ASK1 fusion constructs

Constructs ASK1₄₆₋₂₅₁, ASK1₄₆₋₂₆₇, ASK1₄₆₋₂₈₇, ASK1₈₈₋₂₅₁, ASK1₈₈₋₂₆₇, ASK1₈₈₋₂₈₇ and ASK1₈₈₋₃₀₂ were expressed using pRSFDuet-1 with a cleavage site for a TEV protease. NCAC, TEV protease cleavage and the 2nd NCAC for a removal of cleaved GB1 was performed in the beginning of a His-GB1-ASK1 fusion constructs purification.

2 mL of a Chelating Sepharose Fast Flow (slurry) were incubated with 50 mL of a 0.1 M solution of NiSO₄ for 10 minutes and washed with 50 mL of distilled water and 50 mL of binding buffer (*Tab. 4.5*). Sonicated cells were poured to the column at 4 °C and the proteins bound to slurry non-specifically or weakly were washed away by 200 mL of a washing solution with a low concentration of imidazole (elution buffer diluted 1:9 in binding buffer, *Tab. 4.5*). The protein was eluted from the column at 4 °C with 10 mL of elution buffer (*Tab. 4.5*) and 1.5 mL-fractions were collected. To verify the result of the expression and purification of ASK1, samples from collected fractions were analyzed on SDS-PAGE (*Chapter 4.7*). Prepared ASK1 was in form of a fusion protein with a His-tag, GB1, and with a TEV cleavage site. After the first nickel chelating chromatography, a TEV protease was added to the ASK1 solution to remove the His-tag and GB1.

4.3.2.1 TEV protease cleavage of His-GB1-ASK1 fusion constructs

Tobacco Etch Virus (TEV) protease is an engineered catalytic domain of the Tobacco Etch Virus Nuclear-Inclusion-a endopeptidase. TEV protease is a 27 kDa sequence specific cysteine protease with a strict 7 amino acid cleavage recognition sequence of Glu-Asn-Leu-Tyr-Phe-Gln↓Gly, belonging to the C4 peptidase family. It was prepared in the Department of Protein Structure at the Institute of Physiology AS CR with a concentration of 1 mg·mL⁻¹ and a specific activity of 250 units per 1 mg of a protein (1 unit corresponds to 0.125 μL of TEV protease). After an overnight TEV cleavage, the fusion form of ASK1 construct was cleaved to GB1 with His-tag and ASK1 protein alone.

4.3.2.2 Removal of a cleaved GB1 protein

After a TEV cleavage and dialysis, ASK1 was in a solution with TEV protease and His-tagged GB1. To remove them, a second NCAC was performed.

0.5 mL of Chelating Sepharose Fast Flow (slurry) was incubated with 20 mL of a 0.1 M solution of NiSO₄ for about 10 minutes and washed with 20 mL of a distilled water and 20 mL of a dialysis buffer (*Tab. 4.7*). The protein solution after the dialysis and TEV cleavage was flowed through the column. TEV protease and GB1, both containing His-tag, were captured by nickel ions on the column and ASK1 was eluted alone. The protein solution was loaded on the column three times, for the complete capture of all TEV protease and GB1 protein.

4.3.3 Size exclusion chromatography

SEC is a method separating molecules according to their hydrodynamic volume. The chromatography column is filled with granular porous gel and molecules of dissolved substance are diffused into the pores of polymer matrix. Molecules with larger size than the size of pores are moving through the column smoothly and without any barriers, so they can be eluted first. However smaller molecules are withheld by a polymer matrix and therefore they migrate significantly slower through a column [34].

GE Healthcare Life Sciences HiLoad 26/60 Superdex 75 prep grade column, designed for preparative SEC, was used for a SEC of ASK1. Superdex is a composite matrix of dextran covalently bound to highly cross-linked agarose. The steep selectivity of dextran and the high chemical and physical stability of agarose set up separations with a high resolution. For Superdex 75 prep grade, the steep selectivity curves give unmatched resolution for biomolecules in the molecular weight range from 3 000 up to 70 000 Da. The chromatography media integrate excessive mechanical resistance with a strong hydrophilicity, enabling high flow rates and causing minimal non-specific interactions [35].

SEC buffer (*Tab. 4.6*) of ASK1 filtered with Nylon filter membranes with 0.45 µm pore size and 47 mm diameter (Whatman) was used for a SEC run. Before the measurement, the column was equilibrated with freshly prepared and filtered SEC buffer.

Table 4.6. SEC Buffer.

substance	amount	final concentration
Tris-HCl buffer pH=7.5	40 mL 1M Tris pH=7.5	20 mmol·dm ⁻³
NaCl	58.45 g	0.5 mol·dm ⁻³
EDTA	4 mL 0.5 M EDTA	1 mmol·dm ⁻³
dithiothreitol	1.54 g	5 mmol·dm ⁻³
glycerol	200 g	10 %

Distilled water added to the volume of 2 liters.

The protein solution of ASK1 was concentrated to 2 mL with Amicon Ultra (EMD Millipore, USA) concentrator with cut-off 10 kDa, in the Eppendorf centrifuge 5804R at 1320 g and 4 °C for 2 hours, wherein every two minutes was the sample in a concentrator carefully manually stirred. The protein sample was subsequently filtrated with SPARTAN syringe filter (Whatman), using regenerated cellulose with 0.45 µm pore size and 13 mm diameter and then injected into Watrex HPLC with connected column. Fractions corresponding to the ASK1 were collected and analyzed with SDS-PAGE.

4.4 Expression and purification of TRX

TRX was expressed in pET-15b plasmid with a resistance to the antibiotic ampicilin. The sequence encoding human thioredoxin-1 with a single mutation Cys⁷³ to Ser⁷³ was inserted between restriction sites *Nde*I and *Bam*HI in the pET-15b vector and a cleavage site for a TEV protease followed by 6×His-tag was added to the N-terminus. This expression construct was prepared by my colleague Kateřina Jarosilová.

Expression and purification of TRX was similar to the expression and purification of His-GB1-ASK1 fusion constructs. The purification process consisted of NCAC, TEV protease cleavage, 2nd NCAC for a removal of cleaved GB1 and a SEC performed the next day.

4.5 Protein concentration

The process of a protein concentration is very delicate and risky, as much as it can be a critical step in a protein preparation. A protein is concentrated in a concentrator with a semipermeable membrane, by slow and cautious centrifugation at low speed. During a concentration, despite its careful proceeding, a protein can often form aggregates. Protein aggregation is a process, where misfolded protein molecules or molecules with predominantly hydrophobic surfaces accumulate and clump together, usually because of the interaction between exposed hydrophobic parts.

Solutions of ASK1 and TRX were concentrated with Amicon Ultra (EMD Millipore, USA) concentrator with cut-off 10 kDa, in the Eppendorf centrifuge 5804R at 890-1320 g and 4 °C for several hours, wherein every two minutes was the sample manually stirred. A concentration was stopped, when a protein began to observably precipitate in solution, thus it was considered to be the maximum possible concentration for a given protein construct.

Presence, purity and approximate amount of the protein was controlled and analyzed by SDS-PAGE, the protein molar concentration c ($\text{mol}\cdot\text{dm}^{-3}$) in samples was determined by an absorbance measurement, using the Lambert-Beer equation (*Eq. 1*).

$$A = \varepsilon \cdot l \cdot c \quad (\text{Eq. 1})$$

where A is an absorbance, ε ($\text{dm}^3\cdot\text{mol}^{-1}\cdot\text{cm}^{-1}$) is a molar absorption coefficient and l (cm) is a length of the optical path of a cuvette. The absorbance of a protein sample is measured at a wavelength of 280 nm, where the absorption maximum of amino acids with aromatic ring structures is located, mainly tryptophan, tyrosine and cysteine.

The molar absorption coefficient of a protein was calculated from the primary protein sequence using ProtParam software at a website www.expasy.org., a solvent (buffer) was used as a blank (reference sample). The absorbance was measured at Implen NanoPhotometer P300.

4.6 Dialysis

Dialysis is a method separating individual substances by the size of their molecules. In the purification process, the protein solution is added to a semipermeable dialysis membrane with pores smaller size than the size of protein molecules. Protein remains captured inside the membrane that is located in the large volume of dialysis buffer (Tab. 4.7). However, molecules smaller than the size of membrane pores are compelled to spontaneous diffusion in the direction of a gradient of the electrochemical potential through the semipermeable membrane into the dialysis buffer and vice versa, until reaching the electrochemical equilibrium. After an overnight dialysis, the protein environment corresponds to the used dialysis buffer.

ASK1 was dialyzed at 4 °C in a semipermeable membrane Spectra/Por 2 from Carl Roth GmbH with cut-off 12-14 kDa pores. TRX was dialyzed at 4°C in a semipermeable membrane Spectra/Por 2 from Carl Roth GmbH with cut-off 6-8 kDa pores.

Table 4.7. Dialysis buffer

substance	amount	final concentration
Tris-HCl buffer pH=7.5	20 mL 1M Tris pH=7.5	20 mmol·dm ⁻³
NaCl	11.69 g	200 mmol·dm ⁻³
β -Mercaptoethanol	312 μ L	4 mmol·dm ⁻³
imidazole	5.78 g	85 mmol·dm ⁻³
glycerol	100 g	10 %

Distilled water added to the volume of 1 liter.

4.7 SDS electrophoresis

SDS-PAGE (Sodium dodecyl sulfate polyacrylamide gel electrophoresis) belongs to the electromigration separation analytical methods, the principle of which is based on the different migration speed of electrically charged particles in an electric field. The speed of molecule movement is directly proportional to the size of their charge and indirectly proportional to the size of their particles.

The polyacrylamide gel provides a gel filtration, directing and distributing the movement of different types of molecules according to their shape and size in the gel environment. Sodium dodecyl sulfate is able to generate a negative charge in proteins by causing their denaturation. Tertiary structure of proteins is dependent on the spatial arrangement of the polypeptide chain, which is changing in the presence of SDS molecules forming protein-SDS complex. Negatively charged molecule of SDS attached to the protein is affecting the protein charge, thereby similarly charged proteins are moving in the presence of the electric field at a similar speed and differs only their ability to move through the gel matrix [36]. The movement of large molecules is significantly restricted and withheld by gel pores, while small molecules can move relatively quickly between other particles.

The SDS-PAGE gel in a single electrophoresis run has two parts, a stacking gel and a separating gel. For a gel preparation was used fixed ratio of acrylamide/bis-acrylamide (*Tab. 4.8*). The percentage of acrylamide in a separating gel is selected depending on the size of the target protein in a sample, for our purposes was used 15% separating gel (with 15% acrylamide, *Tab. 4.8*), whose pore size allowed sufficient movement of ASK1 and TRX. The 5% stacking gel (with 5% acrylamide, *Tab. 4.8*) is after solidification of separating gel poured on the top of it and a gel comb is inserted in the stacking gel. The electrophoresis apparatus was filled with the SDS running buffer (*Tab. 4.9*), the voltage used for this technique was 200 V and a single electrophoresis run was completed after one hour.

SDS-PAGE analysis was used to visualize the protein status after each purification step. 10 μL of a protein sample were taken from specific fractions and mixed with 5 μL of a loading buffer (*Tab. 4.9*). The mixture was subsequently heated to 100 $^{\circ}\text{C}$, helping the denaturation and therefore simplifying the SDS-binding to a protein.

To identify the molecular weight of a protein, 5 μL of a solution of the molecular weight standards was loaded to the first lane, Precision Plus Protein Dual Color Standard containing segments with a relative molecular weight of $250 \cdot 10^3$, $150 \cdot 10^3$, $100 \cdot 10^3$, $75 \cdot 10^3$, $50 \cdot 10^3$, $37 \cdot 10^3$, $25 \cdot 10^3$, $20 \cdot 10^3$, $15 \cdot 10^3$ and $10 \cdot 10^3$ was used. Gels were then visualized by incubating with a staining solution containing Coomassie Brilliant Blue R 250 (*Tab. 4.9*) for 1 hour followed by an incubation in destaining solution (*Tab. 4.9*) for few hours.

Table 4.8. Stacking and separating buffers and gels.

Stock solution of acrylamide/bis-acrylamide

substance	amount
acrylamide	29.2 g
bis-acrylamide	0.8 g

Distilled water added to the volume of 100 mL.

Stacking buffer

substance	amount
0.5 M Tris-HCl pH=6.8	50 mL
10% SDS	4 mL

Distilled water added to the volume of 100 mL.

5 % stacking gel

substance	amount
distilled water	2.25 mL
stacking buffer	1 mL
acrylamide/bis-acrylamide	0.5 mL
10% (w/v) APS	75 μ L
TEMED	8 μ L

Separating buffer

substance	amount
1.5 M Tris-HCl pH=8.8	75 mL
10% SDS	4 mL

Distilled water added to the volume of 100 mL.

15 % separating gel

substance	amount
distilled water	1.75 mL
separating buffer	2 mL
acrylamide/bis-acrylamide	3.75 mL
10% (w/v) APS	75 μ L
TEMED	8 μ L

Table 4.9. Buffers for electrophoresis.

SDS-running buffer

substance	amount
Tris	3 g
SDS	1 g
glycine	14.4 g

Distilled water added to the volume of 1 liter.

Loading buffer

substance	amount
1M Tris-HCl pH=6.8	0.6 mL
10% SDS	2 mL
50% glycerol	5 mL
β -Mercaptoethanol	0.5 mL
1% Bromophenol blue	1 mL
distilled water	0.9 mL

Staining buffer

substance	amount
Coomassie Blue R-250	1 g
methanol	450 mL
concentrated acetic acid	100 mL
distilled water	450 mL

Destaining buffer

substance	amount
methanol	100 mL
concentrated acetic acid	100 mL
distilled water	800 mL

4.8 Native gel electrophoresis

Native gel electrophoresis is an electromigration method separating molecules by their electrophoretic mobility, which is directly proportional to the size of their charge and indirectly proportional to their particle size. Native electrophoresis is performed under non-denaturing conditions maintaining the protein's natural structure.

The mobility of proteins is influenced by the electrophoretic forces, depending on the actual physical size of the folded structure, and by the real intrinsic charge of an analyte (because there is no charged denaturing agent used).

This technique is used to verify the interaction between ASK1 and TRX. Prepared samples of ASK1 and TRX had the same amount of substance and contained 5 μL of a loading buffer (*Tab. 4.11*). A complex between ASK1-TBD and TRX was prepared in a molar ratio 1:1 and incubated for 30 minutes on ice. Samples were then loaded to a 15% gel (*Tab. 4.10*) and a native electrophoresis ran in the 1 \times TBE buffer (*Tab. 4.11*) at a constant voltage of 140 V and 4 $^{\circ}\text{C}$ for 5 hours.

Table 4.10. 15 % native gel.

substance	amount
distilled water	2.35 mL
10 \times TBE buffer (<i>Tab. 4.11</i>)	0.6 mL
acrylamide/bis-acrylamide	3 mL
10% (w/v) APS	45 μL
TEMED	4.8 μL

Table 4.11. Buffers for native electrophoresis.

10× Tris–Borate–EDTA (TBE) buffer

substance	amount
Tris	107.8 g
H ₃ BO ₃	55 g
Na ₂ –EDTA·2 H ₂ O	7.4 g

Distilled water added to the volume of 1 liter.

Loading buffer

substance	amount
10× TBE buffer	1 mL
glycerol	3 mL
Bromophenol blue	10 mg

Distilled water added to the volume of 10 mL.

4.9 Circular dichroism

Circular dichroism spectroscopy is an applied photophysical method utilizing the difference in absorbance of left-hand and right-hand circularly polarised components of plane polarised radiation (*Fig. 4.1*) [37]. An electromagnetic wave possesses the circular polarization, if the electric and magnetic field of a wave constantly rotate around the beam's x-y axis with non-changing intensity during the propagation. Plane polarised light rises from two circularly polarised radiation of equal magnitude, left-handed circularly polarized light rotating counter clockwise and right-handed circularly polarized light rotating clockwise [38], presenting two possible spin angular momentum positions for a photon. If left and right circular polarised light are not equally absorbed (they have different magnitude), they obtain different amplitude after passing through a sample and the resulting recombination would maintain an elliptical polarisation. The different magnitude of circular polarised light is present when a chromophore is chiral. A chromophore can be optically active because of its intrinsically chiral structure and its covalent link to another chiral center, or because it is situated in an asymmetric 3D-structure environment [38].

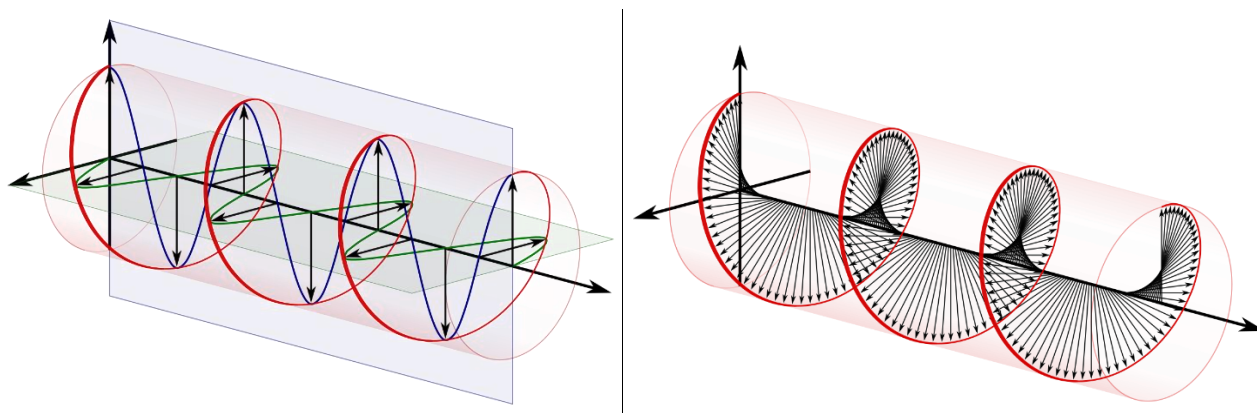


Figure 4.1. Circularly polarised light. The electric field (left) can be divided into horizontal (blue) and vertical (green) component with the right angle between them. The horizontal rightward part is by one quarter of a wavelength relatively ahead from the vertical part, forming quadrature phase connection. The region of horizontal maximum magnitude corresponds to the region of vertical zero magnitude generating a helix alignment (right). Adapted from http://en.wikipedia.org/wiki/Circular_polarization.

The circular dichroism spectra are measured as a function of wavelength. A spectropolarimeter measures the differential absorption ΔA between left L and right R circularly polarised components (Eq. 2) converted to the terms of an ellipticity θ in degrees (Eq. 3, Eq. 4) with a and b as the minor and major axes of the resulting ellipse.

$$\Delta A = A_L - A_R \quad (\text{Eq. 2})$$

$$\theta = \tan^{-1} \frac{b}{a} \quad (\text{Eq. 3})$$

$$\theta = 32.98 \cdot \Delta A \quad (\text{Eq. 4})$$

Many biological molecules are optically active, including proteins. CD spectroscopy is used in protein structural studies analyzing the characteristic structural signatures of conformational protein motifs [39]. The far ultraviolet (far-UV) CD spectrum (190 nm – 250 nm) define and characterize the secondary protein structure, the near-UV CD spectrum (>250 nm) maintains information about the tertiary protein structure [40][41].

The protein chromophores examined by CD spectroscopy cover peptide bonds with the absorption below 240 nm, aromatic amino acid side chains with the absorption range from 260 nm to 320 nm and weak broad absorption of disulfide bonds around 260 nm [42].

The far-UV CD provides characteristic structural signatures for many common protein conformational motifs, such as the α -helix, the β -pleated sheet, the β -turn and random coil conformation (Fig. 4.2). The wavelength 190 nm - 250 nm is the region corresponding to $n \rightarrow \pi^*$ and $\pi \rightarrow \pi^*$ transitions of amide groups, influenced by the geometry of the polypeptide backbone [41].

The deconvolution of CD spectra using K2D method [43] is used to estimate the percentage of a secondary structure content. The far-UV CD is unable to predict neither location of concrete conformational motifs, therefore it is mostly used to investigate changes in a conformation as a function of temperature, of the concentration of ligands and denaturing agents, or upon the complex formation.

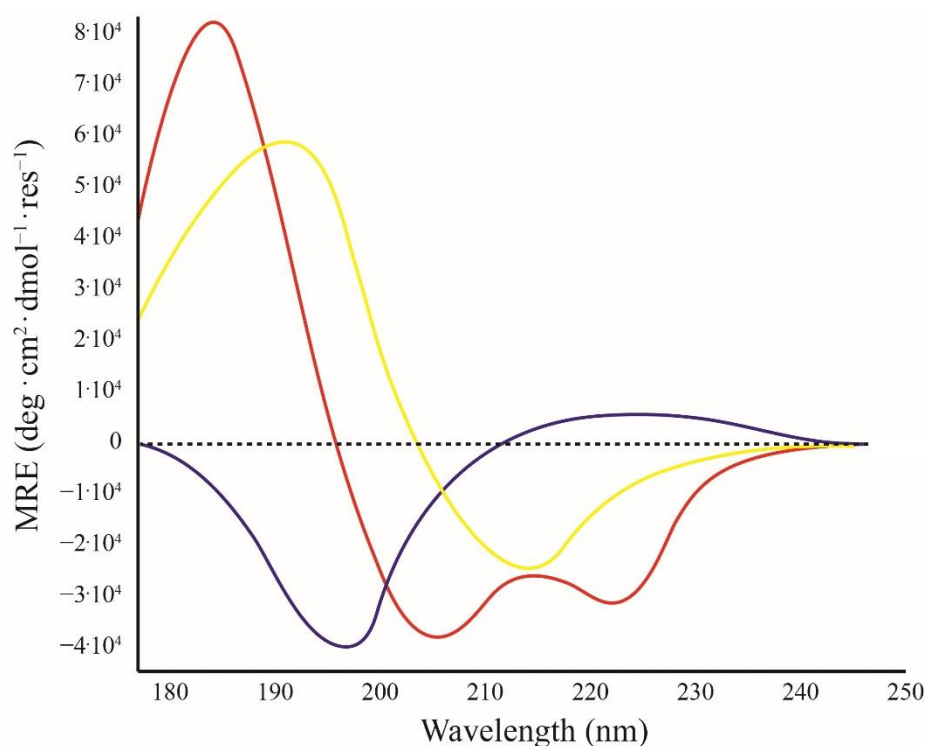


Figure 4.2. Far-UV CD spectrum of poly-L-lysine. The absorption spectrum of the α -helix (red) form, the β -sheet (yellow) form and the intrinsically disordered random coil (blue) form of poly-L-lysine. Y-scale shows Mean Residue Ellipticity (MRE) corresponding to the molar ellipticity of the protein divided by the number of monomer units or residues in the protein molecule. Adapted from <http://www.proteinchemist.com/cd/cdspec.html>.

The near-UV spectra provide information about aromatic side chains of proteins, often present in segments affected by conformational changes. The wavelength 250 nm - 300 nm corresponds to the region of an absorption and dipole orientation of the amino acids phenylalanine, tyrosine, tryptophan, cysteine (S-S disulfide bridges) [40]. The near UV absorption is weaker than the far UV, therefore it is necessary to increase the amount of sample during the measurement. Unlike far-UV CD, analysis of the near-UV spectrum cannot provide a substitution to any particular 3D structure. However, the change in environment of an aromatic side chain contribute significantly to the absorbance spectra in near-UV CD, promising higher probability of a detection than within a far-UV range.

The distinctive vibronic fine structure in the near-UV spectra appears because of the vibronic transitions between different vibrational levels of an excited state and can access individual residues information and provide a characteristic wavelength profile [42]. Phe is characterized by weaker but sharper fine structure peaks between 255 and 270 nm, Tyr is characterized by a peak between 275 and 282 nm and Trp is characterized by a fine-structure peak between 290 and 305 nm. The substantial form and structure of a protein near-UV CD spectrum is affected by (a) the number of concrete type of aromatic amino acid in the protein side chain, (b) by their mobility, (c) by a character of their environment, presence of H-bonding and polar groups, and (d) by their spatial disposition in the protein side chain [42].

The CD spectra were measured in a quartz cuvette from Starna, USA with an optical path length of 1 mm for the far-UV and 1 cm for the near-UV measurements using a J-810 spectropolarimeter from Jasco, Japan at the University of Chemistry and Technology in Prague, in collaboration with Ing. Pavlína Novotná.. A spectral region of 200-260 nm was used for the far-UV CD measurements and for the near-UV CD measurements was used a spectral region of 250 - 320 nm. Conditions of the measurements were set to a scanning speed of 10 nm·min⁻¹, a response time of 8 seconds, a bandwidth of 1 nm, a resolution of 1 nm and a sensitivity of 100 mdeg. The CD measurements were conducted at 22 °C, the far-UV CD spectrum was obtained as an average of 5 accumulations, and the near-UV CD spectrum was obtained as an average of 15 accumulations. A baseline in the spectra was corrected by subtracting the spectra of the corresponding buffer (*Tab. 4.12*) without protein.

Table 4.12. Buffer for CD measurements.

substance	amount	final concentration
Tris-HCl buffer pH=7.5	20 mL 1M Tris pH=7.5	20 mmol·dm ⁻³
NaCl	11.7 g	200 mmol·dm ⁻³
β -Mercaptoethanol	156 μ L	2 mmol·dm ⁻³

Distilled water added to the volume of 1 liter.

After baseline correction, the final spectra were expressed as a mean residue ellipticity MRE (deg·cm²·dmol⁻¹·res⁻¹) calculated using equation 5,

$$\text{MRE} = \frac{\theta_{\text{obs}} \cdot M_w}{c \cdot l \cdot N_R \cdot 10} \quad (\text{Eq. 5})$$

where θ_{obs} is the observed ellipticity in mdeg, M_w is the protein molecular weight, c is the protein concentration in mg·ml⁻¹, l is the path length in cm, and N_R is the number of amino acids in the protein [44].

4.10 Dynamic light scattering

Dynamic light scattering (DLS) is a physical method studying the properties of inhomogeneous and vigorous media used to determine the hydrodynamic radius and diffusion coefficient of particles dispersed in the solution. In protein physics DLS is used to investigate an aggregation behavior, to study the polydispersity and to observe the stability of a purified protein sample [34].

A light wave transition through a solution causes the oscillation of dipole moments acting as a source of a scattered light radiation. In liquids the light scattering possesses different intensity in different sections of the sample, the strongest scattering is caused by colloidal particles with the different refractive index than has the solvent. The intensity of the radiation scattering depends on the scattering vector s (Eq. 6),

$$s = \frac{4\pi n_0}{\lambda} \sin \frac{\theta}{2} \quad (\text{Eq. 6})$$

where λ represents the radiation wavelength, n_0 is the refractive index of a solvent and θ is the scattering angle between the direction of primary and scattered beam [34].

If particles have negligibly small size compared to the wavelength of used radiation, the intensity of a radiation scattering I is independent of s . If the particles are larger than $\lambda/20$, I is directionally dependent of s due to the interference of light waves scattered from different sections in a particle [34].

The progress of an $I(s)$ function is given by the size and shape of the scattering particles with an applicable Guinier approximate equation (Eq. 7),

$$I(s) \cong I(0) \left(1 - \frac{1}{3} R_g^2 s^2\right) \quad (\text{Eq. 7})$$

where R_g is a radius of gyration (the square root of the average squared distance of each scattering spot from the center of a particle) and $I(0)$ is the intensity extrapolated to the zero angle (Eq. 8).

$$\frac{I \sin \theta}{I(0)} = 1 - \frac{1}{3} R_g^2 s^2 \quad (\text{Eq. 8})$$

Instantaneous time value of the radiation scattering intensity $i(t,s)$ randomly fluctuates near the time average of $I(s)$, caused by the concentration, density and temperature fluctuations. The dynamic change of the temporal fluctuations is characterized by the first-order temporal autocorrelation function $g(\tau,s)$, τ corresponds to a lag time (Eq. 9) [34].

$$g(\tau, s) = \lim_{T \rightarrow \infty} \frac{1}{T} \int_0^T i(t, s) i(t + \tau, s) dt \quad (\text{Eq. 9})$$

In the simplest case the fluctuations are caused by a translational diffusion of the monodisperse spherical particles with a diffusion coefficient D (Eq. 10),

$$g(\tau, s) = A [1 + \beta e^{-2Ds^2\tau}] \quad (\text{Eq. 10})$$

where A is the distribution function of relaxation times, β is a coherence factor depending on the geometry of the experimental setup (theoretically $\beta = 1$).

Measured scattered light intensities $I(t)$ as a function of time t were defined and evaluated by the second-order temporal autocorrelation function $g^{(2)}(\tau)$ (Eq. 11).

$$g^{(2)}(\tau) = \frac{\langle I(t)I(t + \tau) \rangle}{\langle I(t) \rangle^2} \quad (\text{Eq. 11})$$

A relation between the first-order and second-order autocorrelation function reflect the equation 12 [45].

$$g^{(2)}(\tau) = 1 + \beta \left[\int_0^{\infty} A(\tau_r) e^{-\frac{\tau}{\tau_r}} d\tau_r \right] \quad (\text{Eq. 12})$$

where τ_r is the relaxation time. The inverse Laplace transform with a constrained regularization algorithm CONTIN was used for a fitting of measured data.

The mean relaxation time of diffusive modes in the CONTIN distribution provide the hydrodynamic radii of the protein molecules (Eq. 13) [45],

$$R_H = \frac{8\pi n_0^2 kT}{3\eta_0 \lambda^2} \sin^2\left(\frac{\theta}{2}\right) \langle \tau_r \rangle \quad (\text{Eq. 13})$$

where k is the Boltzmann constant, T is the temperature and η_0 is the solvent viscosity. R_H is the radius of a corresponding sphere that diffuses at the identical rate as the molecule of interest [34].

ASK1₄₆₋₂₆₇ construct dialyzed to the buffer for a DLS measurement (Tab. 4.13) was selected for a DLS measurement of ASK1. The purpose of this experiment was to determine the presence of aggregates in a sample concentrated to the maximal possible concentration of 3.4 mg·mL⁻¹. For DLS measurements were used: 22 mW He-Ne laser operating at the wavelength of 632.8 nm, ALV CGS/8F goniometer, ALV High QE APD detector, and ALV/LSE-5004 Light Scattering Electronics and Multiple Tau Digital Correlator, in a cooperation with doc. RNDr. Miroslav Štěpánek, Ph.D. at the Department of Physical & Macromolecular Chemistry, Faculty of Science, Charles University in Prague [45].

Table 4.13. Buffer for a DLS measurement.

substance	amount	final concentration
Tris-HCl buffer pH=7.5	20 mL 1M Tris pH=7.5	10 mmol·dm ⁻³
NaCl	11.7 g	100 mmol·dm ⁻³
dithiothreitol	1.08 g	5 mmol·dm ⁻³

Distilled water added to the volume of 2 liters.

4.11 Small angle X-ray scattering

Small-angle X-ray scattering is an established physical method for the low resolution structure determination of biological macromolecules in a solution [46]. High resolution protein structure can be determined by three different techniques: X-ray crystallography, nuclear magnetic resonance (NMR) and cryo-electron microscopy (cryo-EM). The outcome from scattering curves reveals considerably less structural information than can be obtained from crystallography, however SAXS experiments (a) can be accomplished much more promptly, (b) they request simpler sample preparation and cheaper material, (c) they can determine shape and conformation in solution for any proportion of bio-macromolecular system, avoiding the limiting boundaries of NMR and EM methods and (d) SAXS can provide more accurate model of bio-macromolecule by investigating systems in their native environment maintaining substantial flexibility [47].

SAXS data provide a platform for calculating and defining several parameters, such as radius of gyration R_g (Eq. 7, 16); distance distribution function $P(r)$ (Eq. 15); maximum particle dimension D_{\max} ; particle volume V ; intensity $I(0)$ proportional to mass and volume (Eq. 17); molar mass M (Eq. 18).

SAXS uses a scattering signal developed from the difference in electron density ρ of a sample protein solution and a buffer (blank). After the subtraction of the buffer from the protein sample, the scattering curve is radially symmetric caused by the incoherent orientations of particles in a solution. The scattering curve of a homogeneous protein sample is determined by the electron distribution of the particle:

$$I(s) = 4\pi \int_0^{D_{\max}} P(r) \frac{\sin(s \cdot r)}{s \cdot r} dr \quad (\text{Eq. 14})$$

where s represents a scattering vector [48]. The distance distribution function $P(r)$ (Eq. 15) is an autocorrelation function calculated by indirect Fourier transformation of the scattering data to avoid problems with ill-posed Fourier transform of noisy data, particularly problems with the discrete examining of the $I(s)$ over a finite scale [49].

$$P(r) = \frac{r}{2\pi^2} \int_0^{\infty} I(s) \cdot s \cdot \sin(s \cdot r) ds \quad (\text{Eq. 15})$$

The $P(r)$ function is radially averaged, resulting to the determination of the distances between electrons in the sample. $P(r)$ function is zero at $r = 0$ and $r \geq D_{\max}$, where D_{\max} corresponds to the maximum co-axial length. The $P(r)$ function also provide another definition of R_g (Eq. 16).

$$R_g^2 = \frac{\int_0^{D_{\max}} r^2 P(r) dr}{\int_0^{D_{\max}} P(r) dr} \quad (\text{Eq. 16})$$

$I(0)$ is proportional to the molar mass and volume (Eq. 17), evolving independently on the shape of a molecule and depending only on the square of the number of electrons in the particle, what allows to determine molecular weight.

$$I(0) = 4\pi \left(\int_0^{D_{\max}} P(r) dr \right) \quad (\text{Eq. 17})$$

Normalized $I(0)$ provides information about the molar mass M of a molecule (Eq. 18).

$$M = \frac{I(0)\mu^2}{N_A \left(1 - \frac{\rho_s}{\rho_p}\right)^2} \quad (\text{Eq. 18})$$

Where the μ is an average mass per number of electrons N_A is Avogadro's number, ρ_s is a solvent and ρ_p is a particle electron density [47].

SAXS data were collected on the European Molecular Biology Laboratory (EMBL) P12 beamline on the storage ring PETRA III (Deutsches Elektronen Synchrotron (DESY), in Hamburg, Germany). Data were processed and analyzed by prof. Obšil.

Sample preparation for SAXS involved a special care of proteins considering the high sensitivity of this method to aggregates and polydispersity in protein solutions. SAXS was measured in a dilution series of ASK1₈₈₋₃₀₂C-His with a concentration of 4.6 mg·mL⁻¹, 2.3 mg·mL⁻¹ and 1.2 mg·mL⁻¹; TRX with a concentration of 12 mg·mL⁻¹, 6 mg·mL⁻¹, 3 mg·mL⁻¹ and 1.4 mg·mL⁻¹ and ASK1₈₈₋₃₀₂C-His:TRX complex with a concentration of 11.9 mg·mL⁻¹, 6 mg·mL⁻¹, 3 mg·mL⁻¹ and 1.5 mg·mL⁻¹. The distinctive protection of proteins against aggregates generation consisted of a very cautious concentrating, constant temperature of 4° C during the whole sample preparation, careful pipetting and filtering of protein samples and avoiding of a trembling that can also cause a production of aggregates.

5 RESULTS

5.1 Expression and purification of ASK1₈₈₋₃₀₂C-His

The isolation of the desired protein from a complex mixture of *E. coli* cells is an essential first step in protein preparation. Expression and purification of ASK1₈₈₋₃₀₂C-His for biophysical and structural studies were attributed as the main goals of this diploma thesis. This construct was a result of previous work in our laboratory, the protein sequence was chosen based on a secondary structure prediction (*Supplement 2*) and a location of TRX binding domain.

The expression of ASK1₈₈₋₃₀₂C-His was performed from 6 L of LB-media. The purification process consisted of a nickel chelating chromatography (NCAC) and size exclusion chromatography (SEC). The result of each purification step was verified by SDS-PAGE.

5.1.1 Nickel chelating chromatography

ASK1₈₈₋₃₀₂C-His was purified using the batch form of NCAC. A column contained 1 mL of Chelating Sepharose Fast Flow and it was placed at a temperature of 4 °C. Eluted protein was collected into the tube containing 10 mL of a SEC buffer. Samples of 10 µL were taken approximately every 2 mL from the eluted protein and analyzed by SDS-PAGE (*Fig. 5.1*). Electrophoresis showed that the proteins possessed expected molecular weights and a reasonable purity. Next, diluted protein solution was slowly concentrated to a final volume of 2 mL (corresponding to the recommended injected volume for the used column) and filtered with the nylon filter membranes of a 0.45 µm pore size and 47 mm diameter.

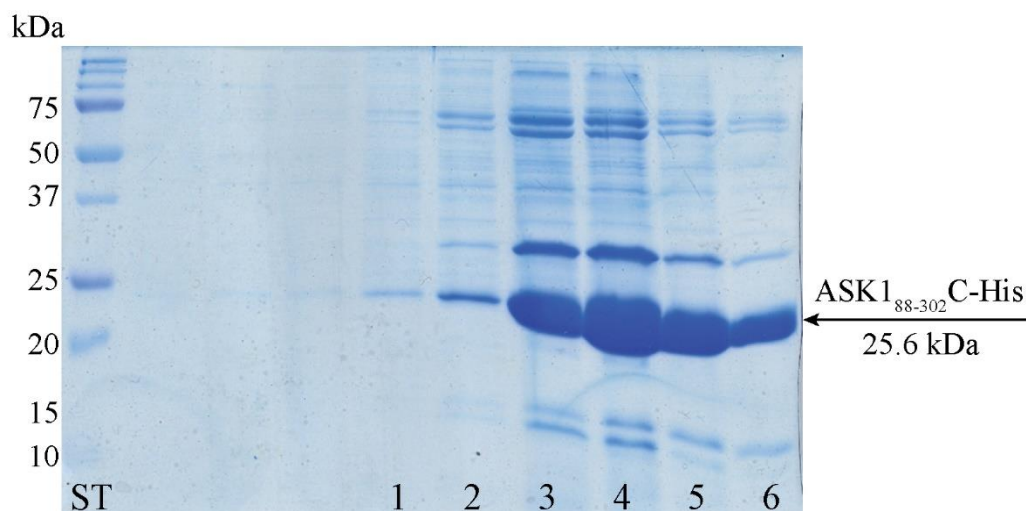


Figure 5.1. 15% SDS-PAGE gel after NCAC of ASK1₈₈₋₃₀₂C-His. Samples of 10 μ L were taken approximately every 2 mL from the eluted protein and mixed with 5 μ L of a loading buffer. 5 μ L of a protein M_w standard (ST) was loaded to the first lane.

5.1.2 Size exclusion chromatography

GE Healthcare Life Sciences HiLoad 26/60 Superdex 75 prep grade column with 330 mL volume and 2.5 mL/min flow was used for a SEC of ASK1₈₈₋₃₀₂C-His. The volume of each fraction was 1.5 mL and 40 fractions were collected to Eppendorf microtubes. A spectrophotometric detector was set to a wavelength of 280 nm and the chromatogram showing the elution profile was recorded (*Fig. 5.2*). Time (and volume, with 2.5 mL/min flow) of collection was chosen to respond to particular molecular weight of an eluted protein according to a column calibration. SDS-PAGE pointed out fractions with ASK1 of sufficient purity and concentration (*Fig. 5.3*). ASK1₈₈₋₃₀₂C-His was expressed from 6 L of LB-media.

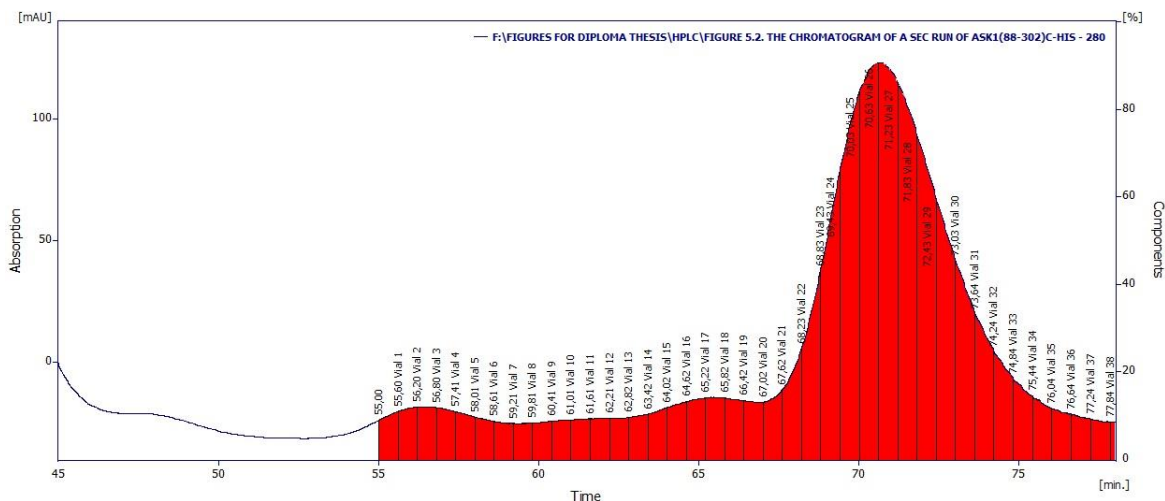


Figure 5.2. The chromatogram of a SEC run of ASK1₈₈₋₃₀₂C-His. The absorption in milliabsorbance units (mAU) is plotted against the time of elution in minutes. Blue line represents absorption signal at a wavelength of 280 nm, red color defines collected fractions with the number of vials. Fractions 22-24, 26, 27, 30-33 were analyzed by SDS-PAGE (Fig. 5.3).

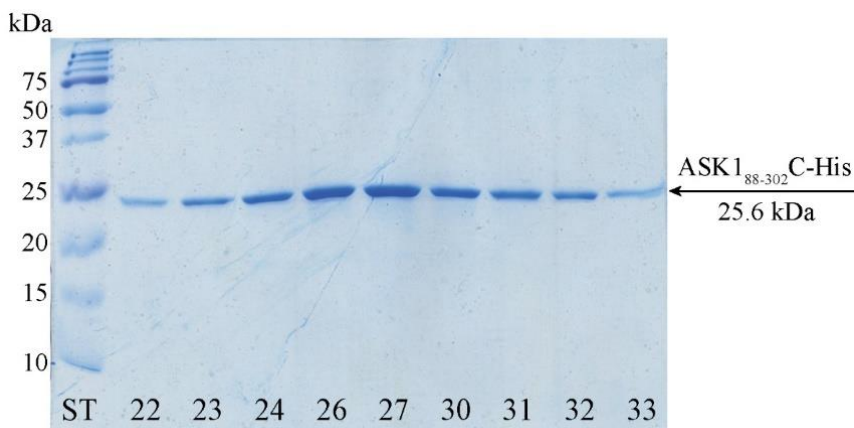


Figure 5.3. 15% SDS-PAGE gel of selected fractions from SEC. A sample of 10 μL was taken from fractions number 22-24, 26, 27, 30-33 and mixed with 5 μL of a loading buffer. 5 μL of a protein M_w standard (ST) was loaded to the first lane. Fractions 23-32 were merged together and the protein was prepared to biophysical studies.

$$M_w (\text{ASK1}_{88-302}\text{C-His}) = 25.6 \text{ kDa}, c (\text{ASK1}_{88-302}\text{C-His}) = 15.6 \mu\text{M} = 0.4 \text{ mg} \cdot \text{mL}^{-1}$$

$$m (\text{ASK1}_{88-302}\text{C-His}) \text{ after SEC} = 6 \text{ mg}$$

Final yield of ASK1₈₈₋₃₀₂C-His from 1 L of LB-media was 1 mg of a pure protein.

5.2 Expression and purification of TRX

Expression and purification of TRX as a binding partner for ASK1 was attributed as the next goals of this diploma thesis. TRX was expressed and purified as a fusion protein with the N-terminal His-tag and a TEV cleavage site.

The expression of TRX was from 3 L of LB-media. The purification process consisted of the NCAC with an overnight dialysis cleaving the construct with a TEV protease and a SEC performed the next day. The result of each purification step was verified by SDS-PAGE.

5.2.1 Nickel chelating chromatography

NCAC column contained 2 mL of Chelating Sepharose Fast Flow and it was placed at a temperature of 4° C. Eluted protein was collected to microtubes, separating several fractions of a 1.5 mL volume. The SDS-PAGE analysis revealed that the expression yield and solubility of TRX is, as expected, very high (*Fig. 5.4*).

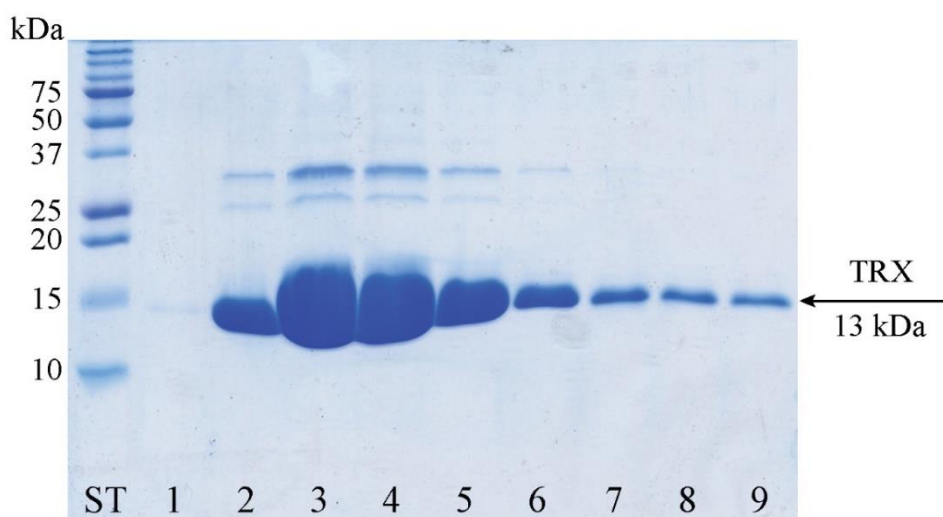


Figure 5.4. 15% SDS-PAGE gel after NCAC of TRX. A sample of 10 μ L was taken from NCAC fractions 1-9 and mixed with 5 μ L of a loading buffer. 5 μ L of a protein M_w standard (ST) was loaded to the first lane. Fractions 2-6 was mixed together and dialyzed with a TEV protease.

5.2.2 TEV protease cleavage

TEV protease used in the following experiment had a specific activity of 250 units per 1 mg of a protein (1 unit corresponds to 0.125 μL of TEV). The approximate concentration after NCAC was determined spectrophotometrically by an absorbance measurement at a wavelength of 280 nm, with the elution buffer (*Tab. 4.5*) as a blank. 10 μL of a 5-times diluted sample was taken after an overnight dialysis with TEV and analyzed by SDS-PAGE. Electrophoresis showed the result of His-tagged TRX cleavage (*Fig. 5.5*). An overnight incubation with a TEV protease was not sufficient enough for a complete cleavage of fusion protein, however the amount of uncleaved protein was relatively low.

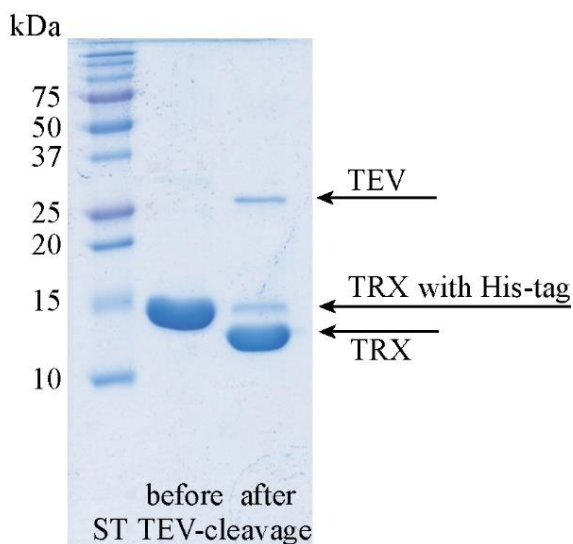


Figure 5.5. 15% SDS-PAGE gel before and after TEV cleavage of TRX.

10 μL of a 5-times diluted sample was taken from a protein before and after TEV cleavage and mixed with 5 μL of a loading buffer. 5 μL of a protein M_w standard (ST) was loaded to the first lane.

$$M_w (\text{TRX with His-tag}) = 13 \text{ kDa}$$

$$M_w (\text{TRX}) = 12.4 \text{ kDa}$$

$$M_w (\text{TEV}) = 27.5 \text{ kDa}$$

5.2.3 Size exclusion chromatography

For a SEC of TRX was used GE Healthcare Life Sciences HiLoad 26/60 Superdex 75 prep grade column with 330 mL volume and 2.5 mL/min flow. The volume of each fraction was 1.5 mL and 40 fractions were collected to Eppendorf microtubes. A spectrophotometric detector was set to a wavelength of 280 nm and the elution profile was recorded into the chromatogram (Fig. 5.6). Time (and volume, with 2.5 mL/min flow) of collection was chosen to respond to particular molecular weight of an eluted protein according to a column calibration. SDS-PAGE revealed that fractions from the beginning of elution profile contain uncleaved fusion protein, therefore only fractions 21-33 were merged together and used for further studies (Fig. 5.7).

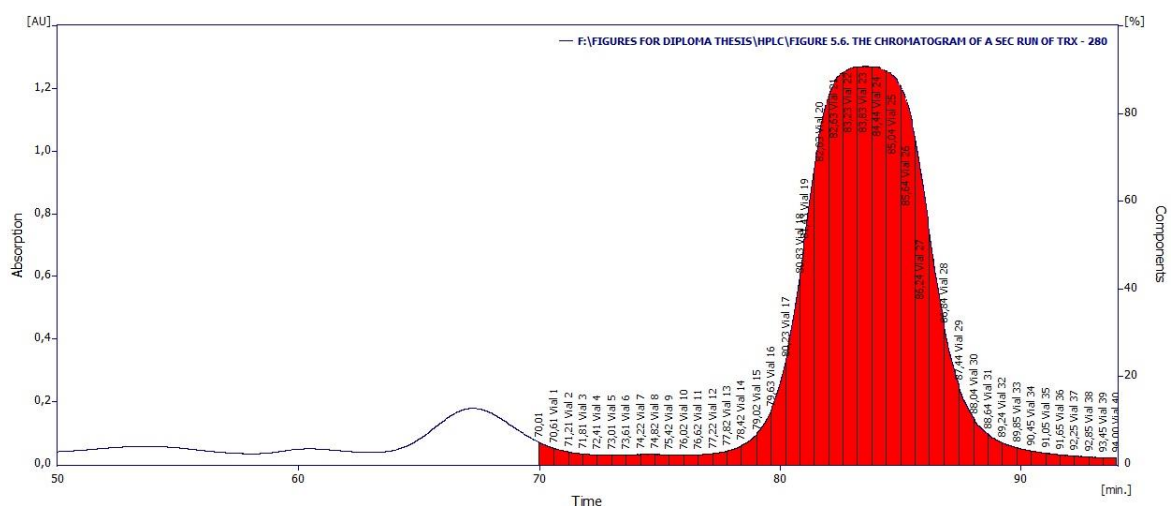


Figure 5.6. The chromatogram of a SEC run of TRX. The absorption in absorbance units AU is plotted against the time of elution in minutes. Blue line represents absorption signal at a wavelength of 280 nm, red color defines collected fractions with the number of vials. Fractions 16-18, 23, 27, 29-32 were analyzed by SDS-PAGE (Fig. 5.7)

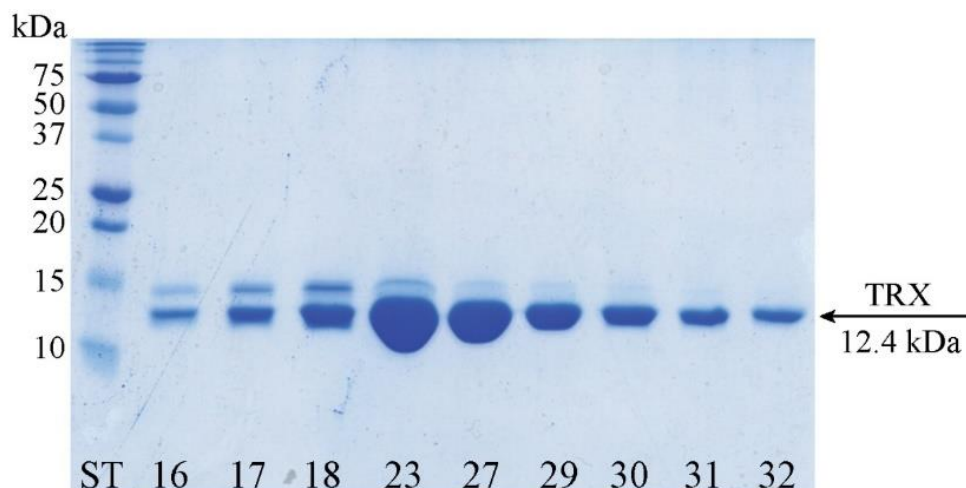


Figure 5.7. 15% SDS-PAGE gel of selected fractions from SEC. 10 μL of a 5-times diluted sample was taken from fractions number 16-18, 23, 27, 29-32 and mixed with 5 μL of a loading buffer. 5 μL of a protein M_w standard (ST) was loaded to the first lane. SDS-PAGE revealed the presence of an uncleaved fusion TRX, fractions 21-33 were merged together.

$$M_w (\text{TRX}) = 12.4 \text{ kDa}, c (\text{TRX}) = 196 \mu\text{M} = 2.55 \text{ mg} \cdot \text{mL}^{-1}$$

$$m (\text{TRX}) \text{ after SEC} = 46 \text{ mg}$$

Final yield of TRX from 1 L of LB-media was 15.3 mg of pure protein.

5.3 Circular dichroism

CD spectroscopy was used to determine the structural changes in ASK1 upon the complex formation. The far-UV CD provides characteristic structural signatures for many common protein conformational motifs, revealing information on the secondary structure. The near-UV CD provides information on the tertiary structure. The CD spectra were measured by a J-810 spectropolarimeter from Jasco, Japan at the University of Chemistry and Technology in Prague, in collaboration with Ing. Pavlína Novotná. The deconvolution of CD spectra using K2D method [43] revealed an approximate secondary structure containing $\sim 35\%$ of α -, $\sim 20\%$ of β - and $\sim 45\%$ of random structure.

ASK1₈₈₋₃₀₂C-His and TRX with a concentration of 8 μM was used for far-UV spectra, ASK1₈₈₋₃₀₂C-His and TRX with a concentration of 26 μM was used for near-UV spectra. CD measurements were performed at 22 $^{\circ}\text{C}$, the final far-UV CD spectrum (Fig. 5.8) included an average of 5 accumulations, and the final near-UV CD spectrum (Fig. 5.9) included an average of 15 accumulations. A baseline in the spectra was corrected by subtracting the spectra of the corresponding buffer without protein.

The far-UV CD spectrum of the ASK1₈₈₋₃₀₂C-His:TRX complex (with 1:1 molar stoichiometry) showed no significant difference when compared with the sum of the individual CD spectra of ASK1₈₈₋₃₀₂C-His and TRX. This suggested that the interaction between ASK1 and TRX does not induce any considerable structural changes in the overall secondary structure.

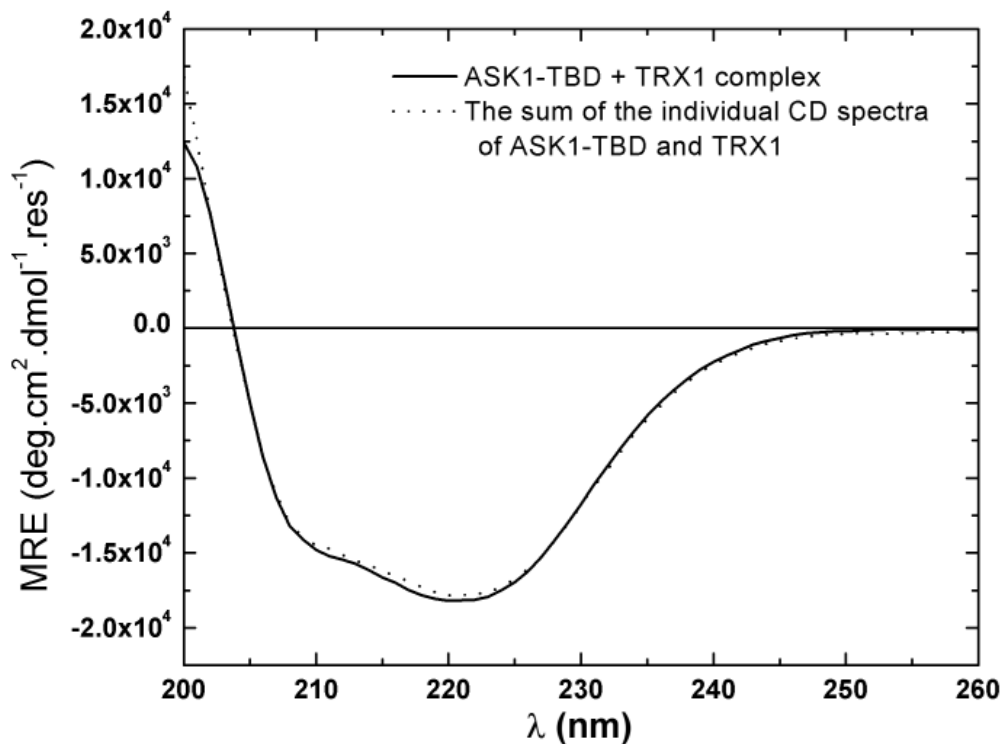


Figure 5.8. Far-UV CD spectrum. The comparison of the far-UV CD spectrum of the ASK1₈₈₋₃₀₂C-His:TRX complex (solid line) with the sum of the individual far-UV CD spectra of ASK1₈₈₋₃₀₂C-His and TRX (dotted line), with the 1:1 molar stoichiometry and the 8 μM concentration. The mean residue ellipticity (MRE) is plotted as a function of the wavelength λ . Spectrum revealed no significant change in a secondary structure of ASK1₈₈₋₃₀₂C-His upon the complex formation.

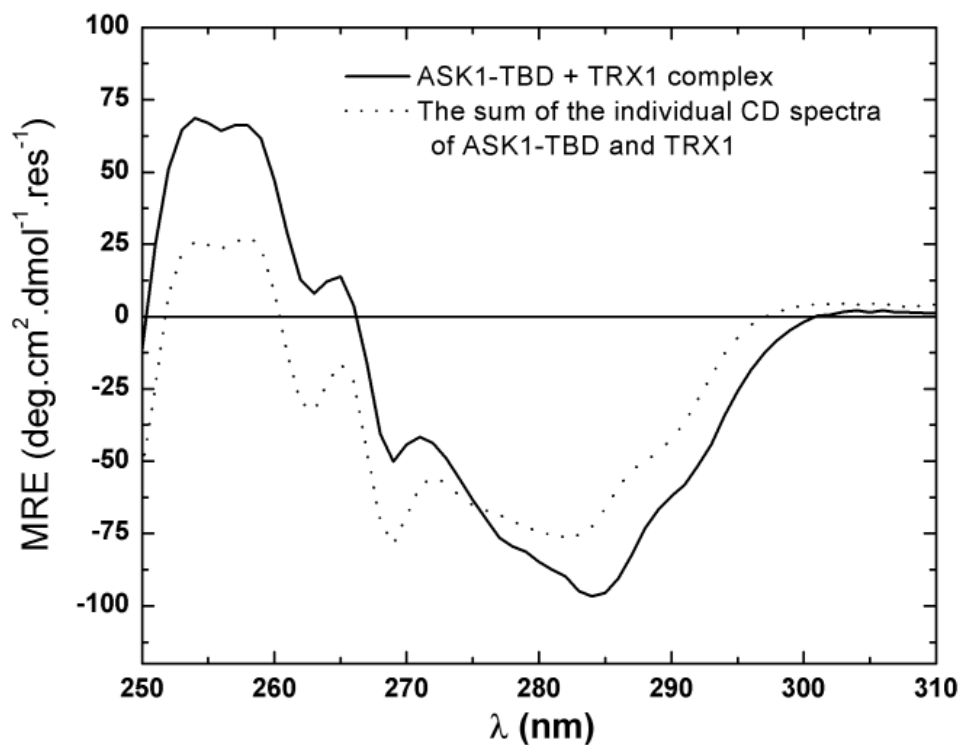


Figure 5.9. Near-UV CD spectrum. The comparison of the near-UV CD spectrum of the ASK1₈₈₋₃₀₂C-His:TRX complex (solid line) with the sum of the individual near-UV CD spectra of ASK1₈₈₋₃₀₂C-His and TRX (dotted line), with the 1:1 molar stoichiometry and the 26 μ M concentration. The mean residue ellipticity (MRE) is plotted as a function of the wavelength λ . The significant differences occurred only in the region from 275 to 295 nm.

Near-UV CD spectra revealed significant differences only in the region from 275 to 295 nm. This suggested the change in a conformation and/or environment of a tryptophan residue, considering a fine-structure peak of a Trp around 290 nm. Since the Trp³¹ is the only tryptophan residue in the active site of an ASK1-TBD:TRX complex, it is likely that observed differences mainly reflected a structural change in the vicinity of TRX Trp³¹ and that this tryptophan is directly involved in the ASK1-TRX interaction.

5.4 Small angle X-ray scattering

One of the goals of this diploma thesis was to prepare samples for SAXS measurements. SAXS can specify and determine the shape and dimension of a protein solution and it was used to acquire the visual insight into the structure of ASK1₈₈₋₃₀₂C-His and its complex with TRX. SAXS data were collected on the European Molecular Biology Laboratory (EMBL) P12 beamline on the storage ring PETRA III (Deutsches Elektronen Synchrotron (DESY), Hamburg, Germany).

The ASK1₈₈₋₃₀₂C-His protein solution was prepared with a concentration range of 1.2 - 4.6 mg·mL⁻¹, the TRX protein solution was prepared with a concentration range of 1.4 - 12 mg·mL⁻¹ and the ASK1₈₈₋₃₀₂C-His:TRX complex solution was prepared with a concentration range of 1.5 - 11.9 mg·mL⁻¹. The experimental data from SAXS measurements were plotted as a dependence of scattering intensity $I(s)$ on the scattering vector s (Fig. 5.10).

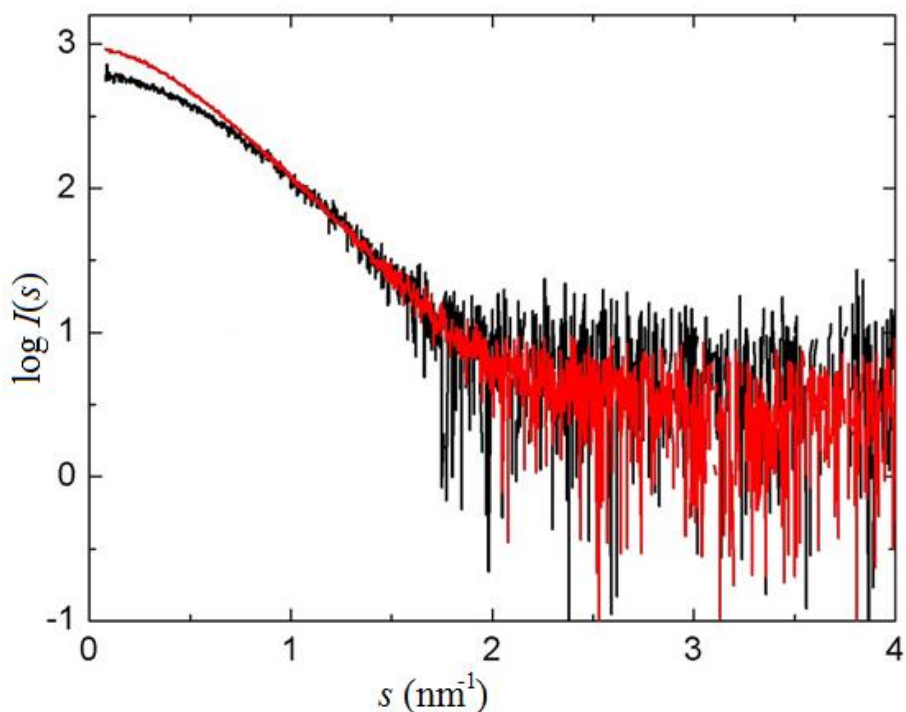


Figure 5.10. The experimental SAXS data. The scattering intensity $I(s)$ as a function of the scattering vector s of ASK1₈₈₋₃₀₂C-His (**black**) with a concentration of 2.3 mg·mL⁻¹ and ASK1₈₈₋₃₀₂C-His:TRX (**red**) with a concentration of 6 mg·mL⁻¹.

For a reference sample was chosen bovine serum albumin solution, a comparison of its forward scattering intensity $I(0)$ with ASK1₈₈₋₃₀₂C-His and ASK1₈₈₋₃₀₂C-His:TRX provided an estimation of the molecular mass of both protein and complex (*Tab. 5.1*).

The linearity of the Guinier region (*Fig. 5.11*) suggested no aggregation in both samples. From the slope of the Guinier plot and from the distance distribution function $P(r)$ (*Fig. 5.12*) was calculated the radius of gyration (R_g) for both ASK1 alone and the ASK1:TRX complex.

Calculated $P(r)$ function also provided the maximum particle distance D_{\max} reflecting maximal dimensions of ASK1₈₈₋₃₀₂C-His and ASK1₈₈₋₃₀₂C-His:TRX. Calculated parameters are listed in *Tab. 5.1*.

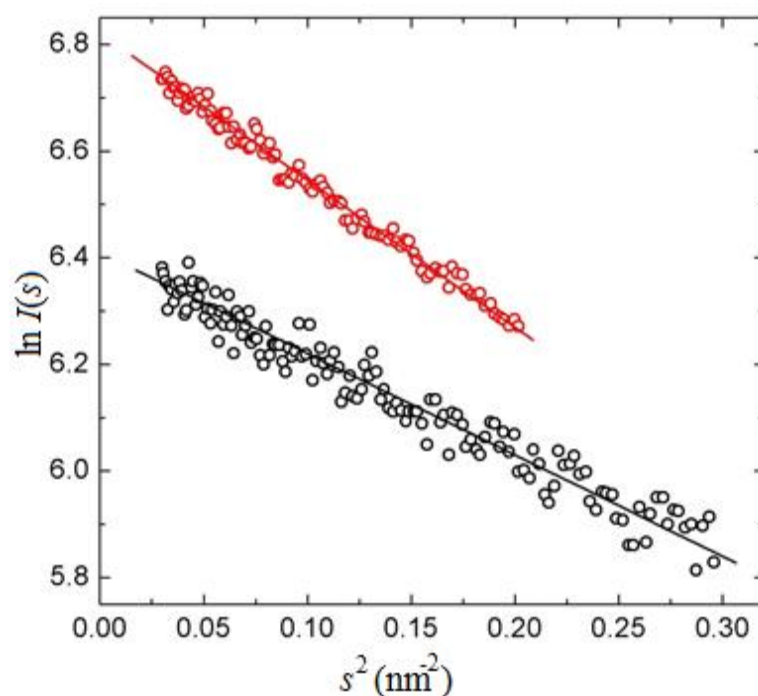


Figure 5.11. Calculated Guinier plot. The scattering intensity $I(s)$ as the function of the scattering vector s^2 confines the Guinier region of ASK1₈₈₋₃₀₂C-His (**black**) with a concentration of 2.3 mg·mL⁻¹ and ASK1₈₈₋₃₀₂C-His:TRX (**red**) with a concentration of 6 mg·mL⁻¹.

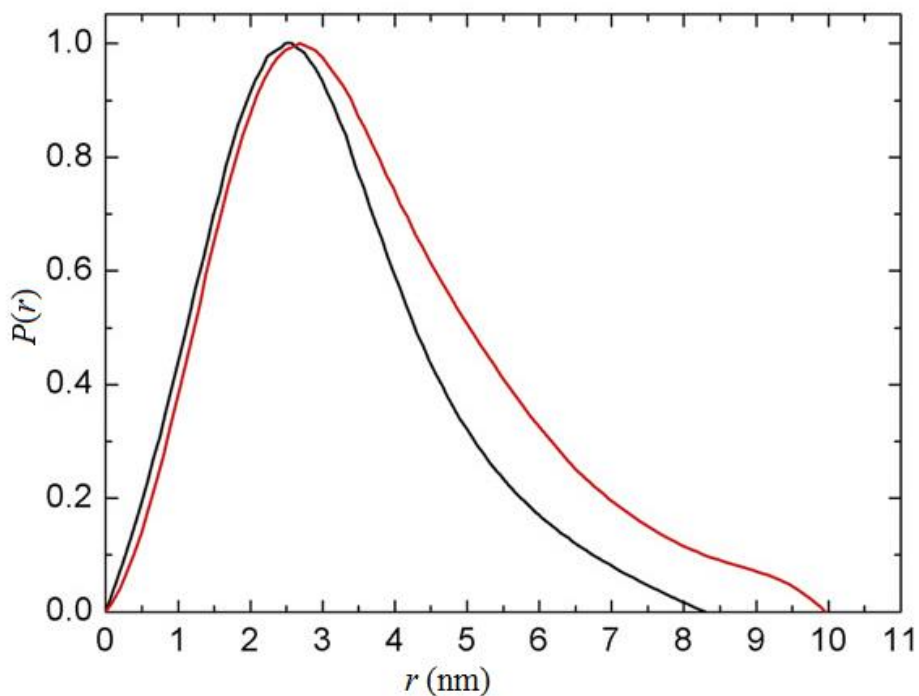


Figure 5.12. The distance distribution function $P(r)$ calculated from the scattering data. The distance distribution function of ASK1₈₈₋₃₀₂C-His (**black**) and ASK1₈₈₋₃₀₂C-His:TRX (**red**) is a real space representation of the scattering data and specifies the proportions of a protein in solution.

Table 5.1. Structural parameters calculated from SAXS data.

Sample	M_w (kDa) calculated	M_w (kDa) real	R_g (Å) from Guinier	R_g (Å) from $P(r)$	D_{max} (Å) from $P(r)$
ASK1₈₈₋₃₀₂C-His	~ 25	25.6	23.7 ± 0.3	24.2 ± 0.2	82
ASK1₈₈₋₃₀₂C-His:TRX	~ 37	38.6	28.9 ± 0.2	29.3 ± 0.1	99

All these data showed that samples were prepared in desired monodisperse conditions without aggregation. Prepared samples enabled a computation of the *ab initio* molecular envelopes, allowing the low-resolution structure determination, provided by prof. Obšil.

5.5 Preparation of ASK1-TBD constructs for protein

X-ray crystallography

In order to fully characterize interaction between ASK1 and TRX, it is necessary to obtain high-resolution structural data using either X-ray crystallography or NMR. We have decided to start with the crystallographic analysis. To increase the probability of successful crystallization, it is necessary to remove all flexible segments of a protein, including affinity tags. Since ASK1₈₈₋₃₀₂C-His does not have a cleavable His-tag, seven different constructs of ASK1-TBD were designed for crystallographic studies.

A cleavage site for a TEV protease followed by 6×His-tag with attached GB1 protein was added to the sequence of a human N-terminal ASK1 with seven different lengths (constructs ASK1₈₈₋₃₀₂, ASK1₄₆₋₂₅₁, ASK1₄₆₋₂₆₇, ASK1₄₆₋₂₈₇, ASK1₈₈₋₂₅₁, ASK1₈₈₋₂₆₇, ASK1₈₈₋₂₈₇, sequence is shown in *Supplement 1*). The purpose of the preparation and testing of seven different constructs of ASK1-TBD with cleavable His-tag was to find a construct with optimal stability and solubility for structural studies.

Purification of His-GB1-ASK1 fusion constructs consisted of the NCAC, TEV protease cleavage, 2nd NCAC for a removal of cleaved GB1 and a SEC performed the next day. The result of each purification step was verified by SDS-PAGE.

5.5.1 Nickel chelating chromatography

ASK1₄₆₋₂₅₁, ASK1₄₆₋₂₆₇, ASK1₄₆₋₂₈₇, ASK1₈₈₋₂₅₁, ASK1₈₈₋₂₆₇, ASK1₈₈₋₂₈₇ and ASK1₈₈₋₃₀₂ were expressed using pRSFDuet-1 with a cleavage site for a TEV protease. NCAC, TEV protease cleavage and the 2nd NCAC for a removal of cleaved GB1 was performed in the beginning of a His-GB1-ASK1 fusion constructs purification.

NCAC column contained 2 mL of Chelating Sepharose Fast Flow and it was placed at a temperature of 4° C. Eluted protein was collected to microtubes, separating several fractions of a 1.5 mL volume.

ASK1₈₈₋₃₀₂ construct was used for initial structural studies and it was expressed from 8 L of LB-media. All other His-GB1-ASK1 constructs were tested with the expression performed from 3 L of LB-media.

The SDS-PAGE analysis after NCAC showed that the proteins possessed expected molecular weights (in cases of well-expressed and soluble constructs) and a reasonable purity (Figs. 5.13 - 5.19). Based on these results, only some constructs were selected for further purification.

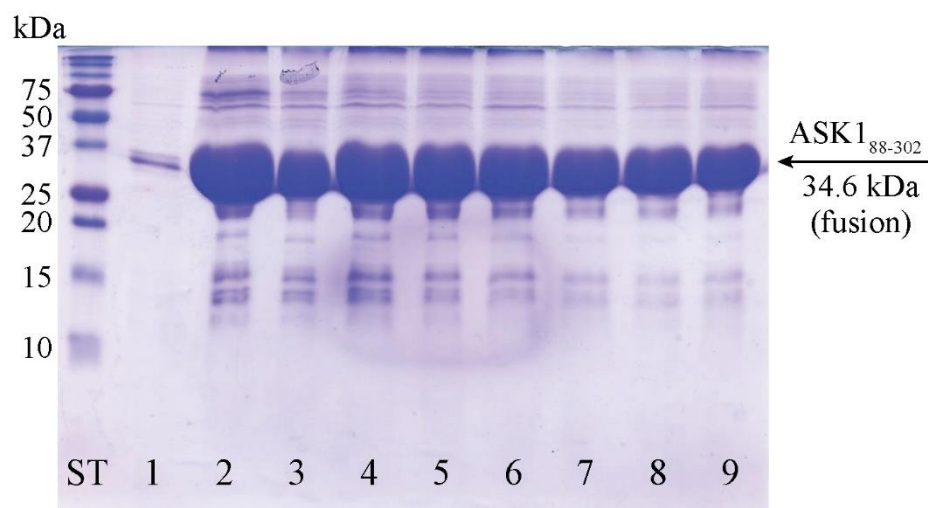


Figure 5.13. 15% SDS-PAGE gel after NCAC of ASK1₈₈₋₃₀₂. Expression from 8 L of LB-media. A sample of 10 μ L was taken from NCAC fractions 1-9 and mixed with 5 μ L of a loading buffer. 5 μ L of a protein M_w standard (ST) was loaded to the first lane. Fractions 2-9 were mixed together and used in the next purification step.

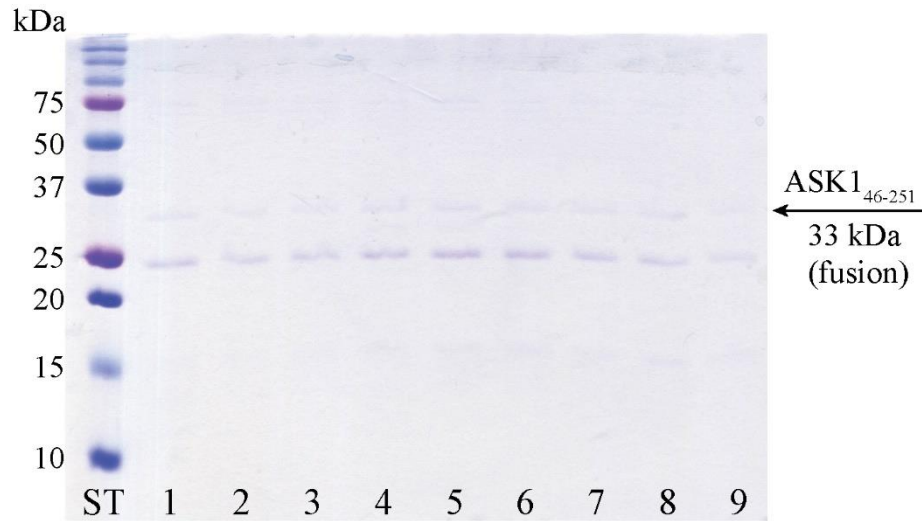


Figure 5.14. 15% SDS-PAGE gel after NCAC of ASK1₄₆₋₂₅₁. A sample of 10 μ L was taken from NCAC fractions 1-9 and mixed with 5 μ L of a loading buffer. 5 μ L of a protein M_w standard (ST) was loaded to the first lane. This construct was not present in a soluble fraction after the expression and thus was not considered for further work.

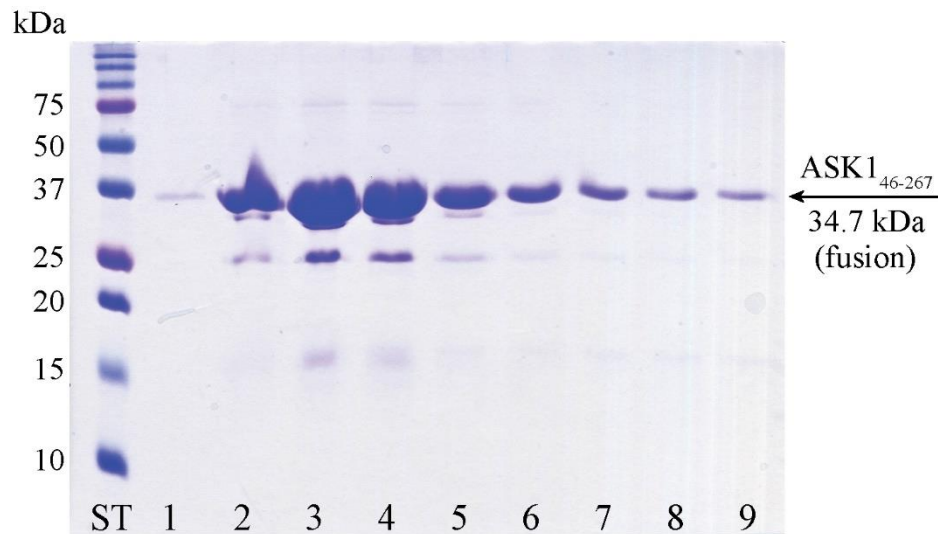


Figure 5.15. 15% SDS-PAGE gel after NCAC of ASK1₄₆₋₂₆₇. A sample of 10 μ L was taken from NCAC fractions 1-9 and mixed with 5 μ L of a loading buffer. 5 μ L of a protein M_w standard (ST) was loaded to the first lane. Fractions 2-5 were mixed together and used in the next purification step. This construct showed the best yield after NCAC.

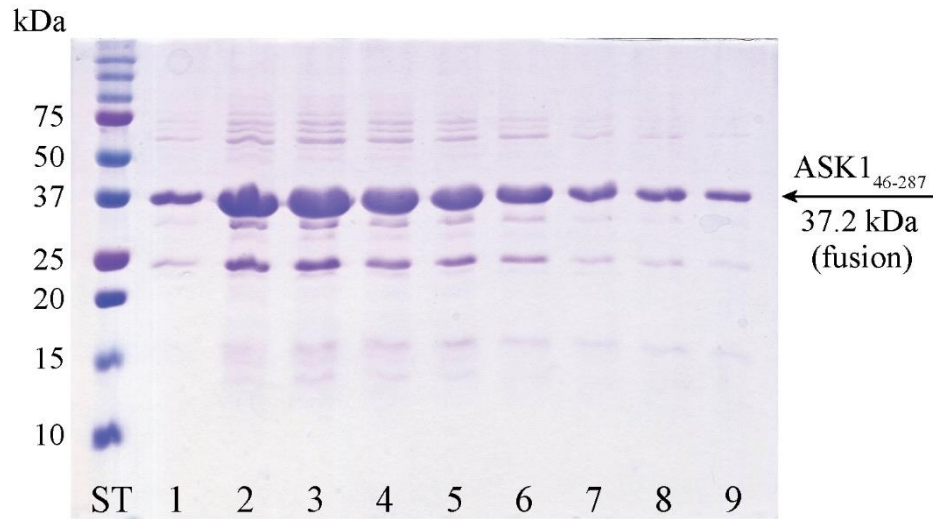


Figure 5.16. 15% SDS-PAGE gel after NCAC of ASK1₄₆₋₂₈₇. A sample of 10 μ L was taken from NCAC fractions 1-9 and mixed with 5 μ L of a loading buffer. 5 μ L of a protein M_w standard (ST) was loaded to the first lane. Fractions 2-6 were mixed together and used in the next purification step.



Figure 5.17. 15% SDS-PAGE gel after NCAC of ASK1₈₈₋₂₅₁. A sample of 10 μ L was taken from NCAC fractions 1-9 and mixed with 5 μ L of a loading buffer. 5 μ L of a protein M_w standard (ST) was loaded to the first lane. This construct was not present in a soluble fraction after the expression and thus was not considered for further work.

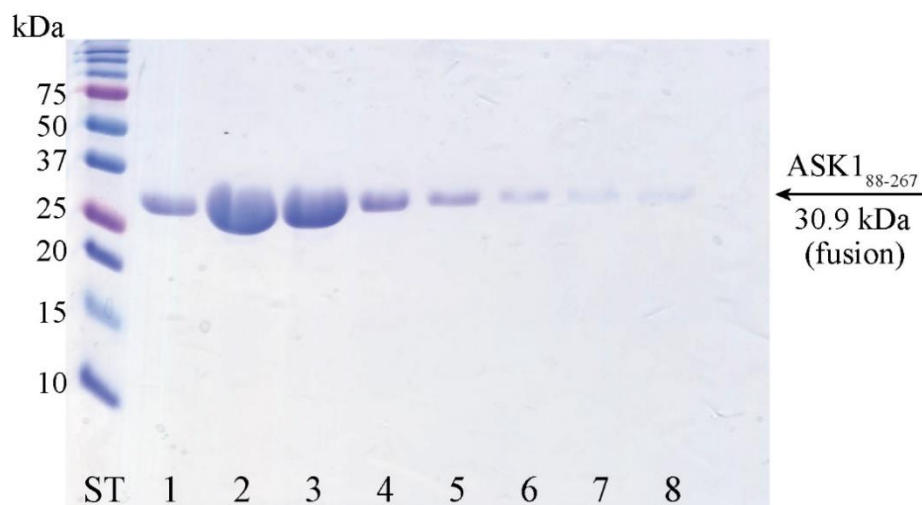


Figure 5.18. 15% SDS-PAGE gel after NCAC of ASK1₈₈₋₂₆₇. A sample of 10 μ L was taken from NCAC fractions 1-8 and mixed with 5 μ L of a loading buffer. 5 μ L of a protein M_w standard (ST) was loaded to the first lane. Fractions 2-5 were mixed together and used in the next purification step.

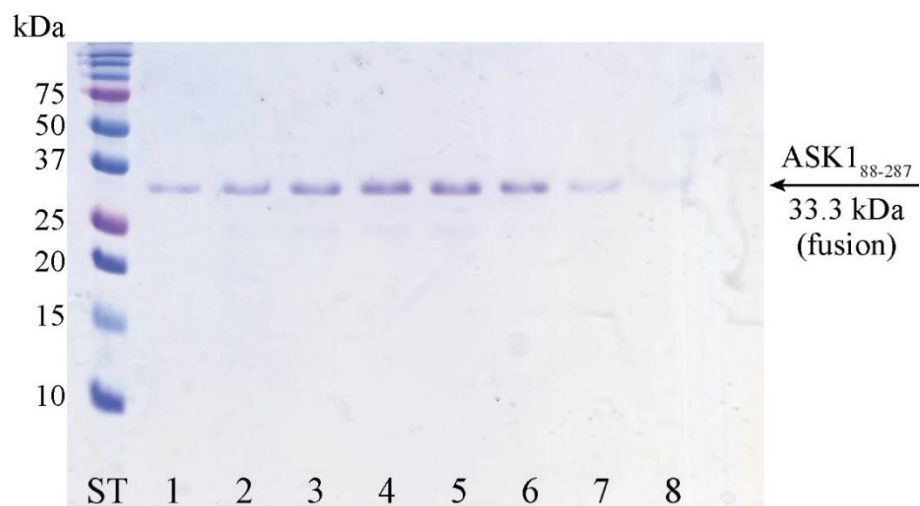


Figure 5.19. 15% SDS-PAGE gel after NCAC of ASK1₈₈₋₂₈₇. A sample of 10 μ L was taken from NCAC fractions 1-8 and mixed with 5 μ L of a loading buffer. 5 μ L of a protein M_w standard (ST) was loaded to the first lane. Fractions 2-6 were mixed together and used in the next purification step.

Obtained gels revealed, that constructs ASK1₈₈₋₃₀₂, ASK1₄₆₋₂₆₇, ASK1₄₆₋₂₈₇, ASK1₈₈₋₂₆₇ and ASK1₈₈₋₂₈₇ exhibit reasonable expression yield and the solubility (Figs. 5.13, 5.15, 5.16, 5.18, 5.19).

On the other hand, constructs ASK1₄₆₋₂₅₁ and ASK1₈₈₋₂₅₁ were not present in soluble fraction (Figs. 5.14, 5.17) and thus were not considered for further work.

5.5.2 TEV-protease cleavage

TEV protease used in the following experiment had a specific activity of 250 units per 1 mg of a protein (1 unit corresponds to 0.125 μ L of TEV). The approximate concentration after NCAC was determined spectrophotometrically by an absorbance measurement at a wavelength of 280 nm, with the elution buffer (Tab. 4.5) as a blank. The fusion part (His-tag and GB1) was cleaved by an overnight incubation with a TEV protease. A sample of 10 μ L was taken from each protein solution after the dialysis with TEV and analyzed by SDS-PAGE (Figs. 5.20 - 5.24). Electrophoresis revealed the complete cleavage of all tested fusion proteins. On every SDS-PAGE gel was also present added TEV protease.

M_w (GB1 with His-tag) = 10.2 kDa

M_w (TEV) = 27.5 kDa

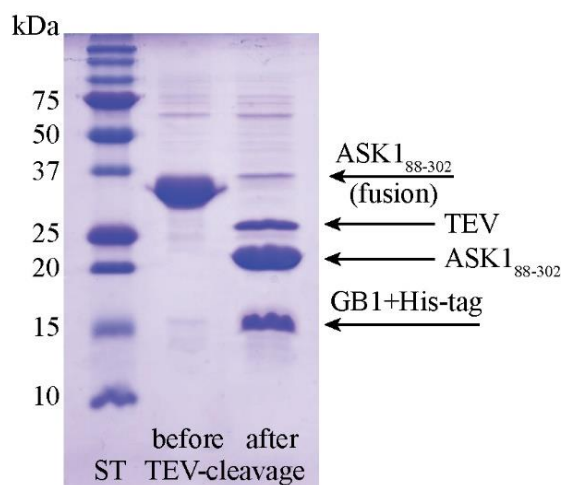


Figure 5.20. 15% SDS-PAGE gel after TEV cleavage and O/N dialysis of ASK1₈₈₋₃₀₂. A sample of 10 μ L was taken from a protein before and after TEV cleavage and mixed with 5 μ L of a loading buffer. 5 μ L of a protein M_w standard (ST) was loaded to the first lane. Molecular weight of ASK1₈₈₋₃₀₂ before TEV cleavage is 34.6 kDa, molecular weight after TEV cleavage is 24.3 kDa.

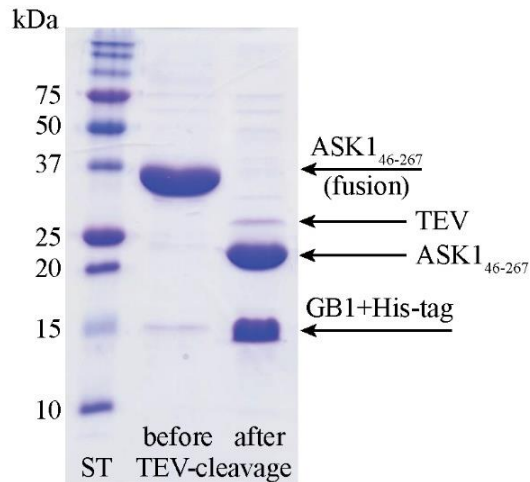


Figure 5.21. 15% SDS-PAGE gel after TEV cleavage and O/N dialysis of ASK1₄₆₋₂₆₇. A sample of 10 μ L was taken from a protein before and after TEV cleavage and mixed with 5 μ L of a loading buffer. 5 μ L of a protein M_w standard (ST) was loaded to the first lane. Molecular weight of ASK1₄₆₋₂₆₇ before TEV cleavage is 34.7 kDa, molecular weight after TEV cleavage is 24.5 kDa.

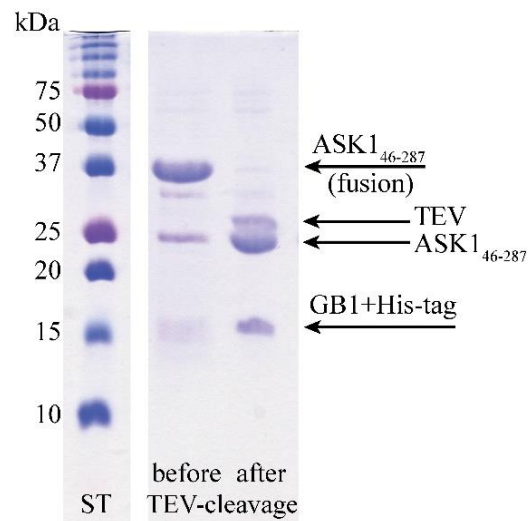


Figure 5.22. 15% SDS-PAGE gel after TEV cleavage and O/N dialysis of ASK1₄₆₋₂₈₇. A sample of 10 μ L was taken from a protein before and after TEV cleavage and mixed with 5 μ L of a loading buffer. 5 μ L of a protein M_w standard (ST) was loaded to the first lane. Molecular weight of ASK1₄₆₋₂₈₇ before TEV cleavage is 37.2 kDa, molecular weight after TEV cleavage is 27 kDa.

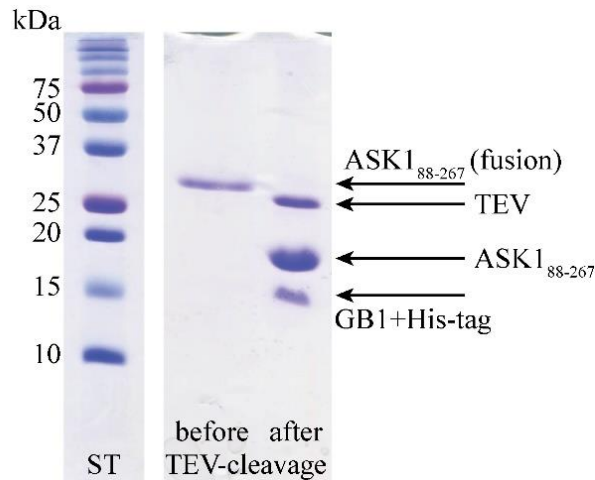


Figure 5.23. 15% SDS-PAGE gel after TEV cleavage and O/N dialysis of ASK1₈₈₋₂₆₇. A sample of 10 μ L was taken from a protein before and after TEV cleavage and mixed with 5 μ L of a loading buffer. 5 μ L of a protein M_w standard (ST) was loaded to the first lane. Molecular weight of ASK1₈₈₋₂₆₇ before TEV cleavage is 30.9 kDa, molecular weight after TEV cleavage is 20.7 kDa.

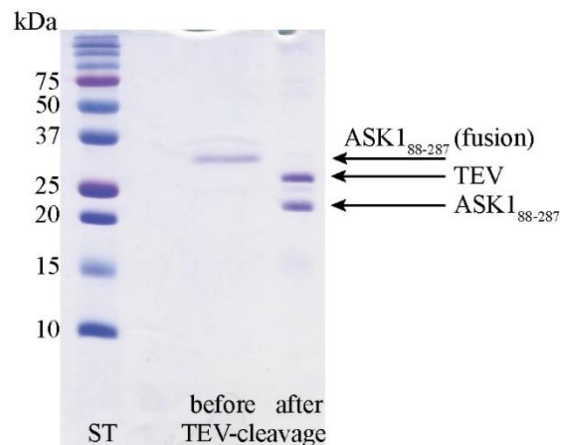


Figure 5.24. 15% SDS-PAGE gel after TEV cleavage and O/N dialysis of ASK1₈₈₋₂₈₇. A sample of 10 μ L was taken from a protein before and after TEV cleavage and mixed with 5 μ L of a loading buffer. 5 μ L of a protein M_w standard (ST) was loaded to the first lane. Molecular weight of ASK1₈₈₋₂₈₇ before TEV cleavage is 33.3 kDa, molecular weight after TEV cleavage is 23.1 kDa. It is likely that the GB1 protein was released by a semipermeable membrane during a dialysis. The yield of this construct was not sufficient for the next purification steps.

5.5.3 Removal of a cleaved GB1 protein

After a TEV cleavage and dialysis, ASK1 was in a solution with TEV protease and GB1. To remove them, a second NCAC was performed. GB1 and TEV protease, both containing His-tag, were trapped on the column, whereas ASK1 was eluted. A sample of 10 μL was taken from each construct after 2nd NCAC and analyzed by SDS-PAGE (Figs. 5.25 - 5.28). Electrophoresis revealed efficient removal of GB1 and TEV. During this procedure, a loss of ASK1 (slight decrease in the concentration) had been observed.

M_w (ASK1₈₈₋₃₀₂) = 24.3 kDa

M_w (ASK1₄₆₋₂₆₇) = 24.5 kDa

M_w (ASK1₄₆₋₂₈₇) = 27.0 kDa

M_w (ASK1₈₈₋₂₆₇) = 20.7 kDa

M_w (GB1 with His-tag) = 10.2 kDa

M_w (TEV) = 27.5 kDa

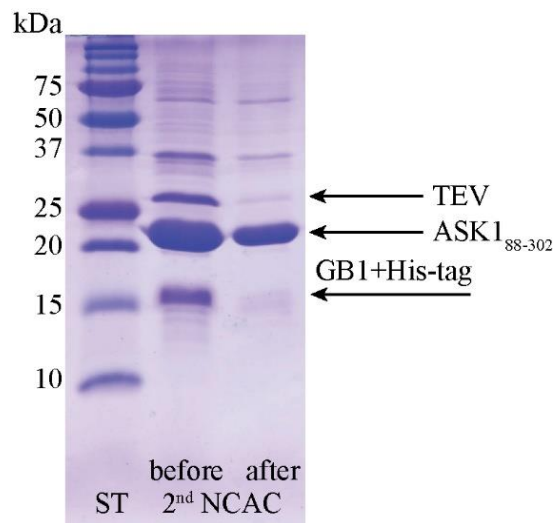


Figure 5.25. 15% SDS-PAGE gel after 2nd NCAC of ASK1₈₈₋₃₀₂. A sample of 10 μL was taken from a protein before and after 2nd NCAC and mixed with 5 μL of a loading buffer. 5 μL of a protein M_w standard (ST) was loaded to the first lane.

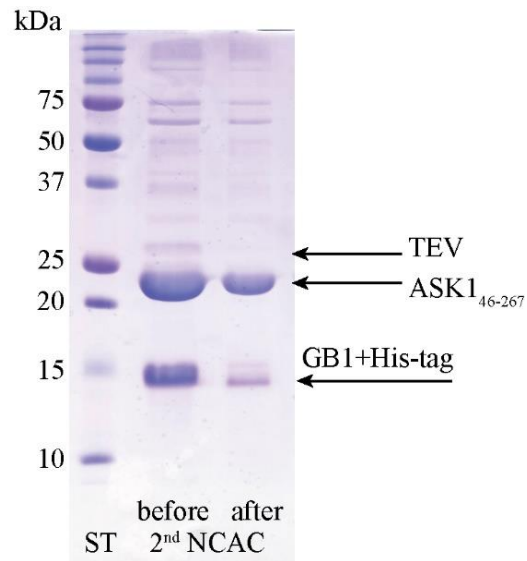


Figure 5.26. 15% SDS-PAGE gel after 2nd NCAC of ASK1₄₆₋₂₆₇. A sample of 10 μ L was taken from a protein before and after 2nd NCAC and mixed with 5 μ L of a loading buffer. 5 μ L of a protein M_w standard (ST) was loaded to the first lane.

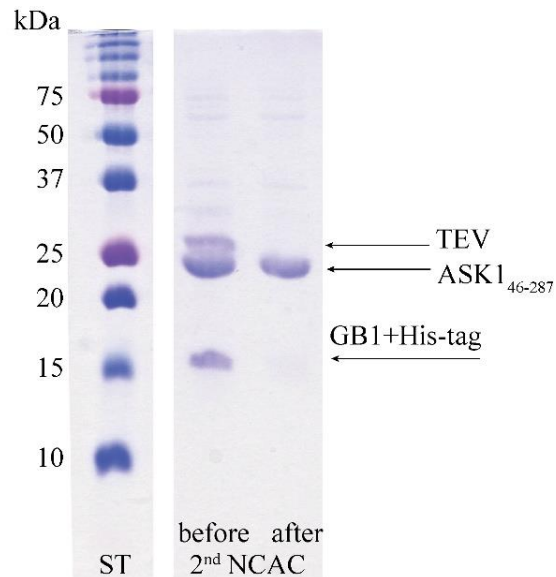


Figure 5.27. 15% SDS-PAGE gel after 2nd NCAC of ASK1₄₆₋₂₈₇. A sample of 10 μ L was taken from a protein before and after 2nd NCAC and mixed with 5 μ L of a loading buffer. 5 μ L of a protein M_w standard (ST) was loaded to the first lane.

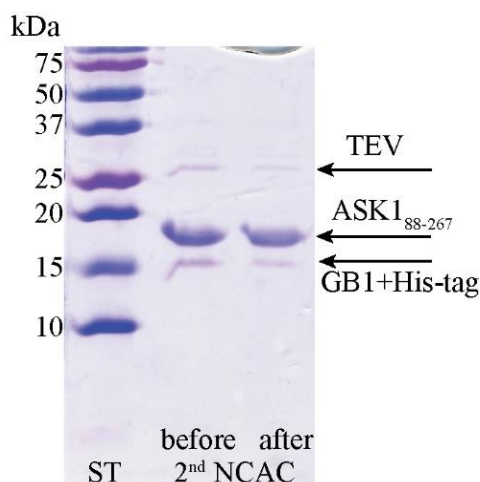


Figure 5.28. 15% SDS-PAGE gel after 2nd NCAC of ASK1₈₈₋₂₆₇. A sample of 10 μ L was taken from a protein before and after 2nd NCAC and mixed with 5 μ L of a loading buffer. 5 μ L of a protein M_w standard (ST) was loaded to the first lane.

5.5.4 Size exclusion chromatography

Protein samples for a SEC were prepared after 2nd NCAC by a slow concentration to a final volume of 2 mL (recommended injected volume for the used column). During protein concentration, several ASK1 constructs partially precipitated, especially ASK1₈₈₋₃₀₂ and ASK1₄₆₋₂₈₇. On the other hand, construct ASK1₄₆₋₂₆₇ showed the best solubility and stability.

GE Healthcare Life Sciences HiLoad 26/60 Superdex 75 prep grade column with 330 mL volume and 2.5 mL/min flow was used for SEC of all ASK1 constructs. The volume of each fraction was 1.5 mL and 40 fractions were collected to Eppendorf microtubes. A spectrophotometric detector was set to a wavelength of 280 nm and the elution profile was recorded into the chromatogram (*Figs. 5.29, 5.31, 5.33, 5.35*). Time (and volume, with 2.5 mL/min flow) of collection was chosen to respond to particular molecular weight of an eluted protein according to a column calibration. SDS-PAGE pointed out fractions with ASK1 of sufficient purity and concentration (*Fig. 5.30, 5.32, 5.34, 5.36*). ASK1₈₈₋₃₀₂ was expressed from 8 L of LB-media, all other constructs were expressed from 3 L of LB-media.

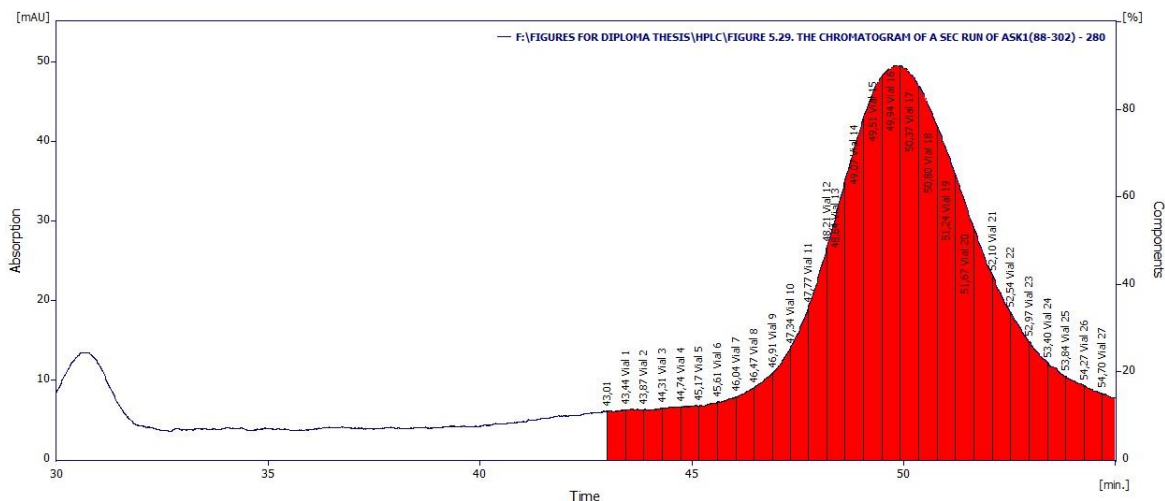


Figure 5.29. The chromatogram of a SEC run of ASK1₈₈₋₃₀₂. The absorption in milliabsorbance units mAU is plotted against the time of elution in minutes. Blue line represents absorption signal at a wavelength of 280 nm, red color defines collected fractions with the number of vials. Fractions 12-20 were analyzed by SDS-PAGE (Fig. 5.30).

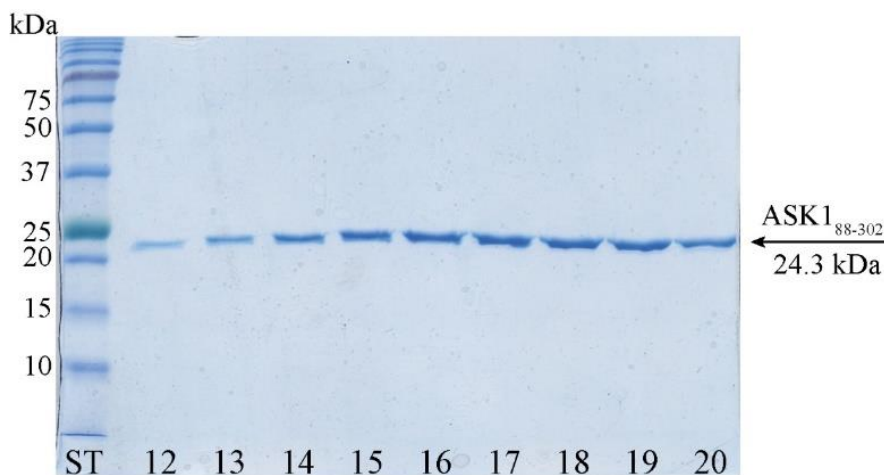


Figure 5.30. 15% SDS-PAGE gel of selected fractions from SEC. A sample of 10 μ L was taken from fractions number 12-20 and mixed with 5 μ L of a loading buffer. 5 μ L of a protein M_w standard (ST) was loaded to the first lane. Fractions 12-22 were merged together.

$$M_w (\text{ASK1}_{88-302}) = 24.3 \text{ kDa}, c (\text{ASK1}_{88-302}) = 12.3 \mu\text{M} = 0.3 \text{ mg} \cdot \text{mL}^{-1}$$

$$m (\text{ASK1}_{88-302}) \text{ after SEC} = 4.2 \text{ mg}$$

Final yield of ASK1₈₈₋₃₀₂ from 1 L of LB-medium was 0.5 mg of pure protein.

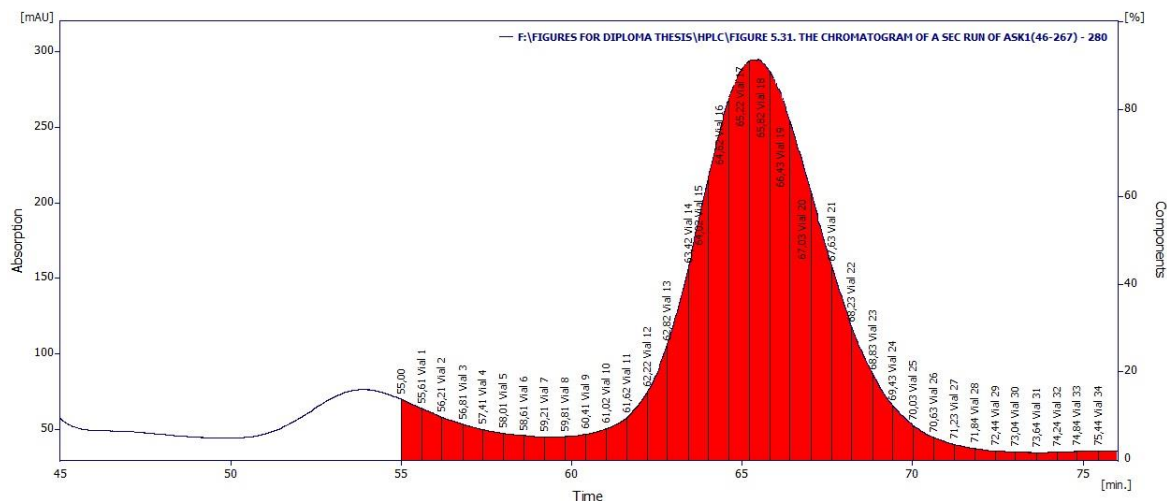


Figure 5.31. The chromatogram of a SEC run of ASK1₄₆₋₂₆₇. The absorption in milliabsorbance units mAU is plotted against the time of elution in minutes. Blue line represents absorption signal at a wavelength of 280 nm, red color defines collected fractions with the number of vials. Fractions 12-14, 16, 18, 22-25 were analyzed by SDS-PAGE (Fig. 5.32).

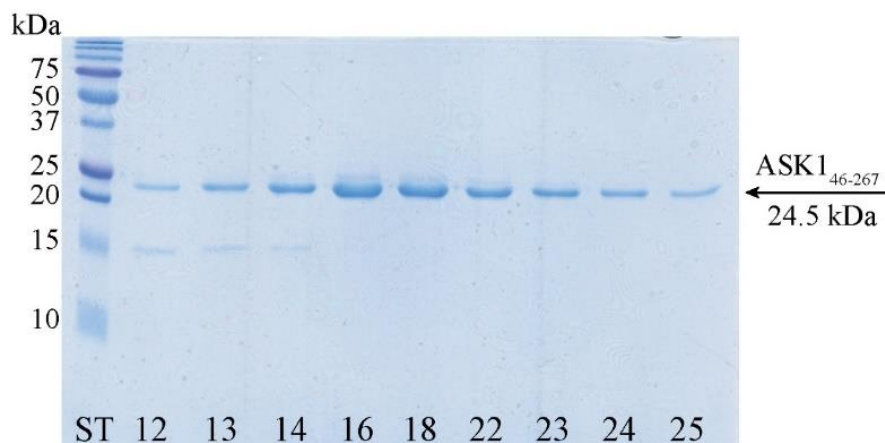


Figure 5.32. 15% SDS-PAGE gel of selected fractions from SEC. A sample of 10 μ L was taken from fractions number 12-14, 16, 18, 22-25 and mixed with 5 μ L of a loading buffer. 5 μ L of a protein M_w standard (ST) was loaded to the first lane. There is a noticeable modest degradation of ASK1₄₆₋₂₆₇ that incurred during the purification process. Fractions 14-23 were merged together.

M_w (ASK1₄₆₋₂₆₇) = 24.5 kDa, c (ASK1₄₆₋₂₆₇) = 28.6 μ M = 0.7 mg \cdot mL⁻¹

m (ASK1₄₆₋₂₆₇) after SEC = 4.5 mg

Final yield of ASK1₄₆₋₂₆₇ from 1 L of LB-medium was 1.5 mg of pure protein.

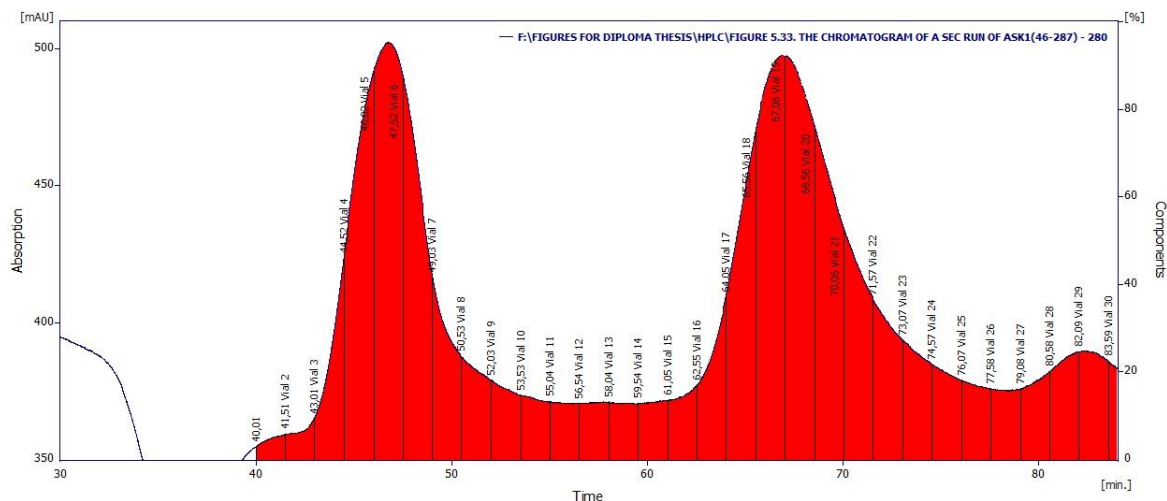


Figure 5.33. The chromatogram of a SEC run of ASK1₄₆₋₂₈₇. The absorption in milliabsorbance units mAU is plotted against the time of elution in minutes. Blue line represents absorption signal at a wavelength of 280 nm, red color defines collected fractions with the number of vials. Fractions 6, 16-19, 21-24 were analyzed by SDS-PAGE (Fig. 5.34).

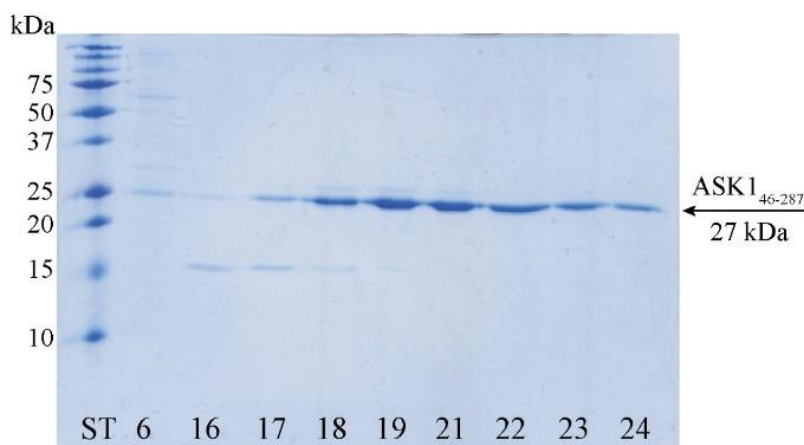


Figure 5.34. 15% SDS-PAGE gel of selected fractions from SEC. A sample of 10 μ L was taken from fractions number 6, 16-19, 21-24 and mixed with 5 μ L of a loading buffer. 5 μ L of a protein M_w standard (ST) was loaded to the first lane. There is a noticeable modest degradation of ASK1₄₆₋₂₈₇ that incurred during the purification process. Fractions 19-24 were merged together.

$$M_w (\text{ASK1}_{46-287}) = 27 \text{ kDa}, c (\text{ASK1}_{46-287}) = 7.4 \mu\text{M} = 0.2 \text{ mg} \cdot \text{mL}^{-1}$$

$$m (\text{ASK1}_{46-287}) \text{ after SEC} = 1.5 \text{ mg}$$

Final yield of ASK1₄₆₋₂₈₇ from 1 L of LB-medium was 0.5 mg of pure protein.

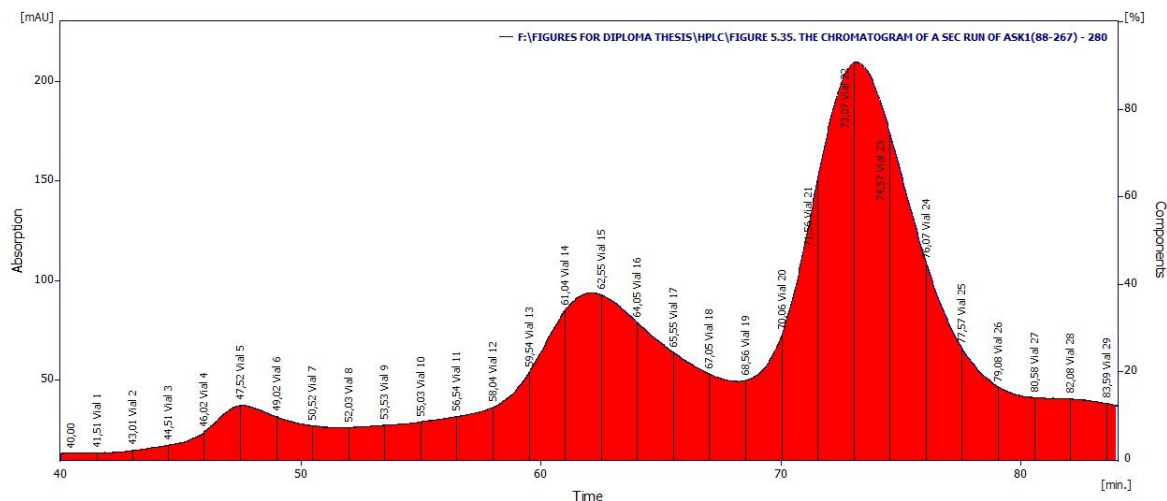


Figure 5.35. The chromatogram of a SEC run of ASK₁₈₈₋₂₆₇. The absorption in milliabsorbance units mAU is plotted against the time of elution in minutes. Blue line represents absorption signal at a wavelength of 280 nm, red color defines collected fractions with the number of vials. Fractions 19-27 were analyzed by SDS-PAGE (Fig. 5.36).

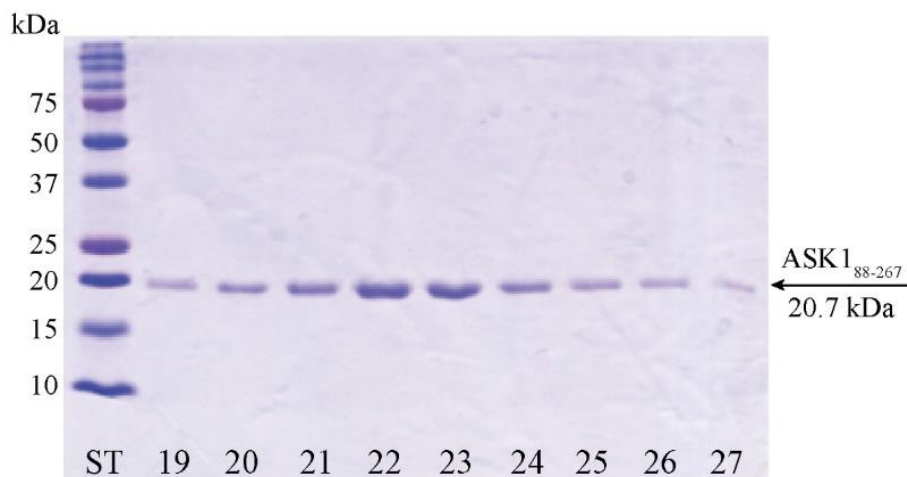


Figure 5.36. 15% SDS-PAGE gel of selected fractions from SEC. A sample of 10 μ L was taken from fractions number 19-27 and mixed with 5 μ L of a loading buffer. 5 μ L of a protein M_w standard (ST) was loaded to the first lane. Fractions 20-24 were merged together.

M_w (ASK₁₈₈₋₂₆₇) = 20.7 kDa, c (ASK₁₈₈₋₂₆₇) = 29 μ M = 0.6 mg·mL⁻¹

m (ASK₁₈₈₋₂₆₇) after SEC = 4.5 mg

Final yield of ASK₁₈₈₋₂₆₇ from 1 L of LB-medium was 1.3 mg of pure protein.

Comparison of a purification of seven different His-GB1-ASK1 fusion constructs indicated the ASK1₄₆₋₂₆₇ as the most promising construct. The final yield 1.5 mg from 1 L of LB-medium suggested that this construct exhibits best expression yield and solubility, thus the ASK1₄₆₋₂₆₇ construct was selected for further structural studies.

5.6 Native gel electrophoresis

Next, the ability of ASK1₄₆₋₂₆₇ to interact with TRX was tested using native gel electrophoresis. Native electrophoresis is a simple method for a rapid determination of a complex formation and a protein-protein interaction in their native state.

The result of this experiment is shown in Fig. 5.37. Lanes A, T and C contained 500 pmol of ASK1₄₆₋₂₆₇, TRX and 1:1 molar ratio of their complex, respectively. The disappearance of TRX band in a complex column and a slight enlargement and shift of ASK1₄₆₋₂₆₇:TRX band suggested proper complex formation.

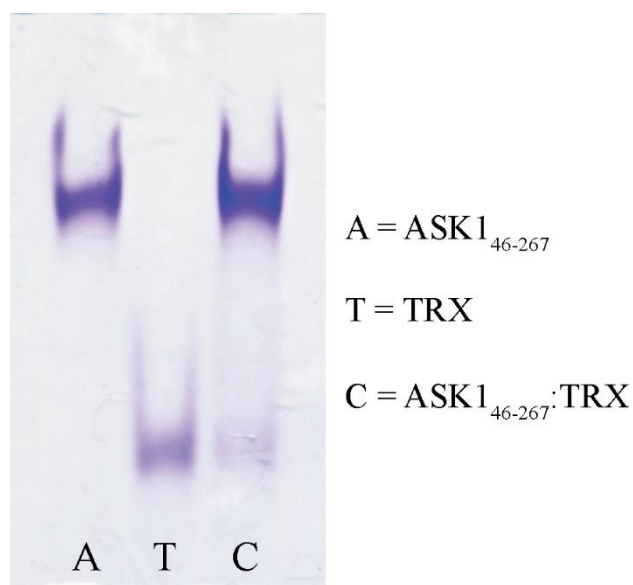


Figure 5.37. 15% native gel of ASK1₄₆₋₂₆₇, TRX and ASK1₄₆₋₂₆₇:TRX complex. 15 μ L of a 500 pmol proteins and a protein complex with 1:1 molar ratio were mixed with 5 μ L of a loading buffer. The disappearance of TRX band in a complex column and a slight enlargement and shift of ASK1₄₆₋₂₆₇:TRX band suggested proper complex formation.

5.7 Dynamic light scattering

Next, DLS was used to determine a polydispersity and aggregation behavior of ASK1₄₆₋₂₆₇ in a solution. ASK1 was dialyzed to the buffer for a DLS measurement and concentrated to the maximal possible concentration of 3.4 mg·mL⁻¹ (further concentration induced visible protein precipitation). The buffer used for DLS measurements is identical to the buffer for the crystallographic studies, it contained a minimal composition of a Tris buffer, NaCl (to maintain a minimum ionic strength of a solution) and a low concentration of a reducing agent (ASK1₄₆₋₂₆₇ has 8 cysteine thiols that easily undergo oxidation). The absence of a glycerol as a stabilizing agent for a protein might also increase the susceptibility to an aggregation.

To check the protein stability at a higher temperature (DLS measurement was performed at 25° C), 10 µL of 5-times diluted sample was taken from ASK1₄₆₋₂₆₇ solution before and after the measurement and analyzed by SDS-PAGE (*Fig. 5.40*) to look for a temperature-dependent proteolytic degradation.

The solvent refractive index was 1.332, the solvent viscosity was 0.89 cP, the temperature was 298.16 K, the wavelength was 632.8 nm and the scattering angle was 90°.

It is necessary to realize that the high molecular-weighted aggregates scatter more strongly than the relatively small non-aggregated proteins and proportions of the individual local maxima do not correspond to the relative quantity of the individual forms in solution.

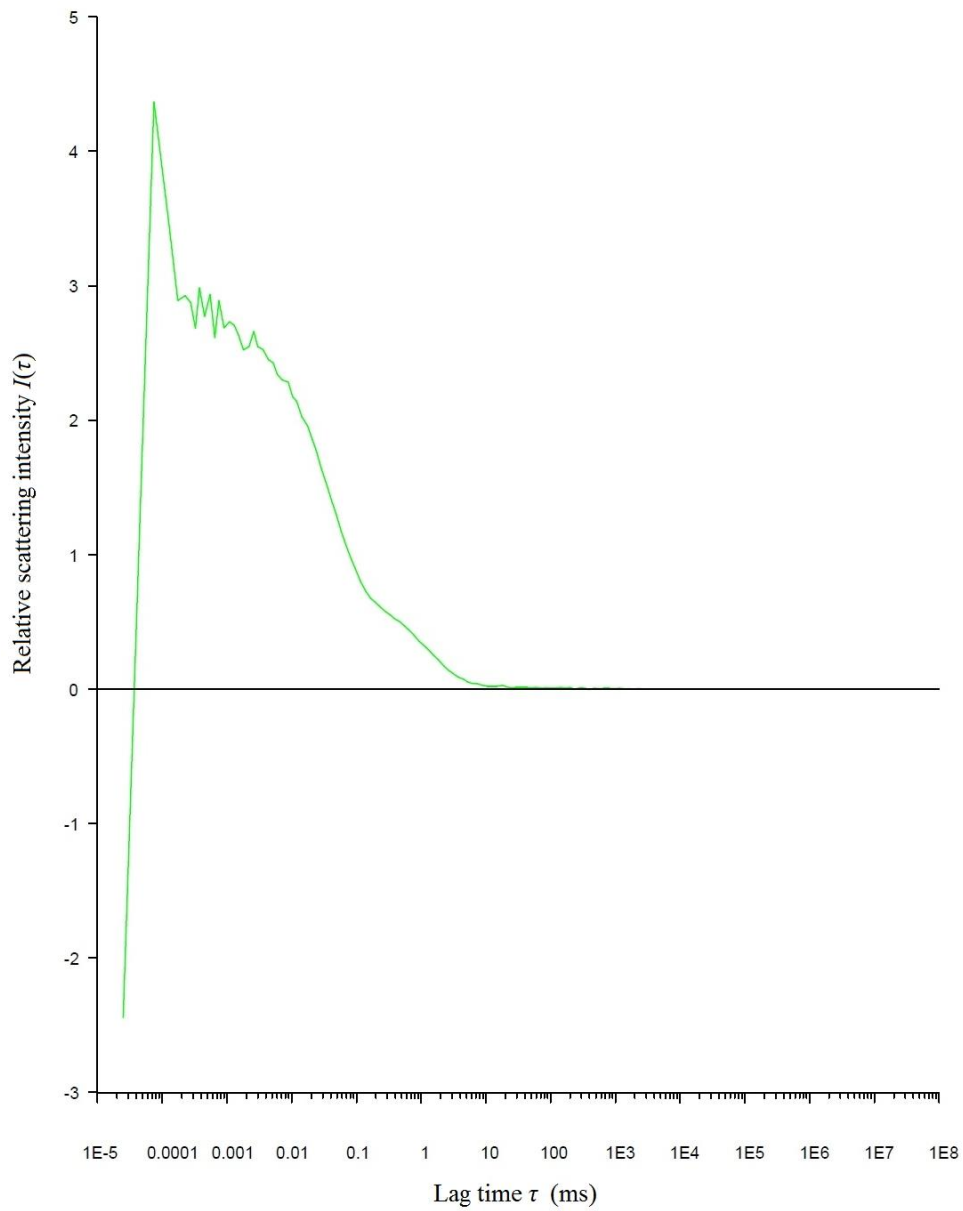


Figure 5.38. Normalized intensity correlation function of ASK1₄₆₋₂₆₇ DLS measurement. The lag time τ of a measurement in milliseconds is plotted against the relative scattering intensity $I(\tau)$. To minimize errors, one measurement lasted for 30 ms and three individual measurements were measured and averaged.

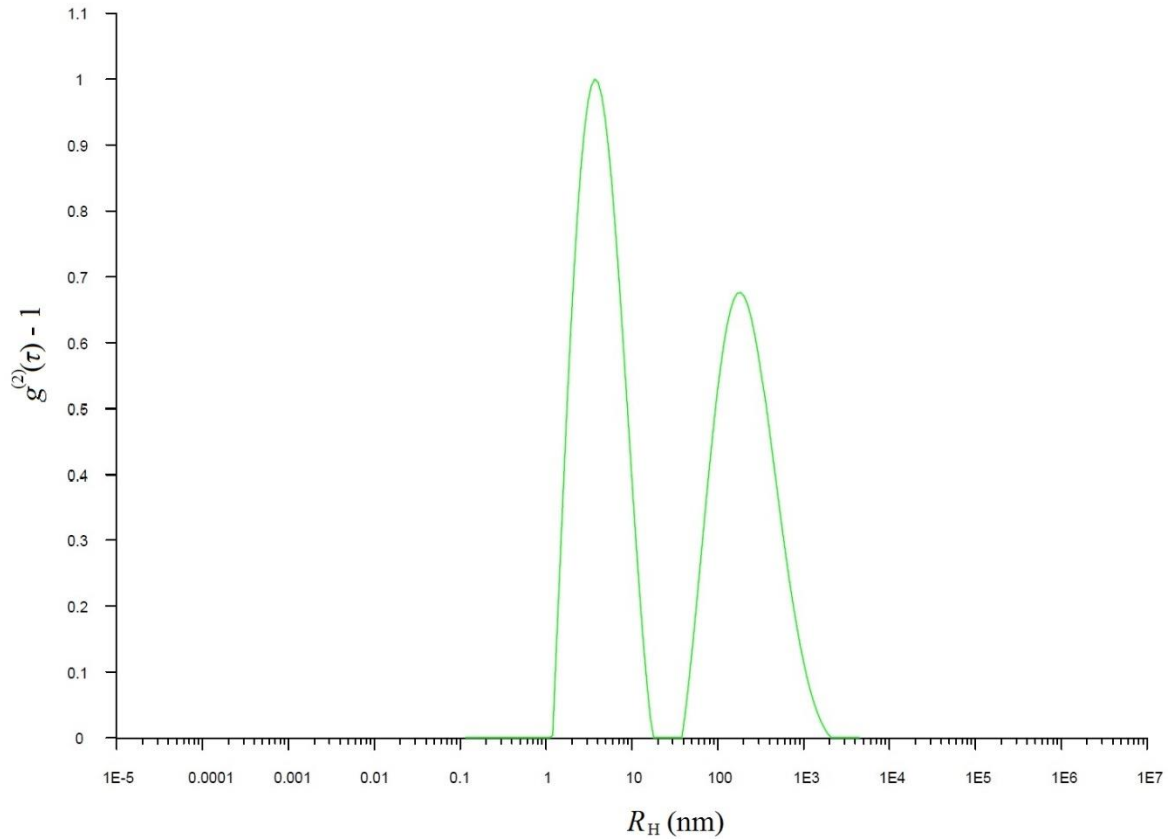


Figure 5.39. Distribution function of the ASK1 DLS measurement. The numerically unweighted hydrodynamic radius in nanometers is plotted against the second-order autocorrelation function $g^{(2)}(\tau)$. The first peak is from 1 nm to 16 nm with the mean peak position at 4 nm and it represents molecules of ASK1₄₆₋₂₆₇. The second peak is from 42 nm to 1920 nm with the mean peak position at 209 nm and represents aggregates. It is obvious from the size of peaks that ASK1₄₆₋₂₆₇ is relatively stable in the buffer at the concentration of $3.4 \text{ mg}\cdot\text{mL}^{-1}$ and during the process of concentration is formed only minimal amount of aggregates.

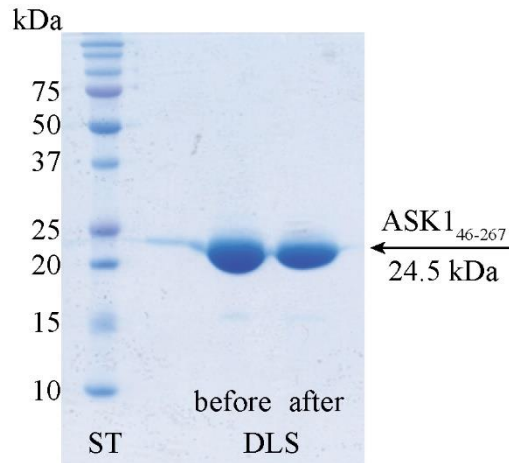


Figure 5.40. 15% SDS-PAGE gel of ASK1₄₆₋₂₆₇ before and after DLS measurements. 10 μ L of a 5-times diluted sample was taken from ASK1₄₆₋₂₆₇ solution before and after measurement and mixed with 5 μ L of a loading buffer. 5 μ L of a protein M_w standard (ST) was loaded to the first lane.

From the size of peaks (*Fig. 5.39*), it is obvious that a protein solution contained low amount of large molecules, in this case aggregates. This suggests that the ASK1₄₆₋₂₆₇ construct is sufficiently stable even in buffer without glycerol and the ASK1₄₆₋₂₆₇ solution does not necessarily require high ionic strength. The SDS-PAGE analysis (*Fig. 5.40*) showed that ASK1₄₆₋₂₆₇ did not suffer from proteolytic degradation, what suggested that this construct is also relatively stable at a temperature of 25 °C.

6 DISCUSSION

This diploma thesis was elaborated to study the TRX binding domain of N-terminal human ASK1 and its complex with TRX. The interaction between ASK1 and TRX is essential in the regulation of MAP kinase signaling pathways influencing the cellular response to stress stimuli from the environment of the cell.

Goals of this diploma thesis can be divided into several parts. First of all, expression and purification of two proteins, ASK1-TBD and TRX were performed.

The ASK1₈₈₋₃₀₂C-His construct was a result of previous work in our laboratory, and after several modification in a purification protocol, we were able to prepare ASK1₈₈₋₃₀₂C-His with a sufficient yield, purity and concentration. The final yield after SEC was 1 mg of ASK1₈₈₋₃₀₂C-His from 1 L of LB-media and the protein purity was checked by SDS-PAGE (*Fig. 5.3*).

The second prepared protein was the binding partner for ASK1, human TRX with a single mutation Cys⁷³ to Ser⁷³. The final yield after SEC was 15.3 mg of TRX from 1 L of LB-medium and the protein purity checked by SDS-PAGE was found to be satisfactory (*Fig. 5.7*).

Next part of this thesis was the study of a secondary and tertiary structure of ASK1₈₈₋₃₀₂C-His and the ASK1₈₈₋₃₀₂C-His:TRX complex using circular dichroism. The analysis of the far-UV CD spectrum of ASK1₈₈₋₃₀₂C-His using K2D method [43] indicated that this protein contains ~35% of α , ~20% of β , and ~45% of random structure. This estimation is in a good agreement with the theoretical prediction (*Supplement 2*) using PSIPRED (~35% α , ~15% β , and ~50% random structure) [50][51] suggesting that produced protein is correctly folded. The CD spectroscopy was also used to monitor structural changes in ASK1 upon the complex formation. The comparison of far-UV CD spectra of ASK1₈₈₋₃₀₂C-His and the ASK1₈₈₋₃₀₂C-His:TRX complex suggested no significant changes in overall secondary structure of ASK1 upon the TRX binding (*Fig. 5.8*). The near-UV CD spectrum, which reflects changes in a tertiary structure, showed significant difference only in the region from 275 to 295 nm upon the complex formation (*Fig. 5.9*). This suggested a conformational change in the region containing tryptophan residue [42].

Since the Trp³¹ located in the TRX sequence is the only tryptophan residue in the ASK1₈₈₋₃₀₂C-His:TRX complex, it is likely that observed differences mainly reflect a structural change in the vicinity of this residue upon the complex formation, suggesting a direct involvement of Trp³¹ in the interaction between ASK1 and TRX.

CD spectroscopy measurements, although easily performable, provide only limited structural information of studied proteins. More sophisticated techniques must be used to obtain detailed structural data. Therefore, we decided to perform SAXS measurements to get insight into the shape and dimension of studied proteins. Thus, sample preparation for SAXS measurements was the next goal of this diploma thesis. It involved a careful preparation of proteins considering the high sensitivity of this method to the aggregates and polydispersity in protein solutions. During the protein expression and purification, it was necessary to keep a constant temperature of 4 °C and to perform very cautious concentration of protein samples. Samples for SAXS experiments were prepared successfully with negligible aggregation and obtained data provided a platform for calculating a radius of gyration R_g , distance distribution function $P(r)$ and maximum particle dimension D_{max} . The molecular mass of the ASK1₈₈₋₃₀₂C-His:TRX complex was estimated by comparing its forward scattering intensity $I(0)$ with a reference solutions of bovine serum albumin. Obtained molecular mass of 37 kDa confirmed the 1:1 molar stoichiometry (theoretical molecular mass of the complex is 38.6 kDa). Both Guinier approximation and $P(r)$ distribution function were used to calculate R_g of ASK1₈₈₋₃₀₂C-His and the ASK1₈₈₋₃₀₂C-His:TRX complex. Obtained values of 2.4 nm and 2.9 nm, respectively, suggested that the complex is more asymmetric than the ASK1 domain alone. The asymmetric shape of the complex was confirmed also by calculations of D_{max} , obtained values were 8.2 nm and 9.9 nm for ASK1₈₈₋₃₀₂C-His and the ASK1₈₈₋₃₀₂C-His:TRX complex, respectively.

In order to fully characterize interaction between ASK1 and TRX, it is necessary to obtain high-resolution structural data using either X-ray crystallography or NMR. We have decided to start with the crystallographic analysis. To increase the probability of successful crystallization, we decided to remove all flexible segments of the ASK1-TBD protein, including affinity tags.

Since ASK1₈₈₋₃₀₂C-His did not have a cleavable His-tag, the ASK1₈₈₋₃₀₂ construct with a C-terminal cleavage site for a TEV protease followed by 6×His-tag with attached GB1 protein was designed for further structural studies and protein X-ray crystallography. However, it became clear after an attempt to express and purify this construct that the C-terminal His-tag increased the solubility of ASK1₈₈₋₃₀₂. After its removal, this construct exhibited only limited stability and solubility (*Fig. 5.30*) and highly precipitated during concentration. Therefore six other His-GB1-ASK1 fusion constructs were designed based on a prediction of the secondary structure (*Supplement 2*), with two alternative starts and three different ends (*Supplement 1*). The aim was to prepare protein as compact as possible, which would be well-crystallizable.

Constructs ASK1₄₆₋₂₅₁, ASK1₄₆₋₂₆₇, ASK1₄₆₋₂₈₇, ASK1₈₈₋₂₅₁, ASK1₈₈₋₂₆₇ and ASK1₈₈₋₂₈₇ were prepared and tested to find a construct with optimal stability and solubility for structural studies. As expected after the experience with the C-terminal His-tag cleavage, the solubility and expression yield of these six constructs were dependent on their C-terminus, while the N-terminal sequence shortening seemed to have a little effect to the final purification yield of a particular construct. The main difference in their solubility is probably caused by changes in the accessibility of their hydrophilic and hydrophobic parts.

Constructs ASK1₄₆₋₂₅₁ and ASK1₈₈₋₂₅₁ were not present in a soluble fraction after nickel chelating chromatography (*Figs. 5.14, 5.17*) and thus were not considered for further work. This suggests that the segment beyond residue Leu²⁵¹ is important for a domain folding and/or covers hydrophobic regions. Its removal probably exposed these regions and caused a protein aggregation.

Constructs ASK1₄₆₋₂₆₇ and ASK1₈₈₋₂₆₇ showed the best behavior and were evaluated as the most promising constructs for further crystallographic studies (*Figs. 5.32, 5.36*). The final yields of these constructs were 1.5 mg and 1.3 mg from 1 L of LB-medium, respectively. With the significantly increased purification yield, the ASK1₄₆₋₂₆₇ construct was selected for further structural studies.

Constructs ASK1₄₆₋₂₈₇ and ASK1₈₈₋₂₈₇ showed insufficient solubility (*Figs. 5.34., 5.24*) and were not considered for further work. According to the prediction of a secondary structure (*Supplement 2*), amino acid residues 270-300 probably form α -helix.

Thus if a part of this α -helix is removed, exposed hydrophobic amino acids start to interact either with each other or with the hydrophobic parts of a protein, causing the aggregation.

After the new construct suitable for crystallography was found, we needed to test both the ability to interact with TRX and the stability under the conditions of a high concentration in a buffer used for a crystallization. In that manner, the next goal of this thesis was to confirm the interaction between ASK1₄₆₋₂₆₇ and TRX by a native gel electrophoresis (*Fig. 5.37*). The disappearance of the TRX band in a complex column and a slight enlargement and shift of the ASK1₄₆₋₂₆₇:TRX band suggest not only proper complex formation, but also that the complex is stable with a 1:1 stoichiometry.

Study of a polydispersity and aggregation behavior of the ASK1₄₆₋₂₆₇ construct was provided by dynamic light scattering. DLS measurement indicated that ASK1₄₆₋₂₆₇ is stable protein with low tendency to aggregate (*Fig. 5.39*). The high molecular weighted aggregates scatter more strongly than the non-aggregated proteins and proportions of the individual local maxima do not correspond to the relative quantity of individual forms in a solution. But even so, DLS showed two well-defined peaks, first with the mean peak position at 4 nm corresponding to the estimated size of ASK1₄₆₋₂₆₇ and the second peak corresponding to aggregates was significantly smaller.

Data presented in this thesis revealed that the construct ASK1₄₆₋₂₆₇ exhibits most promising behavior for crystallization (*Fig. 5.32*). Unfortunately, the recently performed initial crystallographic screening of 5 472 conditions with various buffer compositions, pH, salts and stabilizing agents concentrations did not bring any hit (crystals). Therefore, a chimeric protein, ASK1₄₆₋₂₆₇ construct linked to the enzyme lysozyme, will be designed and used for a future crystallization attempts. Lysozyme crystalize very well under various conditions, therefore it might induce the crystallization of ASK1-TBD, too. Another approach to obtain ASK1₄₆₋₂₆₇ crystals is to perform crystallization in a nitrogen atmosphere under the absence of oxygen, what can protect seven cysteine residues present in ASK1₄₆₋₂₆₇ sequence (*Supplement 1*) from the oxidation. In the case of unsuccessful crystallization, an alternative approach based on NMR spectroscopy will be used for a structure determination. Construct ASK1₈₈₋₂₆₇ with its molecular mass of 20.7 kDa seems suitable for protein NMR measurements.

7 CONCLUSION

- Human ASK1-TBD containing amino acid residues 88-302 with the C-terminal His-tag was successfully expressed and purified
- Human TRX was successfully expressed and purified
- The secondary structure of ASK1₈₈₋₃₀₂C-His and the ASK1₈₈₋₃₀₂C-His:TRX complex was studied by circular dichroism. These measurements suggested the structural change in the vicinity of TRX Trp³¹ altogether with no significant changes in overall secondary structure in ASK1₈₈₋₃₀₂C-His upon the complex formation.
- Samples of ASK1₈₈₋₃₀₂C-His and the ASK1₈₈₋₃₀₂C-His:TRX complex were prepared for SAXS measurements. SAXS data were measured successfully.

- The ASK1-TBD construct for X-ray crystallography was optimized and we suggested ASK1₄₆₋₂₆₇ as the most promising construct for further structural studies
 - Constructs ASK1₈₈₋₃₀₂, ASK1₄₆₋₂₅₁, ASK1₄₆₋₂₆₇, ASK1₄₆₋₂₈₇, ASK1₈₈₋₂₅₁, ASK1₈₈₋₂₆₇ and ASK1₈₈₋₂₈₇ were expressed and purified, with only ASK1₄₆₋₂₆₇ and ASK1₈₈₋₂₆₇ providing high yield and sufficient stability in a solution
 - The interaction between ASK1₄₆₋₂₆₇ and TRX was tested and confirmed by native gel electrophoresis
 - The polydispersity and aggregation behavior of ASK1₄₆₋₂₆₇ construct were studied by DLS and confirmed that ASK1₄₆₋₂₆₇ is sufficiently stable protein with a low tendency to aggregate

8 REFERENCES

- [1] B. Alberts, A. Johnson, J. Lewis, D. Morgan, M. Raff, K. Roberts, and P. Walter, *Molecular Biology of the Cell, Sixth Edition*, vol. 20. Garland Science, 2014.
- [2] H. Ichijo, E. Nishida, K. Irie, P. ten Dijke, M. Saitoh, T. Moriguchi, M. Takagi, K. Matsumoto, K. Miyazono, and Y. Gotoh, "Induction of apoptosis by ASK1, a mammalian MAPKKK that activates SAPK/JNK and p38 signaling pathways.," *Science*, vol. 275, no. 5296, pp. 90–94, 1997.
- [3] M. Saitoh, H. Nishitoh, M. Fujii, K. Takeda, K. Tobiume, Y. Sawada, M. Kawabata, K. Miyazono, and H. Ichijo, "Mammalian thioredoxin is a direct inhibitor of apoptosis signal-regulating kinase (ASK) 1," *EMBO J.*, vol. 17, no. 9, pp. 2596–2606, 1998.
- [4] L. Zhang, J. Chen, and H. Fu, "Suppression of apoptosis signal-regulating kinase 1-induced cell death by 14-3-3 proteins.," *Proc. Natl. Acad. Sci. U. S. A.*, vol. 96, no. 15, pp. 8511–8515, 1999.
- [5] G. Fujino, T. Noguchi, A. Matsuzawa, S. Yamauchi, M. Saitoh, K. Takeda, and H. Ichijo, "Thioredoxin and TRAF family proteins regulate reactive oxygen species-dependent activation of ASK1 through reciprocal modulation of the N-terminal homophilic interaction of ASK1.," *Mol. Cell. Biol.*, vol. 27, no. 23, pp. 8152–8163, 2007.
- [6] A. M. Edelman, D. K. Blumenthal, and E. G. Krebs, "PROTEIN SERINE/THREONINE KINASES," *Annu. Rev. Biochem.*, vol. 56, pp. 567–613, 1987.
- [7] D. Secko, "PROTEIN PHOSPHORYLATION: A GLOBAL REGULATOR OF CELLULAR ACTIVITY | SCQ," 2003. [Online]. Available: <http://www.scq.ubc.ca/protein-phosphorylation-a-global-regulator-of-cellular-activity/>. [Accessed: 20-Apr-2015].
- [8] C. Widmann, S. Gibson, M. B. Jarpe, and G. L. Johnson, "Mitogen-activated protein kinase: conservation of a three-kinase module from yeast to human.," *Physiol. Rev.*, vol. 79, no. 1, pp. 143–180, 1999.
- [9] A. Matsuzawa and H. Ichijo, "Stress-Responsive Protein Kinases in Redox-Regulated Apoptosis Signaling," *Antioxid. Redox Signal.*, vol. 7, pp. 472–481, 2005.
- [10] T. Hayakawa, A. Matsuzawa, T. Noguchi, K. Takeda, and H. Ichijo, "The ASK1-MAP kinase pathways in immune and stress responses," *Microbes Infect.*, vol. 8, no. 4, pp. 1098–1107, 2006.

- [11] S. Shiizaki, I. Naguro, and H. Ichijo, "Activation mechanisms of ASK1 in response to various stresses and its significance in intracellular signaling," *Adv. Biol. Regul.*, vol. 53, no. 1, pp. 135–144, 2013.
- [12] K. Takeda, A. Matsuzawa, H. Nishitoh, and H. Ichijo, "Roles of MAPKKK ASK1 in Stress-Induced Cell Death," *Cell Struct. Funct.*, vol. 28, pp. 23–29, 2003.
- [13] T. Takizawa, C. Tatematsu, and Y. Nakanishi, "Double-stranded RNA-activated protein kinase interacts with apoptosis signal-regulating kinase 1: Implications for apoptosis signaling pathways," *Eur. J. Biochem.*, vol. 269, no. 24, pp. 6126–6132, 2002.
- [14] R. Hayakawa, T. Hayakawa, K. Takeda, and H. Ichijo, "Therapeutic targets in the ASK1-dependent stress signaling pathways.," *Proc. Jpn. Acad. Ser. B. Phys. Biol. Sci.*, vol. 88, no. 8, pp. 434–53, 2012.
- [15] T. Finkel, "Oxidant signals and oxidative stress," *Curr. Opin. Cell Biol.*, vol. 15, no. 2, pp. 247–254, 2003.
- [16] G. Bunkoczi, E. Salah, P. Filippakopoulos, O. Fedorov, S. Müller, F. Sobott, S. a. Parker, H. Zhang, W. Min, B. E. Turk, and S. Knapp, "Structural and Functional Characterization of the Human Protein Kinase ASK1," *Structure*, vol. 15, no. 10, pp. 1215–1226, 2007.
- [17] H. C. Fan, L. I. Ho, C. S. Chi, S. J. Chen, G. S. Peng, T. M. Chan, S. Z. Lin, and H. J. Harn, "Polyglutamine (PolyQ) diseases: Genetics to treatments," *Cell Transplant.*, vol. 23, no. 4–5, pp. 441–458, 2014.
- [18] M. Niso-Santano, R. a. González-Polo, J. M. Bravo-San Pedro, R. Gómez-Sánchez, I. Lastres-Becker, M. a. Ortiz-Ortiz, G. Soler, J. M. Morán, A. Cuadrado, and J. M. Fuentes, "Activation of apoptosis signal-regulating kinase 1 is a key factor in paraquat-induced cell death: Modulation by the Nrf2/Trx axis," *Free Radic. Biol. Med.*, vol. 48, no. 10, pp. 1370–1381, 2010.
- [19] A. L. Peel, N. Sorscher, J. Y. Kim, V. Galvan, S. Chen, and D. E. Bredesen, "Tau Phosphorylation in Alzheimer ' s Disease," vol. 5, pp. 205–218, 2004.
- [20] K. Tobiume, M. Saitoh, and H. Ichijo, "Activation of apoptosis signal-regulating Kinase 1 by the stress-induced activating phosphorylation of pre-formed oligomer," *J. Cell. Physiol.*, vol. 191, no. 1, pp. 95–104, 2002.
- [21] T. Noguchi, K. Takeda, A. Matsuzawa, K. Saegusa, H. Nakano, J. Gohda, J. I. Inoue, and H. Ichijo, "Recruitment of tumor necrosis factor receptor-associated factor family proteins to apoptosis signal-regulating kinase 1 signalosome is essential for oxidative stress-induced cell death," *J. Biol. Chem.*, vol. 280, no. 44, pp. 37033–37040, 2005.

- [22] T. Obsil and V. Obsilova, "Structural basis of 14-3-3 protein functions," *Semin. Cell Dev. Biol.*, vol. 22, no. 7, pp. 663–672, 2011.
- [23] E. H. Goldman, L. Chen, and H. Fu, "Activation of Apoptosis Signal-regulating Kinase 1 by Reactive Oxygen Species through Dephosphorylation at Serine 967 and 14-3-3 Dissociation," *J. Biol. Chem.*, vol. 279, no. 11, pp. 10442–10449, 2004.
- [24] H. Nishitoh, M. Saitoh, Y. Mochida, K. Takeda, H. Nakano, M. Rothe, K. Miyazono, and H. Ichijo, "ASK1 is essential for JNK/SAPK activation by TRAF2.," *Mol. Cell*, vol. 2, no. 3, pp. 389–395, 1998.
- [25] T. C. Laurent, E. C. Moore, and P. Reichard, "Enzymatic Synthesis of Deoxyribonucleotides," *J. Biol. Chem.*, vol. 239, no. 10, pp. 3436–3444, 1964.
- [26] K. F. Tonissen and G. D. Trapani, "Thioredoxin system inhibitors as mediators of apoptosis for cancer therapy," *Mol. Nutr. Food Res.*, vol. 53, no. 1, pp. 87–103, 2009.
- [27] a Holmgren, B. O. Söderberg, H. Eklund, and C. I. Brändén, "Three-dimensional structure of Escherichia coli thioredoxin-S2 to 2.8 Å resolution.," *Proc. Natl. Acad. Sci. U. S. A.*, vol. 72, no. 6, pp. 2305–2309, 1975.
- [28] A. Holmgren, "Thioredoxin," 1985.
- [29] A. E. Damdimopoulos, A. Miranda-Vizuete, M. Pelto-Huikko, J. Å. Gustafsson, and G. Spyrou, "Human mitochondrial thioredoxin. Involvement in mitochondrial membrane potential and cell death," *J. Biol. Chem.*, vol. 277, no. 36, pp. 33249–33257, 2002.
- [30] J. Lu and A. Holmgren, "Thioredoxin System in Cell Death Progression," *Antioxid. Redox Signal.*, vol. 17, no. 12, pp. 1738–1747, 2012.
- [31] a Holmgren, "Thioredoxin. 6. The Amino Acid Sequence of the Protein from Escherichia coli B," *Eur. J Biochem*, vol. 6, pp. 475–484, 1968.
- [32] L. Stryer, A. Holmgren, and P. Reichard, "Thioredoxin. A Localized Conformational Change Accompanying Reduction of the Protein to the Sulfhydryl Form," *Biochemistry*, vol. 6, no. 4, pp. 1016–1020, 1967.
- [33] A. Holmgren, "Effects of Oxidation of Tryptophan Residues in Thioredoxin from Escherichia coli by N-Bromosuccinimide," *J. Biol. Chem.*, vol. 248, no. 11, pp. 4106–4111, 1973.
- [34] "Pokročilé praktikum z fyzikální chemie; Návod k úlohám." [Online]. Available: <http://lynette.natur.cuni.cz/stepanek/vyuka/praktikum.pdf>. [Accessed: 20-Apr-2015].

- [35] “Instruction 28-9920-17 AC for HiLoad 16/600 and 26/60 Superdex 75 prep grade.” [Online]. Available: https://www.gelifesciences.com/gehcls_images/GELS/RelatedContent/Files/1326706518989/litdoc28992017_20120420132119.pdf. [Accessed: 20-Apr-2015].
- [36] H. Ryšlavá, J. Liberda, V. Hýsková, V. Martínek, P. Man, P. Novák, and D. Kavan, “Návody biochemických praktik I,” 2014. [Online]. Available: <https://www.natur.cuni.cz/chemie/biochem/ke-stazeni/biochemicke-praktikum/navody-do-biochemickeho-praktika-2012/>. [Accessed: 20-Apr-2015].
- [37] S. M. Kelly and N. C. Price, “The application of circular dichroism to studies of protein folding and unfolding,” *Biochim. Biophys. Acta*, vol. 1338, no. 2, pp. 161–185, 1997.
- [38] S. M. Kelly and N. C. Price, “The use of circular dichroism in the investigation of protein structure and function,” *Curr. Protein Pept. Sci.*, vol. 1, no. 4, pp. 349–384, 2000.
- [39] N. J. Greenfield, “Applications of circular dichroism in protein and peptide analysis,” *TrAC - Trends Anal. Chem.*, vol. 18, no. 4, pp. 236–244, 1999.
- [40] J. T. Yang, *Circular Dichroism and the Conformational Analysis of Biomolecules*. Springer US, 1996.
- [41] L. Whitmore and B. a. Wallace, “Protein secondary structure analyses from circular dichroism spectroscopy: Methods and reference databases,” *Biopolymers*, vol. 89, no. 5, pp. 392–400, 2008.
- [42] S. M. Kelly, T. J. Jess, and N. C. Price, “How to study proteins by circular dichroism,” *Biochim. Biophys. Acta - Proteins Proteomics*, vol. 1751, no. 2, pp. 119–139, 2005.
- [43] M. a Andrade, P. Chacón, J. J. Merelo, and F. Morán, “Evaluation of secondary structure of proteins from UV circular dichroism spectra using an unsupervised learning neural network,” *Protein Eng.*, vol. 6, no. 4, pp. 383–390, 1993.
- [44] L. Whitmore and B. a. Wallace, “DICHROWEB, an online server for protein secondary structure analyses from circular dichroism spectroscopic data,” *Nucleic Acids Res.*, vol. 32, no. WEB SERVER ISS., pp. 668–673, 2004.
- [45] D. Veisova, L. Rezabkova, M. Stepanek, P. Novotna, P. Herman, J. Vecer, T. Obsil, and V. Obsilova, “The C-terminal segment of yeast BMH proteins exhibits different structure compared to other 14-3-3 protein isoforms,” *Biochemistry*, vol. 49, no. 18, pp. 3853–3861, 2010.

- [46] H. D. T. Mertens and D. I. Svergun, "Structural characterization of proteins and complexes using small-angle X-ray solution scattering," *J. Struct. Biol.*, vol. 172, no. 1, pp. 128–141, 2010.
- [47] C. D. Putnam, M. Hammel, G. L. Hura, and J. a Tainer, "X-ray solution scattering (SAXS) combined with crystallography and computation: defining accurate macromolecular structures, conformations and assemblies in solution.," *Q. Rev. Biophys.*, vol. 40, no. 3, pp. 191–285, 2007.
- [48] D. Kosek, S. Kylarova, K. Psenakova, L. Rezaczkova, P. Herman, J. Vecer, V. Obsilova, and T. Obsil, "Biophysical and Structural Characterization of the Thioredoxin-Binding Domain of Protein Kinase ASK1 and its Interaction with Reduced Thioredoxin.," *J. Biol. Chem.*, pp. 0–25, 2014.
- [49] O. Glatter, "A new method for the evaluation of small-angle scattering data," *J. Appl. Crystallogr.*, vol. 10, no. 5, pp. 415–421, 1977.
- [50] D. T. Jones, "Protein secondary structure prediction based on position-specific scoring matrices," pp. 195–202, 1999.
- [51] D. W. A. Buchan, F. Minneci, T. C. O. Nugent, K. Bryson, and D. T. Jones, "Scalable web services for the PSIPRED Protein Analysis Workbench.," *Nucleic Acids Res.*, vol. 41, no. Web Server issue, pp. W349–57, Jul. 2013.

SUPPLEMENTS

Supplement 1. Amino acid sequence of a human ASK1.

N-terminal ASK1 with amino acid residues 1-320, highlighted are initial and final amino acids of ASK1-TBD constructs used in this diploma thesis. Adapted from a PubMed database.

1	2	3	4	5	6	7	8	9	10	11	12	13	14	15	16	17	18	19	20
M	S	T	E	A	D	E	G	I	T	F	S	V	P	P	F	A	P	S	G
21	22	23	24	25	26	27	28	29	30	31	32	33	34	35	36	37	38	39	40
F	C	T	I	P	E	G	G	I	C	R	R	G	G	A	A	A	V	G	E
41	42	43	44	45	46	47	48	49	50	51	52	53	54	55	56	57	58	59	60
G	E	E	H	Q	L	P	P	P	P	P	G	S	F	W	N	V	E	S	A
61	62	63	64	65	66	67	68	69	70	71	72	73	74	75	76	77	78	79	80
A	A	P	G	I	G	C	P	A	A	T	S	S	S	S	A	T	R	G	R
81	82	83	84	85	86	87	88	89	90	91	92	93	94	95	96	97	98	99	100
G	S	S	V	G	G	G	S	R	R	T	T	V	A	Y	V	I	N	E	A
101	102	103	104	105	106	107	108	109	110	111	112	113	114	115	116	117	118	119	120
S	Q	G	Q	L	V	V	A	E	S	E	A	L	Q	S	L	R	E	A	C
121	122	123	124	125	126	127	128	129	130	131	132	133	134	135	136	137	138	139	140
E	T	V	G	A	T	L	E	T	L	H	F	G	K	L	D	F	G	E	T
141	142	143	144	145	146	147	148	149	150	151	152	153	154	155	156	157	158	159	160
T	V	L	D	R	F	Y	N	A	D	I	A	V	V	E	M	S	D	A	F
161	162	163	164	165	166	167	168	169	170	171	172	173	174	175	176	177	178	179	180
R	Q	P	S	L	F	Y	H	L	G	V	R	E	S	F	S	M	A	N	N
181	182	183	184	185	186	187	188	189	190	191	192	193	194	195	196	197	198	199	200
I	I	L	Y	C	D	T	N	S	D	S	L	Q	S	L	K	E	I	I	C
201	202	203	204	205	206	207	208	209	210	211	212	213	214	215	216	217	218	219	220
Q	K	N	T	M	C	T	G	N	Y	T	F	V	P	Y	M	I	T	P	H
221	222	223	224	225	226	227	228	229	230	231	232	233	234	235	236	237	238	239	240
N	K	V	Y	C	C	D	S	S	F	M	K	G	L	T	E	L	M	Q	P
241	242	243	244	245	246	247	248	249	250	251	252	253	254	255	256	257	258	259	260
N	F	E	L	L	L	G	P	I	C	L	P	L	V	D	R	F	I	Q	L
261	262	263	264	265	266	267	268	269	270	271	272	273	274	275	276	277	278	279	280
L	K	V	A	Q	A	S	S	Q	Y	F	R	E	S	I	L	N	D	I	
281	282	283	284	285	286	287	288	289	290	291	292	293	294	295	296	297	298	299	300
R	K	A	R	N	L	Y	T	G	K	E	L	A	A	E	L	A	R	I	R
301	302	303	304	305	306	307	308	309	310	311	312	313	314	315	316	317	318	319	320
Q	R	V	D	N	I	E	V	L	T	A	D	I	V	I	N	L	L	L	S

Supplement 2. Prediction of a secondary structure of ASK1.

Prediction of a secondary structure of N-terminal ASK1 with amino acid residues 1-320, using the PSIPRED Protein Sequence Analysis Workbench [50][51].

